Theses and Dissertations

Summer 2014

Biodegradable particles as vaccine delivery systems

Vijaya Bharti Joshi
University of Iowa

Recommended Citation

BIODEGRADABLE PARTICLES AS VACCINE DELIVERY SYSTEMS

by

Vijaya Bharti Joshi

A thesis submitted in partial fulfillment
of the requirements for the Doctor of
Philosophy degree in Pharmacy
in the Graduate College of
The University of Iowa

August 2014

Thesis Supervisor: Professor Aliasger K. Salem

Graduate College
The University of Iowa
Iowa City, Iowa

CERTIFICATE OF APPROVAL

_____

PH.D. THESIS

_____

This is to certify that the Ph.D. thesis of

Vijaya Bharti Joshi

has been approved by the Examining Committee
for the thesis requirement for the Doctor of Philosophy
degree in Pharmacy at the August 2014 graduation.

Thesis Committee: _____
Aliasger K. Salem, Thesis Supervisor

_____
Maureen D. Donovan

_____
Douglas R. Flanagan

_____
Peter Thorne

_____
Lewis L. Stevens

AKNOWLEDGEMENTS

I would like to extend heartfelt gratitude to my teachers, colleagues and friends for their support and help that has brought this thesis research to a successful completion.

I am deeply indebted to my supervisor Dr. Aliasger Salem for giving me the grand opportunity to undertake this thesis research. His awe-inspiring personality, stimulating suggestions and encouragement have motivated me throughout this thesis project. In addition, he is always accessible and willing to help his students with their research. As a result, learning became smooth and rewarding for me. I want to express my sincere gratitude for his help, valuable guidance and financial support during the program of study at University of Iowa.

For this thesis research, I owe a debt to Dr. Peter Thorne of the Department of Occupational and Environmental Health and Dr. Gorge Weiner of the Carver College of Medicine for their collaboration in this research work and helpful suggestions during the process. I am also grateful to Dr. Andrea A. Dodd, Dr. Xuefang Jing and Amani Makkouk for assisting me with their expertise during the implementation of my research hypothesis in different disease models. I would like to express my sincere gratitude to Dr. Maureen Donovan, Dr. Douglas Flanagan, Dr. Jennifer Fiegel and Dr. Liu Hong for their valuable suggestions during the progress of this thesis research that has made me a better research scientist. I also want to express my gratitude to Dr. Lewis Stevens for agreeing to be on my thesis committee. His collaboration and insightful discussion regarding the polymer particle delivery systems has been very helpful during the writing process of this dissertation.

This thesis would not have been possible without the assistance of my lab members. I would like to thank Dr. Sean Geary, Amaraporn Wongrakpanich, Kawther,Ahmed Sheetal Reginald D'mello, Kareem Atef Nassar Ebeid, Nattawut LeelakanokKeerthi , Atluri, Behnoush Khorsand Sourkohi and Anh-Vu T Do for their passionate participation in discussion, continuous feedback and collaboration during the experimental conduct. In addition, I will never forget the wonderful time I had during barbeques, group lunches and Halloween gatherings. I would like to

extend a special thanks to Dr. Sean Geary for the training in various immunological assays, providing valuable comments on my writing and proofreading my thesis. Completion of this work would have been difficult without his continuous support. I also want to extend my gratitude to the former members of the lab Dr. Caitlin Lemke, Dr. Yogita Krishnamachari, Dr. Aiman Abbas, Dr. Jessica Graham, Dr. Dahai Jiang and Dr. NaJung Kim for training me in different laboratories techniques during early years of my thesis research. I would like to extend a special thanks to Dr. Yogita Krishnamachari and Dr. Caitlin Lemke for providing me continual technical advice and emotional support during past five years.

A very special thanks to Sandeep Bodduluri and Amaraporn Wongrakpanich aka Kae for always lending an ear when I am stressed and celebrating my successes with me. Their presence and support has helped me stay sane during the difficult times. I also want to thank Neha, Divesh, Shailesh, Amit and Vaibhav for their inexhaustible encouragement and the part they all played during past 10 years in helping me get to this point. They know the true cost of this PhD for me and have supported me throughout. I also want to acknowledge the support from Somnath, Renu, Abhilash, Astha, Guhan, Keshav, the Association of India's Development volunteers, for providing me much needed break from research work and for the fond memories of organizing fundraisers while gaining valuable community exposures with the volunteers.

No words can express my gratitude towards my mother, my father, my lovely sister, Taruna, and my dear brother, Prashant for providing me insurmountable support, hope and conviction to achieve my dreams. This journey would not have been possible without their support. I would like to express my deepest gratitude to my father whom I lost during this period, I miss you dearly.

I also want to acknowledge Kathy Walters, Jean Ross and Chantal Dee for their training on various instruments at Central Microscopy Research Facility. I am also thankful to Lois Baker, Rita Schneider and Debra Goodwin for providing me much needed help in the administrative work during the program of study at University of Iowa.

ABSTRACT

Immunotherapy has been widely investigated in cancer, infectious diseases and allergies for prevention or amelioration of disease progression. In the case of vaccines, the key cellular target in stimulating an effective and appropriate immune response is the professional antigen presenting cell or dendritic cell (DC). Cancer vaccines are primarily aimed at the activation of a tumor-specific cytotoxic T-lymphocyte (CTL) response whilst vaccines to allergies are aimed at reducing IgE responses. Such vaccines normally involve the administration of tumor-associated antigens (TAAs) for cancer, or antigens (Ags) derived from infectious microbes and allergens in the case of allergies. Ags, whether derived from tumor or allergen, can be combined with adjuvants, that include immunostimulatory molecules recognized by the pathogen associated receptors expressed by DCs and can trigger the activation/maturation of DCs. Co-delivery of an appropriate adjuvant with an Ag can stimulate DCs to subsequently promote a robust Ag-specific CTL response which may favor anti-tumor immunity.

Cancer vaccines have been widely investigated in the clinics as a complementary therapy to surgery, radiation and chemotherapy. Activation of CTLs against tumor cells that express TAAs could lead to the complete eradication of a cancer and prevent its reoccurrence. In this study I developed microparticles using a polyanhydride polymer prepared from 1,8-bis(p-carboxyphenoxy)-3,6-dioxaoctane (CPTEG) and 1,6-bis(p-carboxyphenoxy) hexane (CPH) that has shown inherent adjuvant properties. I prepared 50:50 CPTEG:CPH microparticles encapsulating a model tumor Ag, ovalbumin (OVA), and a synthetic oligonucleotide containing an unmethylated CpG motif, CpG, as an adjuvant. CpG has shown significant potential as an adjuvant for TAA-based vaccines leading to significant anti-tumor immune activity. It was shown here that mice vaccinated with OVA-encapsulated 50:50 CPTEG:CPH microparticles developed OVA-specific CTL responses. These mice showed enhanced survival compared to the control treatment groups when challenged with OVA expressing tumor cells.

As a more novel cancer vaccine approach, TAAs from tumor cells undergoing an immunogenic form of apoptosis (which can be triggered by certain chemotherapeutic drugs) can be used as the source of Ags delivered to DCs. The combination of an adjuvant and dying cancer cells can assist in the maturation of DCs so that they promote an effective tumor/TAA-specific CTL response against tumor cells expressing TAAs. In this work a therapeutic in situ tumor vaccine was developed encapsulating a chemotherapeutic drug and CpG. Doxorubicin (Dox) is a widely used chemotherapeutic drug that induces tumor cells to undergo an immunogenic form of apoptosis. Sustained release of Dox within solid tumors in mice can cause the release of a variety of TAAs which can be presented by DCs and, in the presence of CpG, stimulate a strong anti-tumor CTL response. Formulations of poly(lactic-co-glycolic acid) (PLGA) particles loaded with Dox and CpG were prepared anddemonstrated sustained release of their cargo. It was demonstrated, *in-vivo*, that among various formulations of Dox and CpG, that co-delivery of Dox and CpG in the same PLGA particles caused the greatest reduction in tumor growth and longest survival of tumor-challenged mice when compared to treatment groups of PLGA particles delivering Dox and CpG either alone or with an independently loaded combination of particles.

PLGA particles have also been investigated as a prophylactic vaccine delivery system that generates a robust Ag-specific CTL response. This system has been employed for the development of vaccines against various infectious diseases and allergies. However, there has been conflicting opinions regarding the optimum size of PLGA particles required to stimulate an active CTL response. Thus, differently sized PLGA particles encapsulating OVA and CpG were developed to study the relationship of particle size to the magnitude of OVA-specific CTL responses. It was shown that the degree of particle uptake and activation of DCs increased with decreasing size of PLGA particles. It was also demonstrated that immunization of mice with 300 nm sized particles demonstrated a higher proportion of OVA-specific CTLs and promoted increased production of OVA-specific IgG2a antibodies. The immune efficacy of these particles was evaluated with a clinically relevant Ag, Dermatophagoides pteronyssinus-2 (Der p2). Mice vaccinated with different sizes of PLGA particles loaded with CpG and coated with Der p2

v

displayed different magnitudes and types of immune activation against Der p2. The small sized particles decreased the airway hyperresponsiveness associated with allergy-induced asthma. The presence of CpG in the PLGA particle vaccines also reduced the airway hyperresponsiveness.

This thesis research has contributed to the identification and development of a delivery system for Dox in combination with CpG which gives sustained release of these molecules within tumors and enhanced survival in tumor bearing mice. This study also determined optimal sizes of PLGA particle vaccines required to independently stimulate robust Ag-specific immune responses to cancer and allergy.

TABLE OF CONTENTS

ix

LIST OF TABLES

LIST OF FIGURES

xi

xiii

xiv

xv

xvi

LIST OF ABBREVIATIONS

ACK: Ammonium Chloride Potassium

Ag: Antigen

AHR: Airway hyperresponsiveness

APC: Antigen presenting cells

BAL: Bronchoalveolar lavage

CpG: unmythylated phosphodiester cytosine and guanine oligonucleotide

CPH: 1,6-bis(p-carboxyphenoxy) hexane

CPTEG: 1,8-bis(p-carboxyphenoxy)-3,6-dioxaoctane

CTL: Cytotoxic T-lymphocyte

DC: Dendritic Cell

DCM: Dichloromethane

Der p: Dermatophagoides pteronyssinus

DMSO: Dimethyl sulfoxide

Dox: Doxorubicin

DSC: Differential scanning calorimetry

EE: Encapsulation efficiency

ELISA: enzyme-linked immuno-sorbent assay

GM-CSF: Granulocyte macrophage colony-stimulating factor

H&E: Hematoxylin and eosin

HDM: House dust mite

i.p.: intra-peritoneal

IACUC: Iowa Institutional Animal Care and Use Committee

IFN-γ: Interferon-gamma

Ig: Immunoglobulin

IL: Interleukin

ISS-ODN: immunostimulatory oligodeoxynucleotide

KC: Keratinocyte-derived cytokine

LPS: Lipopolysaccharide

MHC: Major histocompatibility class

MIP: Macrophage inflammatory protein

OVA: Ovalbumin

PA: Polyanhydride

PAMP: Pathogen-associated molecular pattern

PBL: Peripheral blood lymphocyte

PBS: Phosphate buffer saline

PCL: Perivascular cuffing lesion

PLGA: Poly(lactic-co-glycolic acid)

PVA: Poly(vinyl alcohol)

PVM-MA: Poly(methyl vinyl ether-co-maleic anhydride)

RT: room temperature

s.c.: subcutaneous

SEM: Scanning electron microscopy

TAA: Tumor-associated antigens

Th1: T-helper 1

Th2: T-helper 2

TLR: Toll-like receptor

TNF-α: Tumor necrosis factor-alpha

XRD: Powder X-ray diffraction

PREFACE

Publications from this thesis research

1.   Joshi VB, Geary SM, Salem AK. Biodegradable particles as vaccine delivery systems: size matters. AAPS J. 2013;15(1):85-94.

2.   Joshi VB, Geary SM, Carrillo-Conde BR, Narasimhan B, Salem AK. Characterizing the antitumor response in mice treated with antigen-loaded polyanhydride microparticles. Acta Biomater. 2013;9(3):5583-9.

3.   Joshi VB, Geary SM, Salem AK. Biodegradable particles as vaccine antigen delivery systems for stimulating cellular immune responses. Hum Vacc Immunother. 2013;9(12):2584-90.

4.   Joshi VB, Geary SM, Salem AK. Production of antigen-loaded biodegradable nanoparticles and uptake by dendritic cells. Methods Mol Biol. (Clifton, NJ). 2014;1139:453-66.

5.   Joshi VB, Adamcakova-Dodd A, Jing X, Wongrakpanich A, Gibson-Corley K, Thorne P, et al. Development of a poly (lactic-co-glycolic acid) particle vaccine to protect against house dust mite induced allergy. AAPS J. 2014:1-11.

CHAPTER 1: INTRODUCTION

Background

Vaccine is a term employed to describe the biological preparations that stimulate a protective immune response. Vaccinations can either be prophylactic, to prevent the onset of disease, or therapeutic where the host already has a disease such as cancer. The exponential growth in vaccine development during the 20th century led to control of smallpox, rabies, plague, cholera, and typhoid in most parts of the developed world (1). These vaccines are generally composed of microbial toxins, attenuated or inactivated microbes that stimulate host immunity to eradicate these microbes. Towards the end of 20th century, in addition to the use of conventional vaccines, the use of recombinant organisms to manufacture protein vaccines led to the development of vaccine carrying a safe immunogen compared to inactivated infectious pathogens. Later, vaccines for several disease causing organisms were combined to target multiple bacterial and viral infections within one vaccine regimen (2). Since then, the expanding research in the field of vaccine development has been focusing on designing vaccine systems that target other potentially fatal diseases. In theory, most contagions that carry specific foreign Ags in the diseased state can be targeted by developing a vaccine that stimulates the host's immune response to eliminate the diseased cells or microbe carrying the foreign Ag. With advancement in immunological understanding of diseases, certain diseased states can be diagnosed by detection of a specific antigen (Ag) present in the body during the diseased state (3, 4). This includes tumor-associated Ags present in most types of cancer, pathogen-associated Ags present during infectious diseases and inflammatory antibodies present against specific antigens (or allergens) during allergic reactions. Vaccines developed against these Ags can selectively eliminate the diseased cells and inhibit disease progression.

Cancer

According to the American Cancer Society there were predicted to be 1,660,290 new cases of cancer and 580,350 deaths due to cancer for the year 2013 in United States (5). Conventional anti-cancer therapies include chemotherapy, radiation and surgery. Recently, targeted therapies using either the small molecule inhibitor, imatinib (marketed as Gleevec® by Novartis), or antibodies, such as trastuzumab (marketed as Herceptin® by Genentech) have been used to inhibit cell signaling pathways in cancer cells to prevent tumor growth and proliferation in patients with chronic myeloid leukemia and breast cancer respectively (6). In general, depending on the stage and severity of the cancer, conventional therapies are used either alone or in combination in an attempt to achieve complete eradication of the tumor and its metastases. However, many cancers, such as melanoma and prostate cancer are essentially non-responsive to therapy once they have metastasized and in the case of those cancers that do respond well to chemotherapy, they often fail to completely eradicate the tumor cells and often drug-resistant variants result in aggressive tumor recurrence. Therefore, there is a requirement for new clinical interventions (7-9). The therapeutic efficacy of conventional anti-cancer treatments could be enhanced by stimulation of anti-tumor immune responses that protect against recurrent metastases. It is now well established that tumors aberrantly express proteins generally not expressed by healthy tissues which are capable of being recognized by the patient's own immune system. These tumor-associated antigens (TAAs) have the potential to be used as the key antigenic molecules for cancer vaccine formulations (10). Cancer/testis Ags are one of the classes of such TAAs which are absent in somatic cells but aberrant expression of these Ags have been reported in many cancers (11). The first cancer/testis Ag to be identified in melanoma patients was MAGE-1 (12) and is expressed in approximately 40 % of melanoma patient tumor samples with no expression in any

normal tissues, except testis (which is an immune privileged tissue[1]), making it an attractive target for anti-tumor immune responses elicited by cancer vaccines (13). Another promising TAA from this class is NY-ESO-1 that has been shown to generate spontaneous immune response in patients carrying NY-ESO-1 positive tumors (14). Other types of TAAs include mutated proteins found only in tumors, of which, mutated Ras-D12 protein, found in 45 % colon adenocarcinomas patients, is an example (15). Novellino et al. have provided an extensive list of TAAs that can be potential targets for cancer vaccines (16). There are certain TAAs that are expressed by a large proportion of many different types of cancer that could therefore be used as antigens in vaccine formulations against multiple cancers (17, 18). Despite the discovery of a wide range of TAA, the only cancer vaccine approved by US Food and Drug Administration (FDA) is Provenge® (Sipuleucel-T),Dendreon's prostate cancer vaccine, that requires isolation of the patient's immune cells, followed by *in-vitro* pulsing of these cells with a prostate-specific protein and then administration of these cells back to the patient (19). Provenge® showed a 4 month improvement in survival for patients compared to placebo control, however this treatment is both costly and labor intensive.

<p style="text-align:center">Allergy and Asthma</p>

Allergies are hyper-immune reactions to generally harmless stimuli that are inhaled, ingested or have come in contact with the skin. Severe cases of allergies are diagnosed using a skin prick test (20). National Health and Nutrition Examination Surveys reported that 54.3 % of the population in the United States are positive for one or more of the most commonly found allergens which include house dust mites, perennial rye, ragweed, German cockroaches, Bermuda grass, cats, Russian thistle, white oak, *Alternaria alternata*, and peanuts (21). Characteristic symptoms for allergy include

---

[1] Tissues that lack adaptive and innate immune response due to specialized mechanism of immune suppression that operate to protect tissues from immune-mediated damage.

vomiting, atopic eczema, dry skin and persistent edema of the nasal mucosa. Allergic reactions to inhaled allergens cause activation of humoral (antibody) immunity directed against the allergen, leading to mucus production, secretion of allergen-specific IgE antibodies and activation of mast cells (22). Chronic exposures to such allergens result in the recruitment of eosinophils and basophils to the site of inflammation and cause pathological damage to the tissues characterized by remodeling of airway and blood vessels (23). All of these factors can contribute to the development of asthma, an allergic reaction to inhaled allergens which causes constriction of the bronchi and difficulty in breathing. While all allergies do not develop into asthma, it has become increasingly evident that asthmatic patients exhibit positive results from skin prick tests for one or more allergens (24). Also, studies have shown that the severity of asthma in allergic patients correlates to the degree of allergen exposures (25). These studies confirm that repeated exposures to allergen can induce asthma. Most of the current therapeutic interventions for asthma include symptomatic treatments that focus on inhibition of inflammatory cytokines (leukotriene receptor antagonist, anti-histamines), mast cell stabilization (cromolyn sodium), anti-IgE activity (omalizumab) and bronchodilation (β2 agonists, inhaled corticosteroids). In the absence of a therapy capable of achieving long-term relief from allergen induced asthma, much research has been focused on the development of vaccines against common allergens. The World Health Organization has approved a regimen of annual vaccination against seasonal allergens that has shown significant reduction in respiratory allergies (26). GRASTEK® (Timothy Grass Pollen Allergen Extract by Merck) is a recently FDA approved allergy vaccine. With the success of preventive vaccinations for seasonal allergies, more robust vaccination strategies are being developed against various allergens (27-29). Use of sublingual and subcutaneous immunotherapy has also shown reduced clinical symptoms of asthma by environmental allergens (30-33). However, such immunotherapy requires repetitive administrations of

increasing doses of allergen for 2 to 3 years, which is inconvenient for the treatment of large populations.

Immune responses to vaccines

Vaccines promote adaptive immune responses that are generated against particular Ag(s), usually administered within the vaccine formulation, and these immune responses can result in humoral (antibody) responses and/or cellular (cytotoxic T-lymphocyte) responses. The majority of successfully formulated vaccines in general use today, or used previously, primarily stimulate humoral immune responses where Ag-specific antibodies produced as a result of the vaccination function by either neutralizing the Ag (e.g. toxins) or by coating (opsonizing) the pathogen with Ag-specific antibody and then stimulating phagocytosis or complement-mediated lysis of the pathogen (34, 35). Humoral responses are generally inadequate at eliminating intracellular pathogens and malignant disease and therefore cellular or cytotoxic T-lymphocyte (CTL) responses are more desirable primarily due to the mechanism by which CTLs recognize Ag (see below).

Cytotoxic T-lymphocyte responses

Cytotoxic T-lymphocyte (CTL) responses are classically stimulated by Ag presenting cells (APCs), in particular dendritic cells (DCs) (36). Ag-specific naïve CTLs can be stimulated to expand and become activated in lymph nodes in the presence of appropriate signals from mature DCs. CTLs recognize Ag in the context of the ubiquitously expressed self-protein, major histocompatibility class I protein (MHC class I). For a vaccine to be effective at generating a CTL response it is necessary to promote DCs to present Ag in association with MHC class I. This can be done with the addition of an appropriate adjuvant or pathogen-associated molecular patterns (PAMPs), such as the oligodeoxynucleotide CpG, which can promote a phenomenon known as cross-presentation (37). The presence of either synthetic or purified PAMPs are recognized

through Toll-like receptors (TLRs) that signal to DCs in such a way as to mimic an infection, thereby promoting to activation/maturation of DCs into efficient immunostimulatory APCs (38). In addition, the mode of delivery of Ag can also influence the degree of MHC class I/Ag presentation. For instance, Ag delivered such that it accesses the cytoplasm (as with certain particulated formulations) or is endogenously expressed (as with adenoviruses) can favor cross-presentation (39, 40). PAMP-stimulated DCs upregulate expression of co-stimulatory B7 molecules (CD80 and CD86) which, along with MHC class I/Ag interaction with the T-cell receptor (TCR) (expressed on the surface of the CTL), are essential signals for CTL activation. (Figure 1). Once activated and expanded/proliferated the Ag-specific CTLs leave the lymph node and travel to the site of the diseased tissue where they specifically eradicate cells expressing MHC class I/Ag. It should be noted that usually Ag will also be presented by DCs in association with MHC class II resulting in activation of T-helper cells potentially capable of enhancing CTL activation (41).

T-helper 1 and T-helper 2 responses

Upon exposure to a vaccine adaptive immune responses are generated that involve Ag-specific responses by B lymphocytes (which produce antibodies) and/or CTLs. Depending on the nature of the vaccine formulation it can favor differentiation of subsets of CD4 T-cells into T-helper cells that secrete discrete suites of cytokines that assist in the development of either humoral or cellular immunity (42). Two major discrete functionally polarized types of T-helper cells are: 1) T-helper 1 (Th1) cells, which primarily secrete IFN- γ and IL-2, and support the development of cellular immunity; and 2) T-helper 2 (Th2) cells, which secrete IL-4, IL-5, IL-9 and IL-13 and promote humoral immunity. Therefore, for the development of vaccines against cancer and infectious diseases it is necessary to simulate Th1 type responses. Vaccines for allergy require inhibition of allergen-induced Th2 dominant inflammatory responses. This could be

achieved by stimulating an allergen-specific Th1 dominant protective response making it a desirable response for the development of vaccines against allergen-induced asthma (Figure 2). The nature of the Th response can be indicated by the relative degree of production of subclasses of immunoglobulin (Ig)-G antibody response. A Th2 dominant immune response is often associated with secretion of IgG1 while Th1 is associated with secretion of IgG2a antibodies in mice (43). Thus, ratio of IgG2a:IgG1 antibodies in serum samples can indicate of the type of Th response present in the treated animal.

<div align="center">Composition of Vaccines</div>

The magnitude, type and specificity of immune response stimulated by a vaccine are partly dependent on the composition of the vaccine. Ag-carrying vaccines can be developed as solutions, ionic complexes, emulsions, attenuated viruses or in the form of polymer micro/nanoparticles encapsulating the Ag within their matrix. The presentation of Ag to the immune system in different forms can lead to differences in the magnitude and type of stimulated immune responses. Besides the presence of preservatives, diluents and other inert constituents, the two active components of vaccines are Ag and adjuvants.

In case of patients already suffering from cancer, a novel approach for in-situ vaccination of tumors has been developed. This involves stimulation of cancer Ag specific immune response by presentation of Ags released from dying tumors of cancer patients. This vaccine approach does not require ex-vivo handling of tumors or vaccination with a specific Ag. In-situ vaccines provide sustained release of anti-cancer drugs and an immunoadjuvant to the solid tumors. While anti-cancer drugs induce immunogenic cell death, Ags/TAAs released from dying tumors, in presence of immunoadjuvant, stimulate tumor-specific immune responses.

<div align="center">Antigen (Ag)</div>

Ag, as a constituent of a vaccine, is often, although not always, in the form of a protein to which an immune response can be mounted because the host harbors Ag-

specific T-lymphocytes and/or B lymphocytes with the potential of being activated. General examples include; microbial protein from an infectious microbe, aberrantly expressed proteins in tumor cells, or an asthma causing allergen. The antigenic material may be in the form of an attenuated pathogen (e.g. chicken pox vaccine) or purified recombinant proteins (e.g. hepatitis B vaccine). Other more novel strategies have been used successfully, for example with the *Haemophilus influenza* type B vaccine where the outer polysaccharide coat (the antigenic material) of the virus is conjugated with a protein to stimulate the immune system.

<u>Ovalbumin (OVA)</u>

In the research presented here ovalbumin (OVA), the albumin protein from chicken egg white, was used as a model tumor antigen. Using OVA in mice tumor model systems allows us to estimate OVA-specific CTL and OVA specific antibody levels using OVA tetramer staining (44) or enzyme-linked immunosorbent assay (ELISA), respectively. These assays provide important tools to monitor the type and magnitude of immune response stimulated by vaccines. In this system, OVA-expressing EG.7-OVA tumor cells were used to challenge mice (45) and the efficacy of vaccines with respect to stimulating OVA-specific antitumor immune responses in prophylactic and therapeutic settings was assessed.

<div align="center">Adjuvants</div>

A plethora of Ags which are under investigation for the development of vaccines are not immunostimulatory (46, 47). A critical step in stimulation of Ag-specific CTL immunity is the complete maturation of DCs that present Ag along with co-stimulatory signals (e.g. from CD80 and CD86 molecules). In a phase I/II clinical study, DCs were isolated from hepatocellular carcinoma patients and pulsed with multiple recombinant TAAs. Vaccination of donor patients with pulsed DCs that were subcultured for 5 days with granulocyte macrophage-colony stimulating factor and interleukin-4 resulted in

induction of T-cell responses against the recombinant TAAs in all 5 patients (48). Thus, for the development of vaccines that induce appropriate maturation of DCs, administration of an adjuvant is required, along with the Ag. Cervarix® (marketed by GlaxoSmithKline), containing the human papilloma virus (HPV)-derived capsid protein (L1 protein) and the TLR-4 agonist, monophosphoryl lipid A, complexed with aluminium hydroxide in sodium dihydrogen phosphate dehydrate buffer, has shown to stimulate protective immunity against HPV infection and therefore providing protection from cervical cancer caused by HPV (49). In a separate study it was shown that when a different TLR-4 agonist, lysophosphatidylcholine (LPC), helps in maturation of DCs *in-vitro* (50) and when incorporated into liposomes with OVA it promotes tumor protection from E.G7 tumor cell challenge (51). PAMPs such as unmythylated CpG oligonucleotide (CpG) and imiquimod (52) may be suitable as adjuvants for certain vaccines (53).

In the research presented in this thesis CpG oligodeoxynucleotides were used as the adjuvant to develop vaccines that stimulate a robust Ag specific CTL response for the prophylactic treatment of intracellular/metastatic disease and generate Th1 skewed antibody response to prevent allergic reactions caused by Th2 inflammation.

CpG oligodeoxynucleotides (CpG)

The ability of bacterial DNA to stimulate innate immunity and to contribute to adaptive immune responses is due to the presence of sequences of single stranded DNA containing unmethylated phosphodiester linked cytosine triphosphate deoxynucleotide (C) and guanine triphosphate deoxynucleotide (G) motifs (CpG) (54). Synthetic CpG sequences or oligodeoxynucleotides (ODNs), which differ from bacterial CpG sequences in that the backbone consists of phosphorothioate linkages, can be recognized by TLR-9, endosomally expressed by DCs. TLR-9 signalling then leads to triggering the maturation of DCs so as to favor the promotion of cellular (CTL) immune responses and thereby mimicking a response to bacterial infection. Depending on their sequence and

immunostimulatory properties, CpG ODN can be classified into three different classes: A, B and C (55, 56).

Class A: Twenty base pair long oligomers containing a single CpG motif and a polyG tail at 3' end of the oligomer. They have been shown to induce maturation of APC and secretion of IFN-γ by DCs (56).

Class B: 18 − 26 base pair oligomers with multiple CpG motifs and a phosphorothioate backbone. They have been shown to induce DC maturation and B cell activation (56).

Class C: Twenty base pair long oligomer with multiple CpG motifs and phosphorothioate backbone. They also contain a TCG dimer at 5'end. They have been shown to induce DC maturation and B cell activation (56).

CpG has been used as an adjuvant to develop vaccines for cancer, allergy and infectious disease (57). Research described in this thesis used CpG-1826 which is a class B ODN and is a 20 base pair DNA oligomer with a sequence 5'-TCCATGACGTTCCTGACGTT-3' (58). All studies for this research were performed with CpG class B and it has been referred to in this text as CpG.

<center>Chemotherapeutic drugs that promote immunogenic cell

death</center>

A major challenge in developing therapeutic cancer vaccines is to target the TAA or combination of TAAs that are aberrantly expressed by cancer/tumor cells to ensure their complete eradication by vaccine-generated TAA-specific immune responses. The two major drawbacks of cancer vaccines that include only one TAA is that: 1) cancer cells may lose expression of the TAA and therefore avoid immune-mediated anti-tumor activity and 2) single TAAs may have limited epitopes that may only be immunogenic in patients expressing appropriate MHC alleles. An alternative approach to overcome these drawbacks is to develop an in situ vaccine system resulting from stimulation of a tumor-

specific immune response through the release of TAAs from dying cancer cells. To explain, accumulating evidence indicates that certain conventionally used chemotherapeutic drugs can induce immune-stimulatory cell death in tumor cells. Treatment of tumors with certain anthracyclines undergo immunogenic apoptosis that is characterized by translocation of calreticulin, a protein normally found in endoplasmic reticulum, to the surface of dying cells (59), which consequently promotes theirengulfment by phagocytes (60). Induction of immunogenic cell death is specific to a few chemotherapeutic agents such as doxorubicin (Dox), in contrast to mitomycin C which fails to induce the immunogenic cell death (61). In another study, dying tumor cells treated with Dox and epirubicin showed increased expression of heat shock protein-70, another marker for DCs to enhance antigen uptake. In the same study, it was also shown that DCs that have internalized Dox and epirubicin treated tumors secrete IFN-γ and IL-12 cytokines promoting T-cell activation (62). *In-vitro* treatment of a cloned stable murine DC cell line with chemotherapeutic drugs showed that at least 15 clinically used anti-cancer drugs induce maturation of DCs (63). In a separate study, treatment of DCs with sub-cytotoxic concentrations of paclitaxel, Dox, mitomycin C, and methotrexate increased the ability of DCs to present Ag to naïve T-cells showing direct assistance of these drugs in stimulation of Ag specific CTL response (64). Additionally, vaccination of mice carrying ovarian cancer (murine ovarian surface epithelial cells) with Dox and cisplatin treated, irradiated murine ovarian cancer cells showed improved survival and induction of cancer-specific CD4+ T-cell immune response (65). Treatment of carcinogen-induced breast adenocarcinomas and fibrosarcomas with Dox has been shown to induce proliferation of antigen-specific CD8 T-cells in tumor-draining lymph and promote CD8 T-cells infiltration in tumors (66). These studies demonstrate that some of the conventional chemotherapeutic drugs have immunomodulatory properties that enhance immunogenicity of dying tumor cells as well as assist maturation of DC and antigen presentation to T-cells. Treatment of cancer with these drugs in association with

an adjuvant can stimulate cancer specific immune responses against TAAs released from dying cancer.

Doxorubicin (Dox)

Among the various chemotherapeutic drugs discussed above, Dox (Figure 3) was chosen in these studies as the anti-cancer agent for the development of an in situ vaccine for potential application to growing tumors in cancer patients. Doxorubicin is an anthracycline used, alone or in combination with other chemotherapeutic agents, for the treatment for many common cancers. Multiple doses of Dox are administered intravenously or intravesically (in bladder carcinoma) as a treatment regimen in an attempt to achieve complete remission. The mechanism of action of Dox is not completely understood, however, most literature suggests that intercalation of Dox between DNA base pairs cause DNA breakage, inhibition of RNA synthesis and inhibition of replication due to the abrogation of topoisomerase II activity (67). Among various side effects associated with chemotherapeutic drugs (gastrointestinal toxicity, inflammation at the site of injection, hair loss, decrease in white blood cell count), induction of cardiotoxicity is the most concerning dose limiting side effect of Dox treatment (68). An increased risk of congestive heart failure was observed in 2.2 % patients treated with injectable Dox solution once every 3 weeks (69). Nevertheless, Dox is often the choice of drug for the treatment of many cancers due to its high potency (70). Recent studies suggest that Dox can potentially assist in stimulation of tumor-specific immune responses which makes it a promising candidate for the development of a novel therapeutic cancer vaccine where the source of tumor antigen is in situ (from the apoptosing tumor cells). Delivery of Dox in liposomal formulations Doxil (marketed in United States) or Caelyx (marketed in Canada and Europe) and Myocet has shown longer circulation times than soluble Dox and also demonstrated reduced cardiotoxocity (71, 72).

Biodegradable polymer particles

A highly desirable goal for new vaccine formulations is that they are safe, inexpensive, stable, and mimic pathogenic infection (73). Biodegradable polymer-based particle vaccines are promising antigen and drug delivery vehicles that offer multiple advantages over the injectable formulations currently available in clinics. These polymer-based delivery systems protect encapsulated molecules from physiological degradation and provide flexibility with respect to the release kinetics of cargo that can be modified by varying the molecular weight or the composition of the polymer backbone (74-77). Compositional and structural modifications to fabricated particles can affect a range of important parameters aside from release kinetics and include; targeting to a specific population of cells or tissue, shielding properties, and particle size, all of which, along with the encapsulate characteristics, can significantly influence the *in-vivo* therapeutic response generated after vaccination or administration. In the case of conventional vaccinations (as opposed to in situ vaccinations), where Ag and adjuvant are a part of the administered formulation, delivering Ag in particles for immune stimulation seems to be important for at least three main reasons: (i) particles are thought to mimic pathogens, due probably to their similar size, and are thus readily phagocytosed by DCs (78, 79); (ii) particles can protect encapsulated Ags from degradation by systemic proteases prior to being phagocytosed (80); (iii) particles can be co-loaded with Ags and one or more adjuvants that can enhance the immunostimulatory power of the DC (80-83); These reasons result in a greater degree of DC activation by particulated Ags when compared to soluble Ags (84).

Biodegradable polymer-based particles can also be used as delivery systems for development of in-situ vaccines. Single injections of therapeutic drug-loaded particles can provide sustained release of the drug to solid tumors and provide a stable pharmacokinetic profile compared to multiple injections of the soluble drug. This potentially decreases the frequency of the drug administration thereby increasing the

chances of patient compliance. Surface modification of biodegradable polymer particles with targeting antibodies can increase the accumulation of particles in the tumor. Currently used drug-antibody conjugates for this purpose are suitable only for the delivery of highly potent drugs to minimize the ratio of drug:antibody molecules in the conjugate. A large number of drug molecules conjugated to one antibody molecule can render the antibody inactive (85-87). Thus, delivering therapeutic drug molecules in particle matrices have the following advantages: (i) particles provide tunable sustained release of encapsulated molecules (88); (ii) particles can prevent or reduce local inflammation at the site of injection caused by soluble dose of therapeutic molecules (89); (iii) polymer particles can provide co-delivery of multiple molecules at the same site; (iv) polymer particles loaded with drug can be surface modified to increase their accumulation in tumors after systemic injection.

Co-delivery of Ag and adjuvant

Possibly one of the most salient properties possessed by polymeric particles, with respect to vaccine applications, is their capacity to co-deliver multiple molecules to the same cell (80, 90). To generate effective protective immune responses against intracellular pathogens and malignant disease a vaccine must ensure both efficient uptake of an Ag by immature DCs, and concomitant stimulation with an adjuvant that drives DC maturation. This can be optimally achieved if adjuvants are co-encapsulated with the Ags within a delivery system. The importance of co-delivery of Ag and adjuvant to the same DC has been elegantly demonstrated to be not only dependent on simultaneous uptake but also on both components being co-delivered in an associated form (80, 91). Many animal and clinical studies have shown improved Ag-specific immune response when Ags are co-delivered with adjuvants (92, 93). Co-encapsulation of Ag and adjuvant within the one particle also avoids uptake by DCs of Ag independently, which under certain conditions may lead to induction of tolerance (94). Aside from co-encapsulation

of the loaded adjuvants it has been shown that certain polymeric particles are capable of exerting a mild to strong adjuvant effects and that can stimulate DC activity (80-82).

<u>Poly(lactic-co-glycolic acid) (PLGA)</u>

PLGA (Figure 4) is a FDA-approved biodegradable and biocompatible synthetic polymer which has been used in humans in the form of sutures (Vicryl®) and for controlled drug delivery for therapeutic drugs (Lupron Depot®). PLGA is prepared by a polycondensation reaction of lactic acid and glycolic acid or by ring opening polymerization of lactide and glycolide dimers (95). PLGA is a biodegradable co-polymer that degrades to lactic acid and glycolic acid which enter the tricarboxylic acid cycle and are metabolized to carbon dioxide and water (88). PLGA is commonly represented as a percent ratio of lactide and glycolide units present in the polymer parent chain. For example, PLGA 75:25 represents 75 % of lactide monomer and 25 % of glycolide. The ratio of lactide to glycolide affects release kinetics of encapsulated molecules, degradation rate of polymer and interaction of the polymer with immune cells (96). When used as vaccine carriers, PLGA particles offer multiple advantages over many other vaccine delivery systems. PLGA is a synthetic polymer which offers high reproducibility during the fabrication process. Ag can be encapsulated in PLGA particles or attached to the particle surface using covalent or ionic bonding or physical adsorption (97). Surface modifications of PLGA particles by conjugating targeting antibodies, biotin, polyethylene glycol (PEG), polyethylenimine (PEI), and mannose have shown to improve the efficacy of vaccines by increasing bioavailability of particles, improving systemic circulation, or by targeting these particles to DCs (97-101). PLGA has been extensively studied as a vaccine delivery system in preclinical settings (75, 102-111). Multiple studies have shown that mice vaccinated with PLGA particles co-encapsulating Ag and CpG invoke stronger Ag-specific IgG (IgG1 and IgG2a) and IFN-γ responses than soluble Ag and CpG (84, 112, 113). Improved immune responses using PLGA

particles co-encapsulating Ag and CpG were also observed over a covalently fused product of Ag and CpG (112). Preclinical studies with PLGA particles have shown stimulation of immune responses where different routes of administration were used. Oral administration of PLGA particles, encapsulating a synthetic peptide PCLUS3-18IIIB (CD4+ T-cell helper epitopes fused with HIV Env CD8+ CTL epitope) with a combination of TLR ligands (macrophage-activating lipopeptide-2, Polyinosinic-polycytidylic acid, and CpG ODN), to mice induces CD8+ T-cells in the intestine providing mucosal immunity against rectal challenge of replication-competent vaccinia virus (114). Intranasal administration of porous PLGA and PLA particles encapsulating hepatitis B surface antigen showed high levels of IFN-γ and IL-2 in spleen homogenates of immunized rats (115). Subcutaneous immunization with PLGA particles encapsulating tumor lysate led to stimulation of CD8+ T-cells and secretion of Th1-type antibodies in mice with melanoma (116). Flexibility in the route of administration offers added advantage in using PLGA particles for development of vaccines.

Polyanhydrides

Biodegradable amphiphilic polyanhydrides (PAs) represent a class of synthetic polymers that are prepared by melt condensation of di-acid monomers in the presence of acetic anhydride and have attractive properties when considered as vaccine vectors (117). PA polymer-based particles degrade through surface erosion which is an added advantage over polyester particles, such as PLGA which undergo bulk degradation. Surface erosion of PA particles ensures sustained release of encapsulated molecules and prevents unwanted degradation of encapsulated molecules which has been otherwise reported to occur in polyester-based particles due to accumulation of acidic byproducts within the particle matrix (118, 119). Additionally, PLGA particles show undesired inflammatory reactions (120) which were not observed with PA particles (121). Microparticles prepared using 1,8-bis(p-carboxyphenoxy)-3,6-dioxaoctane (CPTEG) and 1,6-bis(p-

carboxyphenoxy) hexane (CPH) copolymers (Figure 5) have been shown to be capable of stabilizing the structural integrity of encapsulated Ag and also providing a sustained protein release (117, 122). Various PA polymers have shown strong adjuvant effects that serve as an added advantage for using PAs as a vaccine carrier for stimulating DC maturation, potentially negating the need for co-encapsulation of other adjuvants. The release kinetics, Ag retention and adjuvant effect of polymer particles can be tailored by changing the backbone of the polymer (123). Empty poly(methyl vinyl ether-co-maleic anhydride) (PVM-MA) particles have been reported to act as an agonist to various TLR receptors and consequently can induce upregulation of CD86 in DCs followed by activation *in-vivo* of OVA-specific CD8+ T-cell responses when delivered with OVA (124). In a different study, intradermal vaccination of PVM-MA microparticles encapsulating peanut extract to mice have also been shown to induce high levels of IFN-ɣ when spleens from the vaccinated mice were re-stimulated *in-vitro* confirming the establishment of cell based immunity (125). In a separate study, involving informatics analysis, it was shown that nanoparticles prepared from 50:50 CPTEG:CPH possessed characteristics that resembled those of intracellular pathogens such as *E. coli* and *Y. pestis* (81). These particles promoted surface expression of MHC class I, MHC class II, CD86 and CD40 on DCs (rendering them highly immunopotent), demonstrating lipopolysaccharide (LPS)-like immunostimulatory properties. At the same time, these nanoparticles did not induce an inflammatory cytokine response often associated with LPS exhibiting its ability to support CTL immunity (121). It has been suggested that this adjuvant activity of PVM-MA particles is due to the adsorption of complement protein to the particles which can attract more DCs at the site of delivery (126). Single intranasal vaccination of 50:50 CPTEG:CPH particles encapsulating a *Y. pestis* fusion protein/Ag (delivered with soluble Ag) was capable of generating long term protection against lethal *Y. pestis* challenge as well as inducing high pathogen-specific antibody titers with high

avidity (127). Many of the traits exhibited by 50:50 CPTEG:CPH particles implicate them as strong candidates for vaccine formulations.

Hypothesis

In this research it is proposed that:

1. A) Biodegradable particles co-delivering CpG with model tumor antigen, OVA, (prophylactic vaccine) can protect against challenge with OVA-expressing tumor cells.

    B) Biodegradable particles co-delivering CpG with doxorubicin (in situ therapeutic vaccine) can enhance survival of tumor bearing mice.

2. The size of PLGA particle vaccines affects the magnitude and type of antigen-specific immune responses stimulated in mice.

Rationale

A novel approach to prevent diseases such as cancer and allergies is to develop disease-specific vaccines that generate protective or therapeutic immune responses against the disease. Conventionally, vaccines carry Ag(s) specifically expressed by the target pathogen or disease and an adjuvant that promotes Ag-specific immune stimulation. Multiple reports have shown that co-delivery of Ag and adjuvant to the same DC is key for optimal stimulation of robust Ag-specific immunity that results in the generation of immune memory to prevent recurrences (128). One method to ensure co-delivery of Ag with adjuvant to the same DC is through the use of biodegradable polymer particles as vectors. Polymer particles mimic microbial infection and are readily taken up by DCs to generate robust Ag specific immune responses. Size of these particles can affect the magnitude of particle uptake by DCs and type of immune response developed. Larger sized polymer particle ensures efficient loading of Ag and adjuvant in the particles and sustained release of the encapsulated molecules. On the other hand, small sized

particles mimic the size of naturally occurring infectious microbes. Thus, it is important to explore the relationship of particles size with the degree and type of immune response stimulated by these particles.

In case of allergies, activation of immune system against environmental allergens causes stimulation of inflammatory Th2 responses that can lead to asthma. Activation of the Th1 dominant immunity against allergens using allergen/Ag carrying biodegradable particle vaccines can negatively regulate the activation of Th2 responses that prevent asthma and lung damage associated with exposures to allergens. Steering Th response to Th1 or Th2 is dependent on the nature of the vaccine. The size of biodegradable particle vaccines and presence of an adjuvant can play an important role in the development of Th1 dominant response and prevention of asthma induced by allergen exposures.

In the case of patients suffering from cancer, activation of immune responses against TAAs can function as an adjunctive therapy to conventional treatments to potentially promote complete eradication of metastatic lesions and prevent recurrences. This can be achieved by activating immune response against dying cancer cells from chemotherapy.

While certain chemotherapeutic drugs, such as Dox, induce immunological death of tumor cells and the presence of an adjuvant such as a TLR agonist, can activate DCs that have phagocytosed TAAs released from the dying tumor cells. Administration of chemotherapeutic drugs and adjuvants in biodegradable polymer-based microparticles can ensure continuous sustained delivery of these molecules within the tumor. Subsequently, these DCs travel to the draining lymph node where they can trigger the activation of tumor-specific CTLs.

Thus, for this thesis research I propose the following specific aims:

1. To characterize the anti-tumor immune response in mice vaccinated with Ag and CpG-loaded polyanhydride particles.

2. To develop doxorubicin-loaded, and CpG-loaded, PLGA particles and evaluate their *in-vivo* efficacy in enhancing survival of tumor bearing mice.

3. To investigate the relationship between PLGA particle size and immunopotency in an *in-vivo* vaccination study.

4. To characterize the effect of particle size and presence of CpG in stimulating a protective response against a house dust mite allergen.
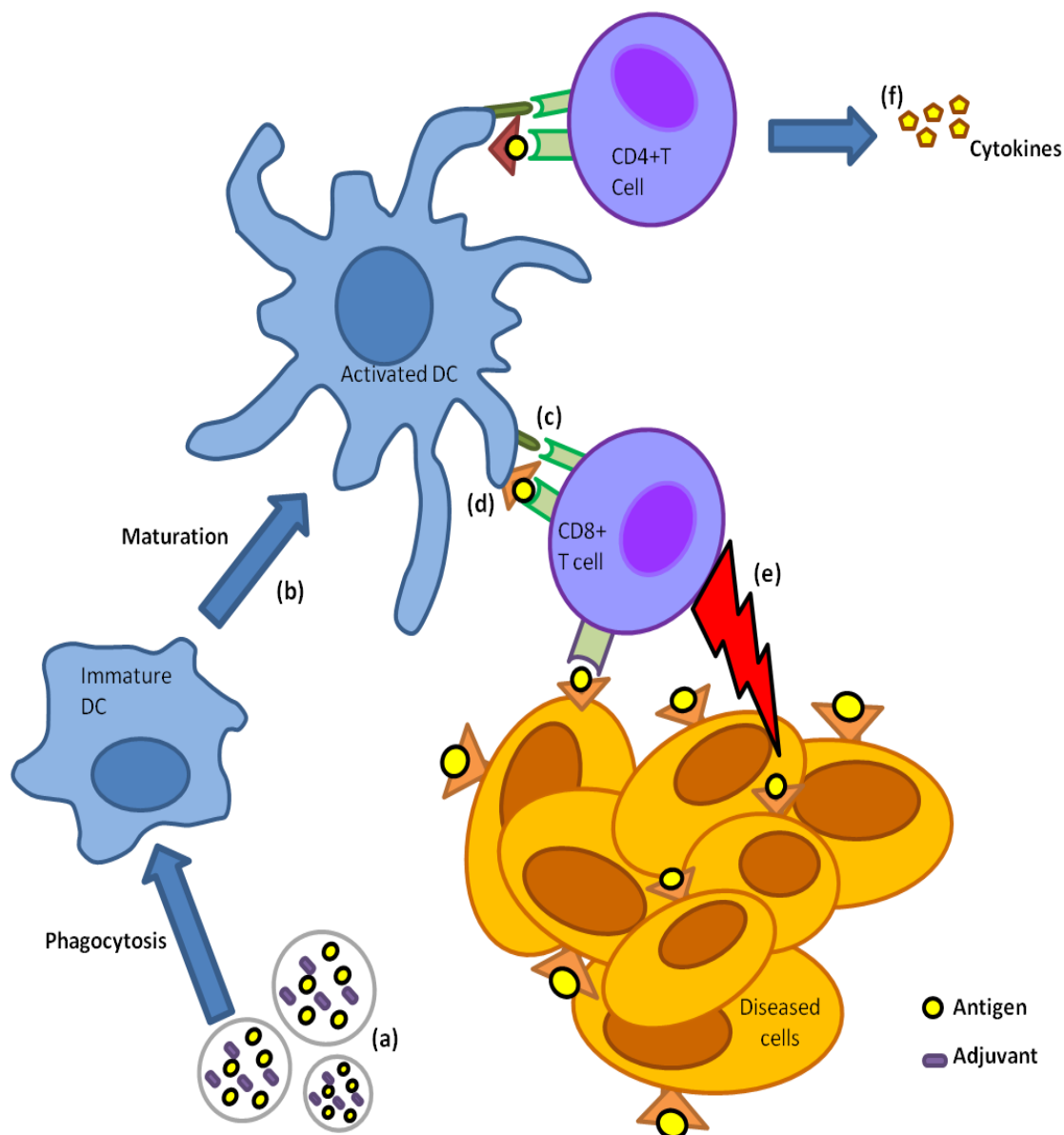
Figure 1: Biodegradable particles co-encapsulating an Ag and an adjuvant (a) are phagocytosed by dendritic cells (DCs). DC due to internalization of a microbial adjuvant activates into a mature DC (b) that are characterized by expression of CD80/CD86 co-stimulatory molecules on its surface (c) along with presentation of Ag (d). Mature DC travel to lymph node and where it prime CD8+ T-cells and CD4+ T-cells. In the presence of co-stimulatory signals, CD8+ T-cells gets activated to cytotoxic T-lymphocytes which travels to peripheral blood eradicating Ag expressing cancerous cells or those infected with intracellular pathogens (e). Activated CD4+ T-cells secretes cytokines (f) which helps in the proliferation of CD8+ T-cells.
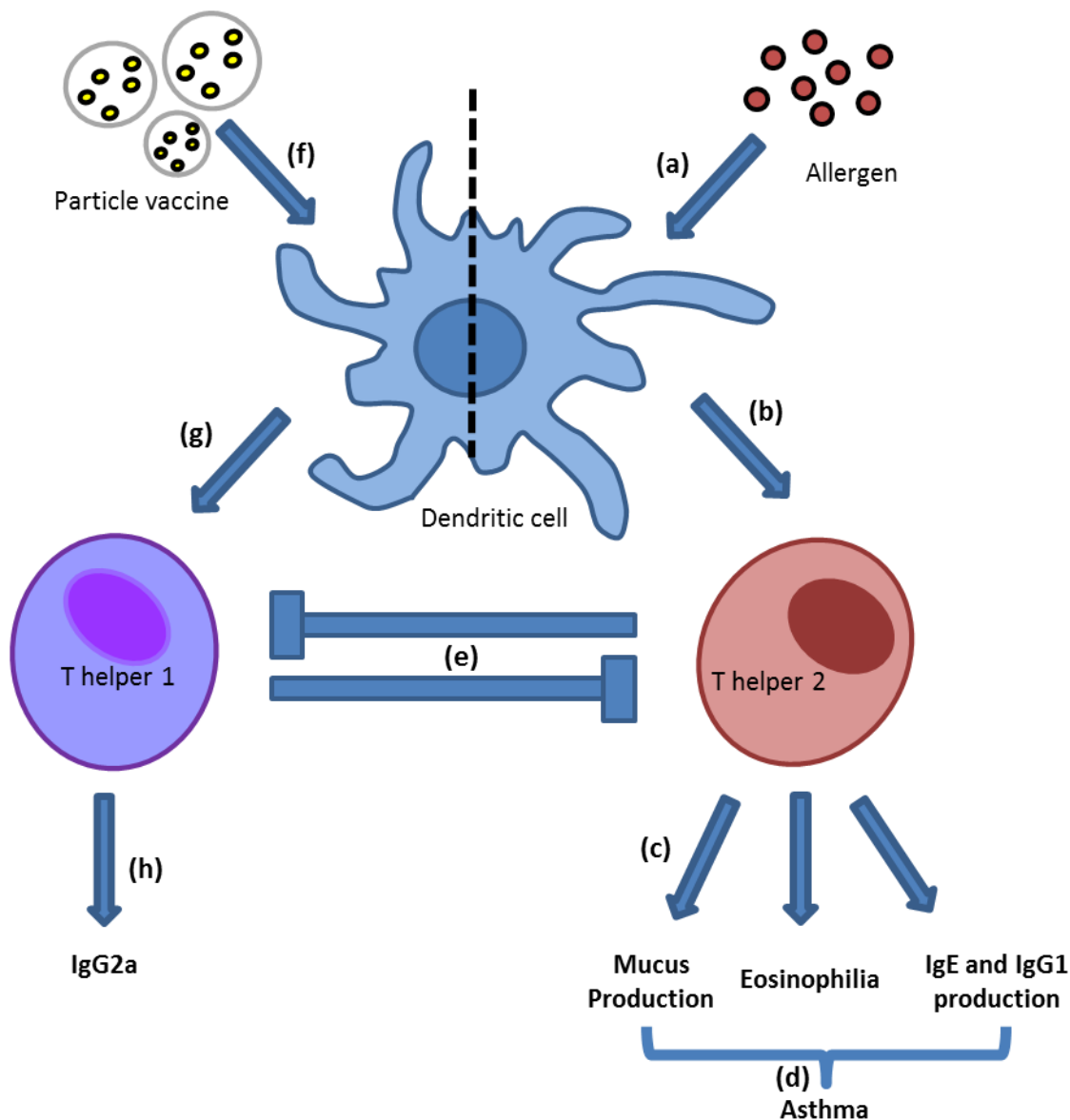
Figure 2 : Exposure to allergen present in the environment (a) are internalized by dendritic cells (DCs). DC after allergen internalization leads to (b) activation of T-helper 2 cells that promote (c) secretion of IgE antibodies and mucus production. Chronic exposure to these allergens can cause eosinophilia. (d) Combination of these inflammatory responses can cause tissue remodeling leading to asthma. (e) Multiple evidences in literature suggest that T-helper 1 (Th1) and T-helper 2 (Th2) response are counter inhibitory pathways and stimulation of Th1 response can down-regulate the activation of Th2 mediated inflammation reaction upon allergen exposures. When biodegradable particles vaccine carrying Ag and adjuvant (f) are internalized by DC, (g) they activate Ag specific Th1 dominant immune response which is (h) characterized by secretion of IgG2a antibodies.
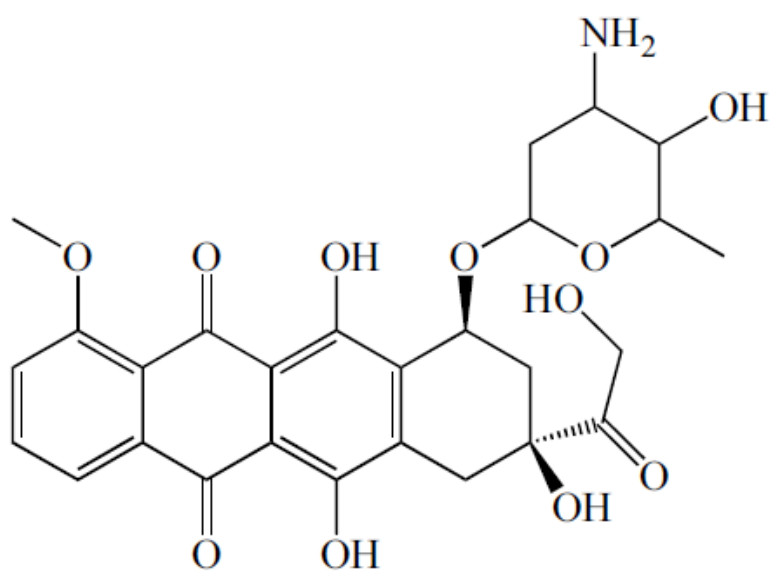
Figure 3 : Chemical structure of doxorubicin (68).
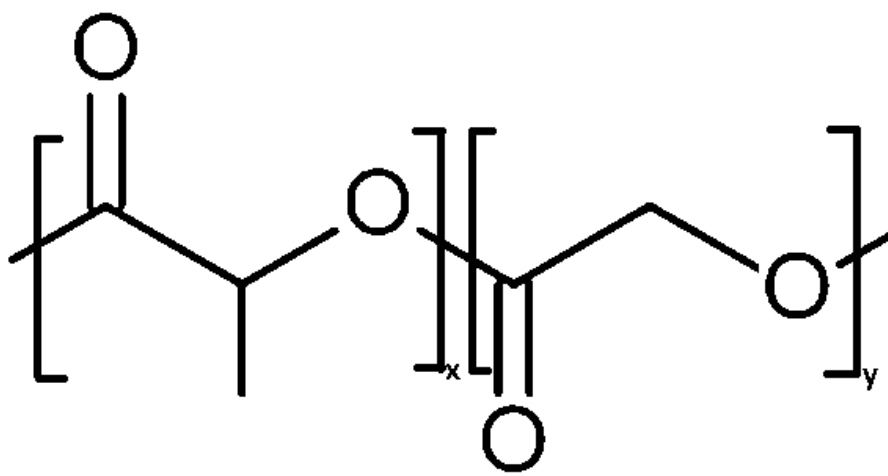
Figure 4 : Chemical structure of poly(lactic-co-glycolic acid) polymer.
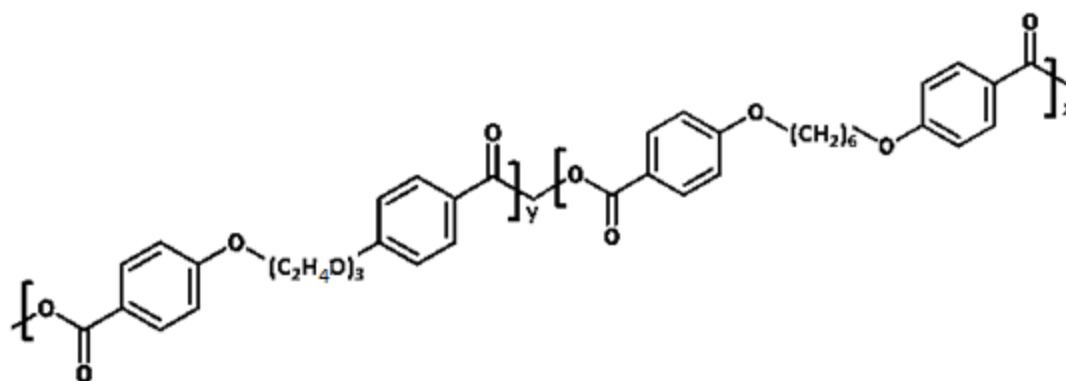
Figure 5: Chemical structure of poly(1,8-bis(*p*-carboxyphenoxy)-3,6-dioxaoctane):(1,6-bis(*p*-carboxyphenoxy) hexane) polymer

CHAPTER 2: A PROPHYLACTIC ANTI-CANCER VACCINE:
ANTIGEN-LOADED POLYANHYDRIDE MICROPARTICLES

Introduction

Cancer is the second most lethal disease (second only to heart disease) in the United States, being responsible for one quarter of human fatalities. Recent data compiled by the American Cancer Society and National Cancer Institute suggests that one in three woman and one in two men in the United States will develop cancer in their lifetime (129). Current anti-cancer therapeutic treatments do not ensure complete eradication of tumors. Also, toxic side effects associated with anti-cancer therapies necessitates the development of vaccines that can establish a protective immunity against cancer. The discovery of tumor-associated antigens (TAAs) as an identification marker of tumor cells (130) and the discovery of the mechanism of dendritic cell (DC)-orchestrated cellular immune responses (131) have made significant contribution to the field of cancer vaccine research. As discussed in Chapter 1, administration of TAA with immune adjuvants to induce DC maturation and resultant cellular immune responses (132) has received significant attention in the development of an effective cancer vaccine. Continual research has been performed to develop delivery systems for TAA and adjuvant to stimulate a cancer specific immune response (133).

The delivery of cancer vaccines through the use of nano- and micro-particle based vectors is showing promise in both clinical and preclinical settings (76). Ideally such vectors should possess a number of favorable traits that include: biocompatibility; capability to co-deliver TAA and adjuvants to DC; possess adjuvant properties; show long shelf life and inexpensive manufacturing procedures (77, 80, 112). In this study amphiphilic polyanhydride microparticles based on 1,8-bis(*p*-carboxyphenoxy)-3,6-dioxaoctane (CPTEG) and 1,6-bis(*p*-carboxyphenoxy) hexane (CPH) (Figure 5) were investigated for their potential as cancer vaccine delivery vehicles CPTEG:CPH (50:50)

microparticles were used, which have previously shown adjuvant properties in generating robust antigen-specific humoral responses and preferential uptake and activation of DC and macrophages (81, 134-136). In addition, CPTEG:CPH copolymers have been shown to be non-toxic, stabilizing to antigens, and biodegradable with 50:50 CPTEG:CPH particles providing a burst release of 10 to 30% of the model TAA, ovalbumin (OVA) followed by sustained release for 30 days (117, 134, 137). Thus, these polyanhydride vectors possess many of the traits desirable for a cancer vaccine vehicle. CpG, an adjuvant capable of triggering DC-mediated Th1 responses (54), was co-encapsulated into CPTEG:CPH particles in an attempt to enhance cellular immune responses. CPTEG:CPH microparticles encapsulating OVA and the synthetic TLR-9 agonist, CpG, are an attractive vaccine that can potentially be used for the stimulation of anti-cancer immunity. In this study the potential of this vaccine in a prophylactic mouse tumor model was assessed. Specific aims for this study are:

1. To develop OVA and CpG encapsulated 50:50 CPTEG:CPH microparticles
2. To evaluate the anti-cancer potential of 50:50 CPTEG:CPH microparticles encapsulating OVA and CpG in a prophylactic mouse tumor model.

Materials and Methods

Fabrication of microparticles loaded with OVA and CpG

50:50 CPTEG:CPH polymer (MW: 8283 with polydispesity of 1.6; glass transition temperature 8 ˚C) was a kind gift from Dr. Balaji Narasimhan, Department of Chemical and Biological Engineering, Iowa State University. Microparticles were prepared using a double emulsion solvent evaporation method derived from Intra et al. (108). Three mg of purified endotoxin-free, chicken egg white ovalbumin (OVA) (Sigma, St Louis, MO) and 3 mg of (or unless specified) endotoxin-free CpG (Integrated DNA Technologies, Coralville, IA) were dissolved in 100 µL of 1% poly(vinyl alcohol) (PVA) (Mowiol®; Sigma, Allentown, PA) solution. This solution was sonicated for 30 seconds

on a power setting of 10, (Sonic Dismembrator Model 100, Fisher Scientific, Pittsburgh, PA) in 1.5 mL of dichloromethane (DCM) containing 200 mg of 50:50 CPTEG:CPH copolymer. This primary emulsion was then sonicated into 8 mL of 1% PVA solution to generate a secondary emulsion, which was then added to 22 mL of 1% PVA solution. Secondary emulsions were stirred in a fume hood for 2 h to allow evaporation of DCM. The resultant suspension of microparticles was collected in a 50 mL centrifugation tube and centrifuged at 2880 xg for 5 min. Pellets obtained were resuspended in 30 mL of deionized water and centrifuged again at 2880 xg for 5 minutes using an Eppendorf centrifuge (Centifuge 5804 R; Eppendorf, Westbury, NY). This step was repeated one more time. Pellets obtained after the last centrifugation were resuspended in 3 mL of deionized water. The suspension of particles was frozen at -20 ˚C for 5 hours. This suspension was lyophilized using FreeZone 4.5 (Labconco Corporation, Kansas City, MO) at -53 ˚C collector temperature and 0.08 mBar pressure. Particles were stored in sealed containers at -20 ˚C until use.

Characterization of microparticles

Microparticles were characterized for their size and charge using a Zetasizer Nano ZS dynamic laser light scattering instrument (Malvern, Southborough, MA). Surface morphology of particles was studied using a Hitachi S-4800 SEM (Hitachi High-Technologies, Ontario, Canada).

Particle size and zeta potential

To measure size and zeta potential, suspensions of lyophilized particles were prepared in deionized water at the concentration of 1 mg/mL. One mL of particle suspension was added to a standard 12 mm square polystyrene cuvette (DTS0012, Malvern, Southborough, MA) and particle size was measured at a backscattering angle of 173°. To measure zeta potential, 1 mL of particle suspension was added to a disposable

folded capillary cell (DTS1070, Malvern, Southborough, MA) and the zeta potential was measured in the automated mode.

<u>Scanning electron microscopy (SEM)</u>

The surface morphology and shape of microparticles was examined using SEM. A suspension of lyophilized particles (1 mg/mL in deionized water) was plated onto a silicon wafer mounted on a SEM stub using a double stick carbon tape. The suspension was left to dry in air for 1 hour. After drying, the silicon wafer was coated with gold-palladium by an argon beam K550 sputter coater (Emitech Ltd., Kent, England) for 2 to 3 minutes. Images were captured using a Hitachi S-4800 SEM (Hitachi High-Technologies, Ontario, Canada) at 8 kV accelerating voltage.

<div align="center">Quantification of OVA and CpG encapsulated in PLGA
particles</div>

To estimate the loading of OVA and CpG, 20 mg of microparticles from each batch were incubated with 500 μL of 0.2 N NaOH for approximately 12 h at room temperature (RT) or until microparticles had fully degraded. This solution was then neutralized using 1N HCl to approximately pH 7. Amounts of OVA and CpG in neutralized samples were quantified as described in the next sections. Loading of OVA and CpG in CPTEG:CPH microparticles was calculated using equation 1. Percentage encapsulation efficiency (% EE) of the fabrication process was calculated as described in equation 2.

Equation 1 : Loading = [Calculated conc. (μg/mL) × Volume (mL)]/ weight of particles (mg)

Equation 2 : % EE = [Weight of particles (mg) × Loading (μg/mg)×100]/Initial weight of drug (μg)

where, Loading = µg OVA or CpG encapsulated per mg of particles, Calculated conc. = Concentration of OVA or CpG estimated in neutralized samples (µg/mL), and Volume = volume of OVA or CpG solution (mL).

Quantification of OVA

For quantification of OVA the micro BCA Protein Assay Kit (Thermo Scientific, Wilmington, DE) was used according to manufacturer's standard protocol. In a 96-well plate, 100 µL of OVA solutions of known concentration (100 µg/mL to 5 µg/mL) and samples of OVA were incubated with 100 µL of working reagent at 37 ˚C for 2 hours. Protein present in the samples reduces Cu^{+2} present in the working reagent to Cu^{+1}. Reduced cuprous ion chelates with 2 molecules of bicinchoninic acid (BCA) present in the working regent to form a purple colored product. The absorbance of this product was measured at 562 nm using a SpectraMax® Plus384 microplate reader (Molecular Devices, Sunnyvale, CA). A standard curve generated from known concentrations of OVA was used to determine OVA concentrations in samples from loading and release studies.

Quantification of CpG

To quantify CpG concentrations, Quant-iT™ OliGreen® ssDNA Assay Kit (Invitrogen, Carlsbad, CA) was used according to the manufacturer's protocol. In a 96-well plate 100 µL of a working reagent was added to 100 µL of standard CpG solutions of different concentrations (16 µg/mL to 0.2 µg/mL) and samples with unknown CpG concentrations. The fluorophore present in the working reagent becomes fluorescent upon binding to single stranded DNA. The plate was incubated at RT for five minutes in the dark. Fluorescence was measured at $\lambda_{excitation}$ 444 nm and $\lambda_{emission}$ 520 nm using SpectraMax® M5 multi-mode microplate reader (Molecular Devices, Sunnyvale, CA). A standard curve generated from known concentrations of CpG was used to determine the concentrations of CpG in samples from loading and release studies.

Prophylactic murine tumor model

The *in-vivo* efficacy of CPTEG:CPH polymer particles encapsulating OVA and CpG were evaluated using a prophylactic murine tumor model developed and optimized by Dr. Sean Geary and Dr. Caitlin Lemke of the Division of Pharmaceutics, College of Pharmacy, University of Iowa (personal communication). Eight to twelve week-old male wild type C57BL/6 mice (Jackson Laboratory, Bar Harbor, Maine) (n = 4/group) were treated with intraperitoneal injections of the following six formulations:

1.   CPTEG:CPH/OVA CpG: OVA and CpG encapsulated in 50:50 CPTEG:CPH microparticles;

2.   CPTEG:CPH/OVA: OVA encapsulated in 50:50 CPTEG:CPH microparticles;

3.   CPTEG:CPH/OVA + soluble CpG: OVA encapsulated in 50:50 CPTEG:CPH microparticles with soluble CpG;

4.   Blank CPTEG:CPH: microparticles equivalent to the dose of OVA particles;

5.   Soluble OVA and CpG: soluble dose of OVA and CpG;

6.   Naïve: untreated mice.

For mice treated with soluble CpG, the particles or solution of OVA was admixed with CpG solution prior to injections. Each mouse was primed on day 0 and similarly boosted on day 7 with the indicated treatments. Doses of 100 µg of OVA and 50 µg of CpG per mouse were consistently used as applicable. On day 14 and day 21, OVA-specific CD8+T-lymphocyte levels were determined from peripheral blood harvested by submandibular bleeds (see section "Estimation of OVA-specific cytotoxic T-cell frequencies in peripheral blood"). On day 28 and day 35, OVA- specific IgG2a and IgG1 antibody titers were measured in serum harvested by submandibular bleeds (see section "Estimation of anti-OVA antibodies in peripheral blood using the enzyme-linked immuno-sorbent assay (ELISA)"). On day 35, mice were subcutaneously challenged with

2 x 10^6 OVA-expressing E.G7 cells (American Type Culture Collection, Manassas, VA) and tumor volumes were monitored over time using equation 3. All animal experiments were carried out in accordance with current institutional guidelines for the care and use of experimental animals.

Equation 3 : Tumor Volume = π/6 x [Diameter 1(mm) × Diameter 2 (mm) × Height (mm)] (138)

where, diameters and height are dimensions of tumor measured using a Vernier caliper.

Estimation of OVA-specific cytotoxic T-cell frequencies in peripheral blood

The frequency of OVA-specific CD8+ T-lymphocytes was determined by tetramer staining, as previously described (44). This protocol was developed and optimized by Dr. Sean Geary and Dr. Caitlin Lemke of the Division of Pharmaceutics, College of Pharmacy, University of Iowa (personal communication). The tetramer used was the H-2K^b SIINFEKL Class I iTAg^{TM} MHC Tetramer (K^b-OVA$_{257}$) labeled with PE (Beckman Coulter, Fullerton, CA). Surface CD8 and CD3 were stained with anti-CD8-FITC and anti-CD3-PE-Cy5 mAbs (eBioscience, San Diego, CA), respectively, to differentiate T-cells from the rest of the leukocyte population. One hundred and fifty – two hundred μL of blood was obtained by submandibular bleeding and added to 5 mL of ammonium chloride potassium (ACK) buffer (150 mM NH$_4$Cl, 10 mM KHCO$_3$, 0.1 mM Na$_2$EDTA in deionized water, store at 4 °C) to lyse red blood cells. After 5 minutes of incubation, peripheral blood lymphocytes were washed two times with 200 μL of PBS containing 2 % (v/v) fetal bovine serum (FBS) and collected by centrifugation at 220 xg. Pellets were re-suspended in 200 μL of cold FACS buffer (PBS with 5 % v/v FBS and 0.1 % w/v sodium azide) and transferred to U-bottom 96-well plate. All subsequent steps were carried out on ice. Cells were centrifuged at 230 xg for 7 minutes at 4 °C and

supernatant was aspirated by one quick flick into the sink. Pellets were re-suspended in 50 µL of 5 µg/mL Fc receptor block (anti-mouse CD 16/32; eBioscience, San Diego, CA) solution prepared in FACS buffer. After 15 minutes of incubation on ice 50 µL of tetramer solution (diluted to 1:100 using FACS buffer) was added to each well, mixed and incubated for 30 minutes. This was followed by addition of 100 µL of CD8 and CD3 antibodies diluted in FACS buffer to 10 µg/mL. After 20 minutes of incubation, cells were centrifuged at 230 xg for 7 minutes at 4 °C and supernatant was aspirated by one quick flick into the sink. Cells were re-suspended in 200 µL of FACS buffer and centrifuged again for washing. This step was repeated twice for removal of the unbound antibodies. Cells were then fixed and permeabilized using BD Cytofix/Cytoperm™ Fixation/Permeabilization Solution Kit with BD GolgiPlug™ (BD Biosciences, San Diego, CA). According to manufacturer's protocol, cells were re-suspended in 100 µL cytofix solution. After 10 minutes of incubation 100 µL of 1X permwash-mix was added to each well. This was followed by centrifugation of cells at 660 xg for 15 minutes at 4 °C. After aspiration of supernatant, cells were re-suspended in 200 µL FACS buffer and samples were acquired using a FACScan flow cytometer (Becton Dickinson, NJ) and analyzed with FlowJo software (Tree Star Software, San Carlos, CA).

Estimation of anti-OVA antibodies in peripheral blood

using the enzyme-linked immuno-sorbent assay (ELISA)

To estimate levels of the OVA-specific IgG1 and IgG2a antibodies in peripheral blood, serum samples were analyzed using ELISA developed by Dr. Sean Geary and Dr. Caitlin Lemke of the Division of Pharmaceutics, College of Pharmacy, University of Iowa (personal communication). Approximately 200 µL of peripheral blood were collected into 1.5 mL eppendorf tubes and incubated at RT for 1 hour. After the incubation, blood clots were removed from eppendorf tubes and samples were

centrifuged at 3000 xg for 10 minutes at 4°C. Supernatants containing serum were collected and stored in -20 °C until used for analysis.

ELISA microwell plates (Corning, Lowell, MA) were incubated overnight (or longer) at 4°C with 250 µL of 5 µg/mL of OVA solution in PBS to coat the plates with OVA. Plates were then washed three times with 150 µL of PBS-Tween buffer (0.05% v/v Tween-20 in PBS). Five µL of serum samples were diluted to 250 µL in PBS-Tween buffer and added to 96-well plates coated with OVA. Serial half-dilutions of serum samples were prepared in different wells using PBS-Tween buffer. Dilutions of known concentration of anti-OVA IgG2a were also prepared as the positive control for the experiment. The tray was then incubated overnight at RT. Plates were then washed 3 times with 150 µL of PBS-Tween buffer. This was followed by addition of 100 µL anti-IgG2a antibody linked to alkaline phosphatase (Southern Biotech, Birmingham, AL). After 3 to 4 hours of incubation, the plates were washed three times with 150 µL of PBS-Tween buffer. This was followed by addition of 100 µL of SIGMAFAST™ p-Nitrophenyl phosphate solution (Sigma, Milwaukee, WI) in the dark. Absorbance was measured after 2 hours at 405 nm using a SpectraMax® Plus384 microplate reader (Molecular Devices LLC,Sunnyvale, California). Samples titers were calculated as the dilution factor of serum that yields absorbance 3 times higher than blank controls. A similar procedure was employed to estimate levels of anti-OVA IgG1 antibodies where known concentration of anti-OVA IgG1 antibody was used to prepare standard curve. Samples were treated with anti-IgG1 antibody linked to alkaline phosphatase (Southern Biotech, Birmingham, AL) for the measurement of IgG1 antibodies in serum samples.

Statistical Analysis

Groups were compared by one-way analysis of variance (ANOVA) followed by Tukey post-hoc test to determine significant differences ($p < 0.05$) in the mean values between pairs of treatment groups. . Survival curves of treatment groups follow a right

skewed distribution. Thus, analysis of survival curves was performed using a non-parametric log-rank (Mantel-Cox) test. All statistical analysis was performed using Prism 5 (GraphPad Prism, La Jolla, CA).

Results

Fabrication and characterization of 50:50 CPTEG:CPH microparticles

The 50:50 CPTEG:CPH microparticles were prepared using a double emulsion solvent evaporation process as described in materials and methods. When OVA alone was used, encapsulation efficiencies of 78.6 % were obtained, yielding 11.8 µg of OVA encapsulated per mg of microparticles (Table 1). However, for encapsulation of CpG, high concentrations of CpG in the water phase led to formation of aggregates during the preparation of the primary emulsion (Figure 6). Destabilization of the primary emulsion was curtailed by decreasing the CpG:polymer (w/w) ratio from 0.015 to 0.001. This alteration did not affect microparticle size but resulted in low loading of CpG and OVA. The possibility that the presence of nucleic acid is responsible for the destabilization of the primary emulsion was confirmed by the observation that microparticle aggregation also occurred when herring sperm DNA oligonucleotide was used instead of CpG. When CpG and OVA were co-encapsulated, the loading efficiency of OVA was only 12 % and CpG was 21 % giving 1.8 µg OVA/mg of particles and 0.2 µg CpG/mg of particles. The mean diameter of all microparticle preparations was between 1 to 3 µm. The zeta potential of blank microparticles was -0.63 mV, which did not change significantly upon encapsulation of OVA and CpG into the microparticles (Table 2). SEM revealed that various microparticle preparations possessed spherical shape and smooth morphology (Figure 7).

Magnitude of antigen-specific cytotoxic T-lymphocytes in

vaccinated mice

Male C57BL/6 mice were vaccinated with CPTEG:CPH microparticles encapsulating OVA plus/minus soluble or co-encapsulated CpG. Each mouse was primed on day 0 and boosted on day 7 with an intraperitoneal injection of an equivalent dose of 100 µg of OVA and 50 µg of CpG except in the CPTEG:CPH/OVA particles where each mouse received 100 µg of OVA and 11 µg of CpG. OVA-specific T-lymphocytes in the peripheral blood from mice on days 14 and 20 were evaluated using a tetramer binding assay. As shown in Figure 8, no significant changes were observed in the vaccinated mice with the exception of the group vaccinated with CPTEG:CPH/OVA, which displayed the greatest levels of OVA-specific T-lymphocytes on both days. In addition, on day 20, the levels of OVA-specific T-lymphocytes in the group vaccinated with CPTEG:CPH/OVA were found to be significantly ($p < 0.05$) increased as compared to naïve and blank CPTEG:CPH particles (Figure 8).

Vaccination of mice with CPTEG:CPH microparticles

promotes high levels of IgG1 antibody production

Male C57BL/6 mice were vaccinated with varying preparations of OVA and/or CpG encapsulated in CPTEG:CPH particles as described in section "Prophylactic murine tumor model". On day 28 after the priming vaccination, serum titers of OVA- specific IgG1 and IgG2a antibodies were measured using ELISA. Results revealed that mice receiving CPTEG:CPH/OVA CpG generated significantly ($p < 0.05$) higher OVA-specific antibody responses (both IgG1 and IgG2a) than all other formulations (Figure 8). This response was further increased on Day 35. All vaccinated mice show higher titers for IgG1 antibodies suggesting the activation of Th2 dominant immune response.

Tumor protection studies

Thirty-five days after the initial boost with the various microparticle formulations, C57BL/6 mice were challenged with a lethal dose of an OVA-expressing tumor cell line (E.G7). Tumor volumes were monitored over the subsequent 28 days and revealed all formulations to have significantly enhanced protective effects when comparing tumor volumes on day 14 to untreated (naïve) mice and mice treated with blank microparticles (Figure 10). Analysis of survival revealed that mice treated with CPTEG:CPH/OVA or CPTEG:CPH/OVA + soluble CpG had significantly ($p < 0.05$) improved survival over all other groups (Figure 11 (B)) on day 14. At the end of the study, 75 % of mice from CPTEG:CPH/OVA and 50 % of the mice survived from group treated with CPTEG:CPH/OVA + soluble CpG were surviving and one mouse from CPTEG:CPH/OVA group showed complete rejection of tumor. At the end of 30 days, the median survival of the CPTEG:CPH/OVA group was undefined and CPTEG:CPH/OVA + soluble CpG was 27.5 days.

Discussion

To date, studies with biodegradable CPTEG:CPH polyanhydride particles have involved the encapsulation of pathogen-derived antigens, which have subsequently demonstrated protection against infectious pathogens such as *Clostridium tetani* (139) and *Yersinia pestis* (127). However, the potential for the amphiphilic CPTEG:CPH microparticles, specifically, to be used as cancer vaccines has yet to be explored. In this study, the cancer vaccine potential of CPTEG:CPH microparticles encapsulating a model TAA, OVA, was investigated. Development of cancer vaccines are often challenging since there is a need to invoke a cell-mediated immune response instead of, or as well as, a humoral response. Delivery of antigen in particles, rather than in free form, is required for the successful generation of an adaptive tumor-specific cytotoxic T-lymphocyte (CTL) response capable of eradicating the primary tumor and, more importantly, its

metastatic lesions (140). If a particulated cancer vaccine delivery system is to be successful it must fulfill a number of requirements (76), including: (i) protection of the TAA; (ii) efficient delivery of TAA and adjuvant signals to dendritic cells; and (iii) concomitant stimulation of dendritic cells leading to subsequent stimulation of an immune response capable of eradicating the tumor (76). Microparticles made from CPTEG:CPH have shown to stabilize encapsulated antigens (141, 142) and their ability to activate dendritic cells is comparable to that of LPS, a TLR 4 agonist (117, 127, 143). It has been speculated that the structural similarity of 50:50 CPTEG:CPH particulates to LPS (144) leads to effective immune activation resulting in long term antibody production (145). Thus, 50:50 CPTEG:CPH particles fulfill many of the traits required for a potentially successful cancer vaccine vector.

Amphiphilic CPTEG:CPH particles have previously shown high encapsulation efficiency of different model proteins using various particle preparation methods (117, 127). In this study, OVA was shown to be efficiently encapsulated in CPTEG:CPH microparticles using a double emulsion solvent evaporation method. However, co-encapsulation of CpG and OVA into CPTEG:CPH microparticles (CPTEG:CPH/OVA CpG) was found to be much less efficient. High concentrations of CpG in the water phase resulted in precipitation of CPTEG:CPH co-polymers during the preparation of the primary emulsion. Decreasing the CpG concentration prevented this aggregation but the CPTEG:CPH/OVA CpG particles showed reduced loading of CpG as well as OVA with less CpG. Further studies are required to characterize the CPTEG:CPH polymer and CpG precipitate. All particle formulations were hygroscopic and required in a dessicator at -20 ºC. Also, unlike PLGA particles, CPTEG:CPH microparticles stored at -20 ºC are difficult to resuspend after 3 weeks of storage. This is due to the formation of aggregates, possibly due to the hygroscopic nature of the CPTEG:CPH polyanhydride co-polymer. The interaction of CPTEG:CPH co-polymer with drug molecules in combination with its

hygroscopic nature are two major challenges in developing CPTEG:CPH microparticles as a successful vaccine delivery system.

It was found that certain CPTEG:CPH-based formulations could provide significant, albeit incomplete, prophylactic protection against tumor-challenge. Mice vaccinated with CPTEG:CPH/OVA afforded the greatest protection. What was particularly unexpected was that these mice showed both increased survival and significantly decreased tumor volumes (day 14) over mice vaccinated with CPTEG:CPH/OVA CpG. It has been shown previously that a higher proportion of IgG2a antibodies relative to IgG1 antibodies potentially indicates the production of antigen-specific cytotoxic T-cells (146), which is key to eradicating cancer (147). However, the ratios of IgG2a:IgG1 antibodies shown here were low (< 0.25) for all particulate treatment groups, suggesting Th2-biased immune response. The observed Th2 response by the CPTEG:CPH/OVA formulation was not surprising since CPTEG:CPH particles encapsulating different antigens have been previously shown to generate Th2 responses. However, co-encapsulation of CpG in CPTEG:CPH/OVA CpG particles failed to increase the IgG2a:IgG1 ratio. This was unexpected since CpG has been previously reported to promote Th1 immune responses (148, 149). One possible explanation for this observation is that the adjuvant properties of 50:50 CPTEG:CPH particles resulted in abrogation of the normal effect of CpG. In other words, 50:50 CPTEG:CPH particles have been shown previously to possess strong adjuvant properties (134) and therefore, when added in relatively high doses compared to the CpG, could result in a phenotypic dominance. It has also been reported that LPS can abrogate effects of CpG (150) and, since 50:50 CPTEG:CPH particles are LPS-like in their effect on dendritic cell activation (81), it is possible that 50:50 CPTEG:CPH particles have a similar dominating influence over dendritic cells and therefore subsequent immune responses. The OVA-specific CTL responses were marginally, but significantly, increased in mice vaccinated with CPTEG:CPH/OVA whilst none of the other treatment groups displayed significant

increases relative to the naïve group. This may explain why the CPTEG:CPH/OVA group exhibited the greatest tumor protection and improved survival ($p < 0.05$). Notably, one mouse from the CPTEG:CPH/OVA group was sacrificed due to tumor burden during a prolonged period of the study. One mouse from the same group successfully rejected the tumor showing no traces of tumor growth, resulting in an undefined median survival for that group. These promising results further support development of the CPTEG:CPH polymeric carriers as an antigen delivery systems for cancer vaccines.
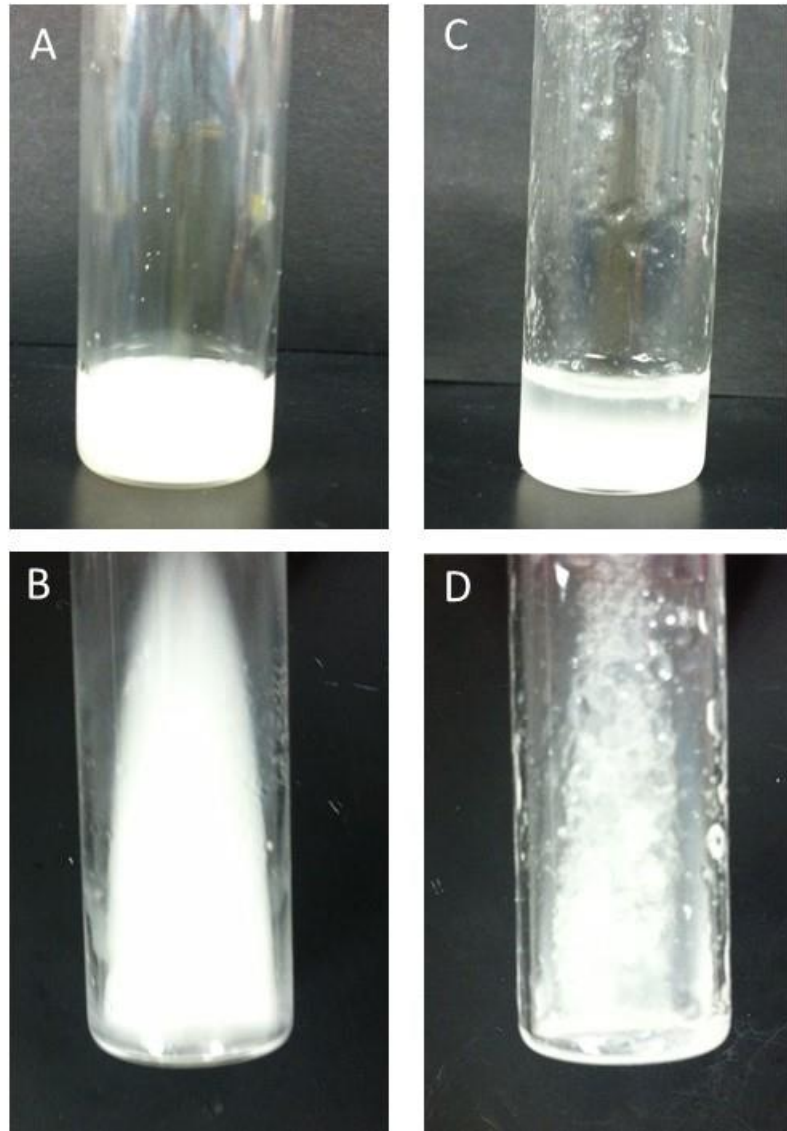
Figure 6 : Primary emulsion (w/o) of (A & B) 3 mg of OVA; (C & D) 3 mg of CpG dissolved in 100 μL of 1% PVA was emulsified in 1.5 mL of DCM containing 200 mg of polymer. B and D are slant views of the glass vial. Emulsification of OVA in PLGA produced a uniform emulsion (A & B). However, emulsification of CpG solution in PLGA showed precipitation (C &D).
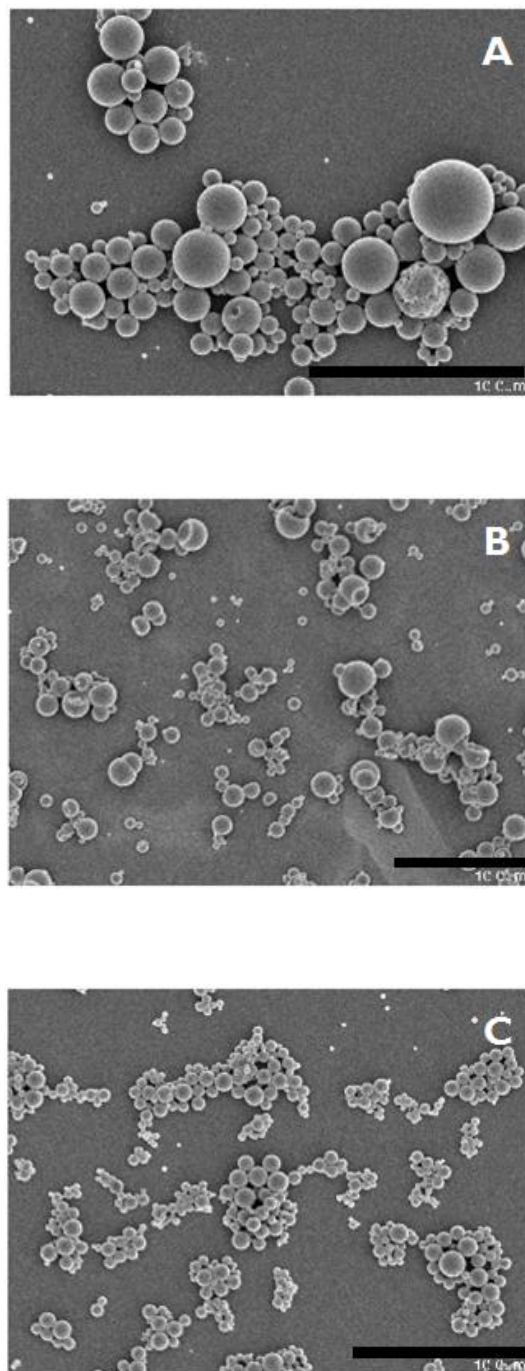
Figure 7 : SEM microphotographs of different CPTEG:CPH microparticle formulations. SEM images of A: Blank CPTEG:CPH microparticles; B: CPTEG:CPH microparticles encapsulating OVA; C: CPTEG:CPH microparticles encapsulating OVA and CpG. Size bar represents 10 μm.
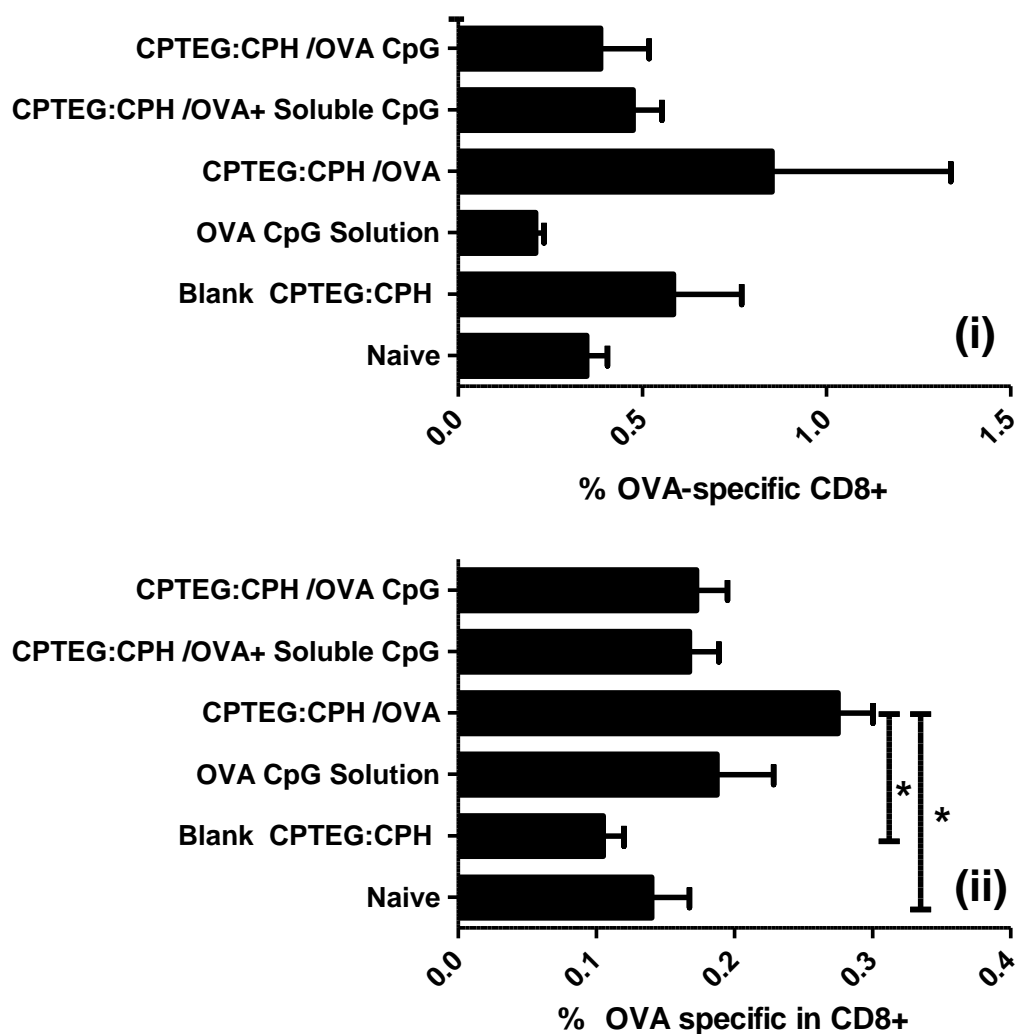
Figure 8: Analysis of OVA-specific T-cell frequency in PBLs of mice vaccinated with different CPTEG:CPH microparticle formulations. Mice were primed (day 0) and boosted (day 7) with PBLs were stained using a fluorescently tagged tetramer, designed to bind to OVA-specific CD8+ T-cells, on day 14 (i) and day 20 (ii) post primary vaccination with indicated microparticle formulations. All groups were statistically compared using ANOVA followed by a Tukey post-hoc analysis (*p < 0.05).
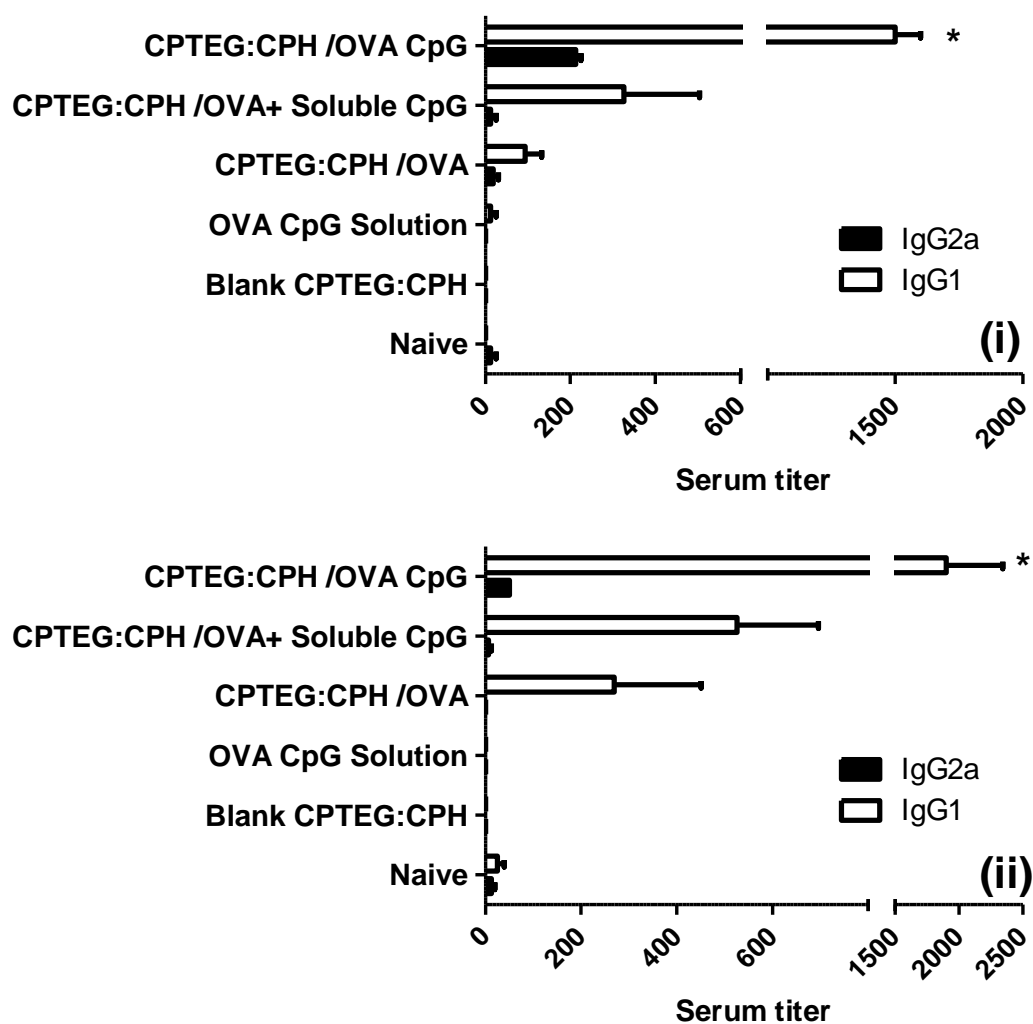
Figure 9 : Comparative serum titers of IgG2a and IgG1 OVA-specific antibodies after vaccination with different CPTEG:CPH microparticle formulations. On (i) day 28 and (ii) day 35 post primary vaccination with indicated treatments, OVA-specific IgG1 and IgG2a titers were measured in sera using ELISA. All groups were compared using ANOVA followed by Tukey post-hoc analysis (*p < 0.01). CPTEG:CPH/OVA CpG group showed significantly higher serum titers for IgG1 when compared with all groups on day 28 and day 35.
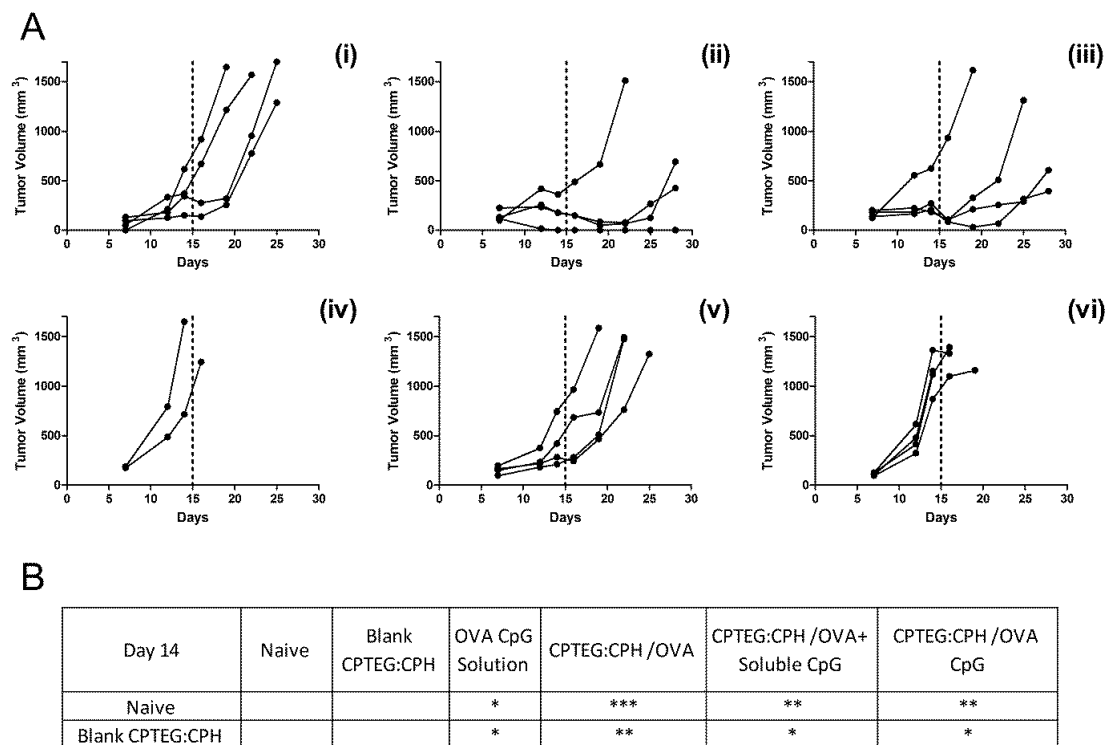
Figure 10 : The prophylactic anti-tumor effect of vaccinating mice with different CPTEG:CPH microparticle formulations. Thirty-five days prior to subcutaneous challenge with E.G7-OVA tumor cells, mice were vaccinated with the following microparticle formulations on day 0 (prime) and day 7 (boost): (i) OVA and CpG encapsulated in CPTEG:CPH; (ii) OVA encapsulated in CPTEG:CPH; (iii) OVA encapsulated in CPTEG:CPH with soluble CpG; (iv) blank CPTEG:CPH particles; (v) soluble OVA and CpG; (vi) Naïve. (A). Tumor volumes were recorded and each curve represents the tumor growth of each individual mouse. Tumor volumes from each treatment group were statistically compared using ANOVA followed by Tukey post-hoc analysis. (***$p < 0.001$; **$p < 0.01$; *$p < 0.05$). (B). Summary of those groups that were significantly different from naïve and blank CPTEG:CPH groups. All other group pairings showed no significant differences.

A

B

Day 14	naïve	Blank CPTEG:CPH	OVA CpG Solution	CPTEG:CPH/OVA	CPTEG:CPH/OVA+ Soluble CpG	CPTEG:CPH/OVA CpG
Naive			*	**	*	*
Blank CPH-CPTEG			*	*	*	*
OVA CpG Solution				*	*	
Median survival (days)	16	15	22	undefined	27.5	23.5
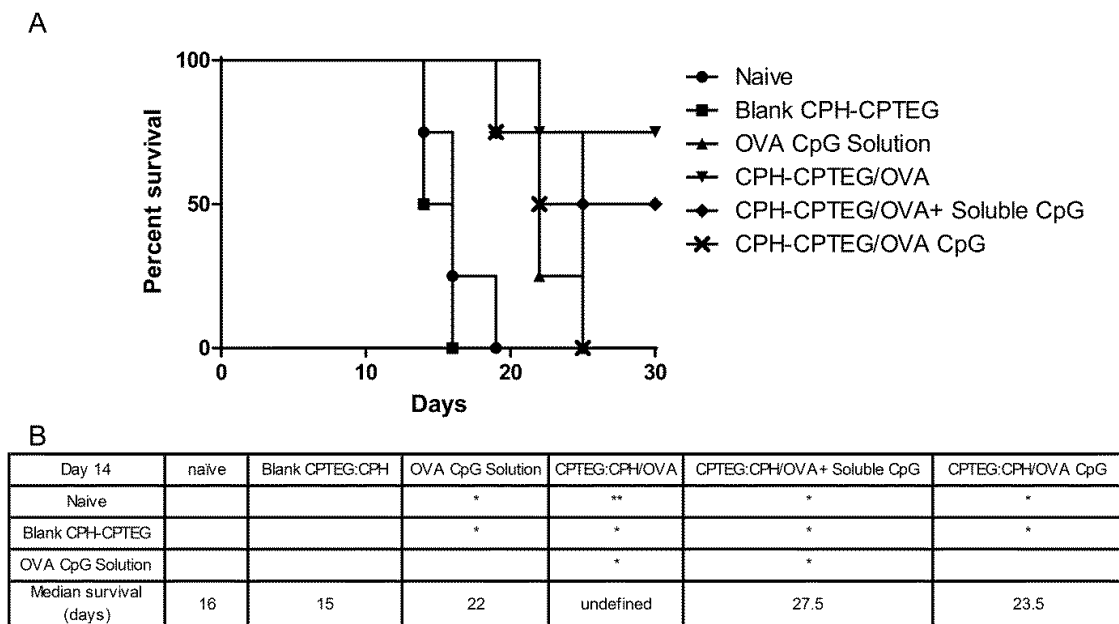
Figure 11 : Survival curve of mice bearing E.G7-OVA tumors. Mice were primed (day 0) and boosted (day 7) with OVA and CpG encapsulated in CPTEG:CPH microparticles; OVA encapsulated in CPTEG:CPH microparticles; OVA encapsulated in CPTEG:CPH microparticles with soluble CpG; Blank CPTEG:CPH microparticles; Soluble OVA and CpG. (A). Survival of mice in each treatment was recorded along with naïve group. (n = 4). (B). Survival curves were analyzed using the Mantel-Cox test and the groups with significant differences between them are displayed. (**$p < 0.01$; *$p < 0.05$).

Table 1 : Loading efficiency and loading mass of OVA and CpG encapsulated CPTEG:CPH microparticles.

Group	% Encapsualtion efficiency	Loading (µg/mg of polymer)
OVA loaded CPTEG:CPH	78.6	OVA:11.8
OVA and CpG loaded CPTEG:CPH	OVA: 12.0	OVA:1.8
	CpG: 21.0	CpG: 0.2

Table 2 : Particle size and zeta potential of CPTEG:CPH microparticles as measured by Zetasizer Nano ZS.

	Particle size (µm)	Polydispersity index (PDI)	Zeta potential (mV)
Blank Particles	3.08	0.25	-0.63 $\pm$ 3. 81
OVA loaded CPTEG:CPH	2.02	0.54	-3.50 $\pm$ 10. 10
OVA and CpG loaded CPTEG:CPH	1.57	0.52	-5.24 $\pm$ 7. 24

CHAPTER 3: RELATIONSHIP BETWEEN THE SIZE OF PLGA PARTICLES LOADED WITH OVA AND CpG WITH THE MAGNITUDE OF THE ANTIGEN SPECIFIC IMMUNE RESPONSE GENERATED

Introduction

The worldwide prevalence of malignant and intracellular pathogenic diseases necessitates the development of novel prophylactic and therapeutic vaccine strategies. A major consideration for development of such vaccines is stimulation of an adaptive immune response which involves generation of cytotoxic T-lymphocytes (CTLs) capable of recognizing pathogen-associated antigens (Ag) (Figure 1). These Ags are endogenously expressed by diseased cells (147). Vaccines to intracellular diseases need to trigger the activation of dendritic cells (DC) in a fashion that maximizes CTL activation. When DCs are activated they can stimulate either Th1-type or Th2-type biased immune responses. Stimulation of antigen-specific CTL tends to be correlated with Th1-type responses. Whether a vaccine generates a primarily Th1-type or Th2-type immune response is largely dependent on the properties of that vaccine (151-153). It has become increasingly evident that in order to generate a Th1-type response, the Ag should be delivered to DCs in a particulated form (154-156). Multiple advantages of using particle based delivery system for antigens have been described in Chapter 1, section "Biodegradable polymer particles".

A wide range of viral and non-viral particulated vaccine delivery systems showing optimum activation of DCs and/or T-cell proliferation have been reported in the literature (78, 143, 157-159). Poly (lactic-co-glycolic acid) (PLGA)-based delivery systems are non-toxic biodegradable delivery vehicles (160) which can provide sustained delivery of Ag and are an attractive approach to stimulating Ag-specific immune responses. However, there are considerable discrepancies regarding the optimum size of

PLGA particles needed to stimulate adaptive immunity. Some studies have shown that larger micron-sized particles, due to smaller surface area:volume ratio, provide a longer duration of release of Ag resulting in enhanced Ag presentation by DCs and stronger CTL responses (143, 161-163). In one study, T-cells isolated from lymph nodes of mice immunized with 2 to 8 μm Ag-encapsulated PLA particles showed higher *in vitro* T-cell proliferation and cytokine secretion compared to the activity of T-cells isolated from mice immunized with 200 nm or 400 nm sized particles (164). In another study, intranasal vaccination of rats with 5 μm-sized PLGA particles encapsulating hepatitis B surface antigen (HBsAg) showed higher particle uptake by alveolar macrophages and higher anti-HBsAg antibody titers when compared to mice vaccinated with HBsAg encapsulated in 12 μm-sized PLGA particles (165). In this study, it was also reported that rat alveolar macrophages uptake higher fraction of 5 μm-sized PLGA particles were compared to the uptake of 12 μm-sized PLGA particles. These studies suggest that sustained release of antigen for long durations in combination with higher uptake of these particles by antigen presenting cells are required for generating an antigen-specific immune response. This idea was further validated with 1000 nm-sized PLGA particles encapsulating BSA which generated a higher IgG antibody response compared to antibody responses in mice vaccinated with 500 nm and 200 nm-sized particles (166). On the other hand, some studies have implied that Ag delivery systems should mimic viruses or bacteria for effective stimulation of DCs and have shown that nanoparticles generate a high number of activated DCs (167) and stronger CTL responses (157, 158, 168). However, polymer nanoparticles can lose their cargo before reaching DCs, as they have lower loading efficiencies than larger particles, and thus co-loading of adequate doses of Ags and adjuvants is more challenging (169). Identification of the optimal size of particles would help in the fabrication of an efficient vaccine formulation with the capacity to generate a robust Ag-specific immune response capable of anti-tumor activity.

In this study, a model antigen ovalbumin (OVA) with CpG oligodeoxynucleotides (CpG) were co-loaded into different sized PLGA particles, with the aim of investigating the relationship between the size of the PLGA vaccine particless and the magnitude of the *in-vivo* antigen-specific immune response stimulated.

<u>Materials and Methods</u>

<u>Fabrication of different sizes of PLGA particles loaded</u>
<u>with OVA and CpG</u>

Particles were prepared using the double emulsion solvent evaporation method (adapted from Chapter 2) followed by differential centrifugation to separate groups of differently sized particles. For preparation of particles, 2 mg of OVA (Sigma, St Louis, MO) and 1.5 mg of CpG (Integrated DNA Technologies, Coralville, IA) were dissolved in 100 µl of 1 % poly (vinyl alcohol) (PVA) (Mowiol®; Sigma, Allentown, PA) solution and is called water1 phase. The initial amount of OVA and CpG were adapted from a previously optimized protocol developed by Dr. Yogita Krishnamachari (personal communication). Two hundred mg of PLGA (Resomer® RG 503; PLGA 50:50 with viscosity: 0.32 – 0.44 dl/g, Boehringer Ingelheim KG, Germany) was dissolved in 1.5 mL of dichloromethane (DCM) to create the oil phase. A primary emulsion was prepared by sonication of the water1 phase into the oil phase for 30 seconds using a sonic dismembrator (Model 100 equipped with an ultrasonic converter probe, Fisher Scientific, Pittsburgh, PA) at 10 watts which was then emulsified into another 1 % aqueous PVA solution using two different methods. In <u>method - 1</u>, the primary emulsion was homogenized for 30 seconds in 30 mL of 1 % PVA solution using an Ultra-Turrax homogenizer (T 25 basic with 12.7 mm rotor; IKA-werke, Wilmington, NC) at 13500 rpm/min. In <u>method - 2</u>, the primary emulsion was emulsified into 8 mL of 1 % PVA solution for 30 seconds using the Sonic Dismembrator at 10 watts. This secondary emulsion was added to 22 mL of 1 % PVA. Secondary emulsions were stirred in a fume

hood to allow DCM to evaporate. Particles were then transferred to a 50 mL conical tube and sequentially centrifuged at 200 rpm (7 xg), 1000 rpm (164 xg), 4000 rpm (2880 xg) and 7000 rpm (6790 xg) for 5 minutes. For sequential centrifugation, particles were first centrifuged at the lowest speed. After this first centrifugation, the supernatant was transferred to a new 50 mL conical tube and centrifuged at the next higher speed. These centrifugation speeds were optimized to provide satisfactory yields and adequate size distributions of PLGA particles. Pellets obtained in 4 conical tubes were resuspended in 30 mL of deionized water and centrifuged again for 5 min at their respective speeds. This step was repeated once more. The pellets obtained after the last wash were resuspended in 3 mL of deionized water. These particle suspensions were frozen at -20°C for 5 hours. These frozen suspensions were then lyophilized using a FreeZone 4.5 freeze dryer (Labconco Corporation, Kansas City, MO) at -53 °C collector temperature and 0.08 mBar pressure. The dried particles were stored in sealed containers at -20 °C until use.

<div align="center">

Characterization of different sizes of PLGA particles

loaded with OVA and CpG

</div>

Scanning Electron Microscopy (SEM)

The morphology of the particles was examined using scanning electron microscopy (SEM), as described in Chapter 2, section "Scanning electron microscopy (SEM)". Briefly, a suspension of particles was placed on a silicon wafer mounted on a SEM stub. It was coated with gold-palladium with an argon beam K550 sputter coater (Emitech Ltd., Kent, England). Images were captured using a Hitachi S-4800 SEM (Hitachi High-Technologies, Ontario, Canada) at 8 kV accelerating voltage.

Measurnment of PLGA particles sizes

The average size of particles was calculated from SEM images using ImageJ software (U. S. National Institutes of Health, Maryland, USA). Deposition of particle

suspensions on a flat surface forms an annulus-shaped cast and the distribution of particles within that cast depends on the size of the particles (170-172). Different sizes of particles in the suspension form concentric circles within the cast. Thus, to calculate the size distribution of particles in a suspension, multiple SEM images of a dried drop of suspension were taken across a chosen diameter of the drop. The sizes of particles were measured in each image using the Image J software and the average size was calculated from many particles ($n \geq 100$).

Estimation of *in-vitro* release of OVA and CpG from PLGA particles

Fifty mg of particles were added to 3 mL of PBS at pH 7.4 and incubated in a 37 ˚C incubator shaker running at 200 rpm/min. At predetermined time intervals, the suspension of particles was centrifuged at the speed used for collection of these particles during the fabrication procedure. Three hundred to four hundred microliters of the supernatant was removed after centrifugation and replaced in fresh PBS. The particles were resuspended and incubated in the 37˚C incubator shaker until the next time point. Samples were analyzed using standard BCA™ and OliGreen® assay kits to quantify OVA and CpG release, respectively. using a SpectraMax® M5 multi-mode microplate reader (Molecular Devices, Sunnyvale, CA) as described in Chapter 2, section "Quantification of OVA" and section "Quantification of CpG".

Quantification of OVA and CpG encapsulated in PLGA particles

Quantification of OVA and CpG encapsulated in different sizes of PLGA particles was performed using the procedure mentioned in Chapter 2, section "Quantification of OVA and CpG encapsulated in PLGA particles". Loading of OVA and CpG in differently sized particles was calculated using the equation 1. Percentage encapsulation efficiencies (%EE) were calculated with equation 2.

Equation 1: Loading = [Calculated conc. (µg/mL) × Volume (mL)]/ weight of particles (mg)

Equation 2: % EE = [Sum of (weight of different sizes of PLGA particles (mg) × Loading (µg/mg)) × 100]/Initial weight of drug (µg)

where, Loading = µg OVA or CpG encapsulated per mg of PLGA particles, Calculated conc. = calculate concentration of OVA or CpG in neutralized samples and Volume = volume of OVA or CpG solution (ml)

Confocal microscopy to study uptake of PLGA particles

JAWS II (CRL-11904, American Type Culture Collection, Manassas, VA) cells, an immature DC cell line derived from C57BL/6 bone marrow, were treated with different sizes of rhodamine B (Sigma, St Louis, MO)-loaded PLGA particles. Particles were prepared by double emulsion solvent evaporation, as described in section "Fabrication of different sizes of PLGA particles loaded with CpG and OVA". In Lab-Tek® Chamber Slides with 8 wells, 10^4 cells were incubated with 1 ng of rhodamine-loaded PLGA particles for 24 hours at 37 ˚C. Cells were then washed three times with PBS and fixed by incubation of cells with 4 % glutaraldehyde solution for 10 minutes. Cells were mounted in DAPI containing Vestashield® mounting media (Vector Laboratories, Inc., Burlingame, CA). Images were acquired using a Zeiss 710 confocal microscope (Carl Zeiss Microscopy, Thornwood, NY).

Flow cytometry to quantify uptake of PLGA particles

Alexa fluor 488 conjugated OVA (AF488-OVA) was loaded into differently sized PLGA particles to compare the extent of particle uptake by JAWS II cells. AF488-OVA was prepared according to a protocol optimized by Dr. Dahai Jiang (personal communication) using an Alexa Fluor® 488 succinimidyl ester kit (Invitrogen Life Technologies, Grand Island, NY). One batch of 40 mg OVA was prepared and used for all subsequent studies. After conjugation, OVA was lyophilized and PLGA particles of different sizes were prepared using the double emulsion solvent evaporation method, as

described in the section: "Fabrication of different sizes of PLGA particles loaded with CpG and OVA". To study the uptake of PLGA particles, 10^4 JAWS II cells/well were incubated in a 6 well plate with 1 μg of AF488-OVA loaded in of PLGA particles of different sizes at 37 ˚C for 24 hours. Cells were washed with PBS and incubated with propidium iodide at a final concentration of 1μg/ mL (Sigma, St Louis, MO) to stain dead cells. Samples were acquired on a flow cytometer (Becton Dickinson FACScan™ with BD CellQuest Pro software) and then analyzed using the FlowJo analysis package (Tree Star Software, San Carlos, CA).

Assessment of activation of bone marrow derived dendritic cells (BMDCs)

Preparation and culture of BMDCs

Mice were euthanized according to University of Iowa Institutional Animal Care and Use Committee (IACUC) guidelines. Bone marrow derived dendritic cells were prepared using a modified standard protocol described by Lutz *et. al.* (173) and developed by Dr. Sean Geary of the Division of Pharmaceutics, College of Pharmacy, University of Iowa (personal communication). The donor mouse was injected intraperitoneally (i.p.) with 87.5 mg/kg ketamine and 2.5 mg/kg xylazine and euthanized. After removing skin and muscles from legs, the femur and tibia were isolated and epiphyses were incised at their extremities to expose the medullar cavity. Bone marrow was flushed out using a 30 gauge needle with 5 mL of growth media (RPMI 1640 with 10% fetal bovine serum) into a petri dish. Cells were collected in a 15 mL tube and collected following centrifugation at 240 xg for 10 minutes. The supernatant was removed and the pellet was resuspended in 10 mL of fresh growth medium. The cells were then counted using a hemocytometer. Two million cells were plated in a sterile bacteriological petri dish with 10 mL of growth medium containing 20 ng/mL granulocyte macrophage colony-stimulating factor (GM-CSF) and incubated at 37 ˚C

with 5 % carbon dioxide. After 3 days, cells were given an additional 10 mL of growth medium containing 20 ng/mL of GM-CSF. On day 6 and day 8, 10 mL of media was removed from the petri dish and transferred to a 15 mL tube and cells were collected by centrifugation at 240 xg for 10 minutes. The supernatant was removed and cells were re-suspended in 10 mL of fresh growth medium with GM-CSF (20 ng/mL). This volume was then transferred back to the petri dish. Adequate differentiation (> 90%) into BMDCs required 8 - 10 days, after which cells can be maintained in 10 ng/mL concentration of GM-CSF or used for experiments.

Flow cytometry of BMDCs to quantify the expression of
CD86 and MHC class I molecules

Relative expression of CD86 and MHC class I surface molecules in DCs serve as markers for the assessment of DC activation. To estimate the up-regulation of these surface molecules by different sizes of PLGA particles, 10^5 BMDCs were incubated in a 6 well plate with 4 µg of OVA and 2 µg of CpG loaded in different sizes of PLGA particles for 48 hours at 37 ˚C. After the incubation, the cells were flushed from the plate using 5 mL PBS and collected in 15 mL tubes which were centrifuged at 230 xg for 5 minutes. Supernatant was removed and cells were re-suspended in fresh PBS. This step was repeated twice to wash the cells. Cells obtained were stained with fluorescently tagged antibodies using a protocol developed and optimized by Dr. Sean Geary and Dr. Caitlin Lemke of the Division of Pharmaceutics, College of Pharmacy, University of Iowa (personal communication). Pellets obtained after the last wash were resuspended in 50 µL of 5 mg/mL Fc receptor block (Anti-mouse CD16/32; eBioscience, San Diego, CA) solution prepared in FACS buffer (PBS with 5% v/v BSA and 0.1% azide) and transferred to U-bottomed 96-well plates. After 15 minutes of incubation on ice 50 µL of anti-CD86 or anti-MHC class I monoclonal antibodies (eBiosciences, San Diego, CA), diluted in FACS buffer to 10 µg/mL, were added to each well. After 20 minutes of

incubation, cells were centrifuged at 230 xg for 5 minutes at 4 °C and the supernatant was aspirated by one quick flick into the sink. Cells were resuspended in 200 µL of FACS buffer and centrifuged again for washing. This step was repeated twice for removal of the excess of antibodies. Cells were re-suspended in 200 µL of PBS containing 4% paraformaldehyde and incubated at RT for 10 minutes. Samples were then acquired on the FACScan flow cytometer (Becton Dickinson FACScan, Franklin Lakes, NJ) and analyzed using the FlowJo analysis package (Tree Star Software, San Carlos, CA).

Immunization of mice with different sizes of PLGA particles

The *in-vivo* efficacy of different sizes of PLGA particles encapsulating OVA and CpG was evaluated using a prophylactic murine model developed and optimized by Dr. Sean Geary and Dr. Caitlin Lemke of the Division of Pharmaceutics, College of Pharmacy, University of Iowa (personal communication). Four groups of male C57BL/6 mice (n = 4) were treated with OVA and CpG loaded PLGA particles with a median size of (a) 17 µm, (b) 7 µm, (c) 1 µm, (d) 300 nm. One additional group of mice was treated with (e) soluble OVA and CpG, and one group of mice remained (f) naïve. Each mouse (groups a – e) was primed on day 0 and boosted on day 7 with an intraperitoneal injection of an equivalent dose of 100 µg of OVA and 50 µg of CpG. Frequencies of OVA-specific cytotoxic T-lymphocytes in the blood were measured on day 14 and 21 using tetramer staining, and OVA-specific IgG antibodies were measured on day 28 using an ELISA assay.

Estimation of OVA-specific cytotoxic T-lymphocyte frequencies in peripheral blood

To estimate the proportion of OVA specific cytotoxic T-lymphocytes (CTLs), peripheral blood lymphocytes (PBLs) were stained with phycoerythrin-labeled H2-Kb SIINFEKL Class I iTAgTM MHC Tetramer (Kb-OVA257) (Beckman Coulter, Fullerton,

CA). PBLs were also double stained with anti-CD8 and anti-CD3 monoclonal antibodies (eBioscience, San Diego, CA) which allows CTLs to be differentiated from the rest of the lymphocyte population (44). Cells were stained with a protocol described in Chapter 2, section "Estimation of OVA specific cytotoxic T-cell frequencies in peripheral blood". Briefly, PBLs were obtained by submandibular bleeding and red blood cells were lysed using ammonium chloride/potassium (ACK) buffer (150 mM NH_4Cl, 10 mM $KHCO_3$, 0.1 mM Na_2EDTA in deionized water, stored at 4 °C). Lymphocytes were collected at 220xg and stained with anti-CD8, anti-CD3 and Kb-OVA257. These cells were washed and fixed with a BD Cytofix/Cytoperm™ Fixation/Permeabilization Solution Kit with BD GolgiPlug™ (BD Biosciences, San Diego, CA). Samples were acquired using a FACScan flow cytometer (Becton Dickinson, NJ) and analyzed with FlowJo software (Tree Star Software, San Carlos, CA).

Estimation of anti-OVA antibodies in peripheral blood
using the enzyme-linked immuno-sorbant assay (ELISA)

Delivery of Ag and adjuvant induces mixed IgG subtype antibody responses that can have a significant effect on tumor regression (151, 152). It has been reported that higher proportions of IgG2a antibodies relative to IgG1 antibodies correlates with secretion of a set of cytokines that favor CTL proliferation (153). Thus, the IgG2a:IgG1 ratio reflects the phenotype of antigen-specific responses generated as a result of vaccination (174). To estimate levels of these antibodies in peripheral blood serum, titers were determined using a protocol described in Chapter 2, section "Estimation of anti-OVA antibodies in peripheral blood using the enzyme-linked immuno-sorbent assay (ELISA)". Briefly, serum samples were collected via submandibular bleeding. Serial dilutions of the serum samples were then incubated on ELISA microwell plates (Corning, Lowell, MA) that had been previously coated with 5 µg/mL of OVA solution in PBS. Plates were then washed with PBS-Tween (0.05% v/v Tween-20 in PBS), followed by

incubation with alkaline phosphatase conjugated anti-IgG antibodies (Southern Biotech, Birmingham, AL). Excess antibody was then washed followed by addition of p-nitrophenylphosphate in the dark. Absorbance was measured after 2 hours at 405 nm using SpectraMax® Plus384 microplate reader.

Statistical Analysis

All experiments were repeated at least in triplicate. The size distributions of particles in the treatment groups did not follow the Gaussian distribution. Thus, the size distributions of treatment groups were compared by non-parametric Kruskal-Wallis one-way analysis of variance followed by Dunns post-hoc analysis to compare all pairs of treatments and identify the pairs of the treatment groups that showed significant difference ($p < 0.05$) in the size distribution. Results for all other experiments were compared by one-way analysis of variance (ANOVA) to analyze if the mean values of treatment groups were different. This was followed by a Tukey post-hoc analysis to compare all pairs of treatments and identify pairs of the treatment groups that showed significant differences ($p < 0.05$) in their mean values. All statistical analyses was performed using Prism 5 (GraphPad Prism, La Jolla, CA).

Results

Preparation and characterization of differently sized PLGA particles co-loaded with OVA and CpG

Polydisperse PLGA particles prepared from a double emulsion solvent evaporation process were segregated into four size-ranges of PLGA particles (A, B, C and D) by differential centrifugation at 7 xg, 164 xg, 2880 xg and 6790 xg, respectively. The box-plots in Figure 12 show the median, first and third quartile of the size distribution of all four batches which were found to be significantly different ($p < 0.001$) from each other. Particles of group D and C are nanoparticles and microparticles

respectively with narrow size ranges. In group B, 50 % of particles are within the range of 2.9 µm to 9 µm which are easily phagocytosed by APCs whereas in group A, 50 % of particles are within the range of 13 µm to 20 µm which are difficult to be phagocytosed by APCs as shown in Figure 15. These size ranges were selected to delineate the effect of different sizes of PLGA particles in producing an *in-vivo* response. Table 3 displays the mean and median size of the four different batches of particles. In order to generate the required range of particle sizes, two methods were used where the secondary emulsions were prepared by homogenization and sonication in Method - 1 and Method - 2 respectively. Method - 1 resulted in particles with median sizes of 17 µm and 7 µm. Whilst method - 2 resulted in a higher percentage of smaller sized particles predominantly with median sizes of 300 nm and 1 µm as described in Table 4. Encapsulation efficiency and Ag loading of different formulations are presented in Table 5 and Table 6 respectively. In this study, each batch of particles is defined by its median size. Each batch of particles had distinct size distributions and had smooth and spherical morphologies as shown in Figure 13.

<div align="center">

Percentage release of OVA and CpG is dependent on the

size of PLGA particles

</div>

All sizes of PLGA particles show a burst release of encapsulated molecules. However, the extent of the burst release decreases with increasing particle size. Figure 14 describes the percentage release of OVA (Figure 14 (i)) and CpG (Figure 14 (ii)) at different time points showing that the release of encapsulated molecules was governed by the size of PLGA particles. Particles of 300 nm in size released most of its cargo in approximately 48 hours. This can be attributed to the 300 nm PLGA particles exhibiting lower loading and possessing a larger surface area to volume ratio relative to larger sized particles. All other particle groups demonstrated release of only a fraction of encapsulated molecules in the burst release. It should be noted that the release studies

were performed in PBS at 37 °C. The presence of enzymes and serum could modify these release profiles *in-vivo*.

Size-dependent uptake of PLGA particles in a dendritic cell line

Uptake of differently sized PLGA particles by dendritic cells was studied using Zeiss laser scanning microscope-710 (Carl Zeiss, Gottingen, Germany). JAWS II cells were incubated with rhodamine-loaded PLGA particles of different sizes. Confocal microscopy demonstrated a very large uptake of 300 nm sized particles. Particles of sizes 7 µm and 1 µm were also internalized by JAWS II cells. Seventeen micron sized particles were not readily taken up by dendritic cells because of the excessively large particle size. Figure 15 is the representative image from each treatment group. The difference in the uptake of particles in different size groups clearly shows that particle uptake decreased with increasing size.

Efficiency of uptake of PLGA particles is dependent on size

Flow cytometry of JAWS II cells incubated with AF488-OVA loaded particles gave an insight into the degree of antigen delivery efficiency by differently sized particles. In comparison with delivery of non-particulated AF488-OVA, PLGA particles of sizes 7 µm, 1 µm and 300 nm were significantly more efficient (p < 0.001) in delivering AF488-OVA to JAWS II cells (Figure 16 (i)). The significant shift of median fluorescence intensity shows that the size of PLGA particles can be correlated to antigen delivery efficiency. PLGA particles that were 300 nm in size generated the maximum intracellular delivery of antigens. Figure 16 (ii) displays representative histograms showing the relative fluorescence shift of the live cells treated with different sizes of particulated and non-particulated AF488-OVA. Particle sizes of 7 µm, 1 µm and 300 nm

demonstrated a significant uptake of AF488-OVA in the treated population of cells as compared to the 17μm particles and the non-particulated AF488-OVA treatment.

Particle-mediated activation of BMDC is size dependent

DCs show enhanced surface expression of MHC and CD80/CD86 co-stimulatory molecules on activation (175). To understand the effect of particle size on stimulating BMDC, the relative surface expression of CD86 and MHC class I molecules on BMDC was assessed subsequent to treatment with different sizes of PLGA particles carrying 4 μg of OVA and 2 μg of CpG. It was shown that after 48 hours treatment, 300 nm sized particles generated the highest fraction of activated BMDCs as shown in Figure 17. This could be attributed to its high antigen delivery efficiency as discussed earlier. Particle sizes of 7 μm, 1 μm, and soluble antigen also showed a significant increase ($p < 0.001$) in the fraction of stimulated BMDCs when compared with untreated populations. In contrast, 17 μm sized particles did not show any significant up-regulation of activation markers by 48 hours of treatment. This size dependency in activation of BMDCs shows that particulated antigen delivery is more effective than soluble antigen delivery but also that the size plays a major role in the activation of DC.

Magnitude of antigen-specific cytotoxic T-lymphocytes *in-vivo* is determined by particle size

Male C57BL/6 mice (n = 4) were treated with different sizes of particulated and non-particulated OVA and CpG. Each mouse was primed on day 0 and boosted on day 7 with an intraperitoneal injection of an equivalent dose of 100 μg of OVA and 50 μg of CpG. Peripheral blood lymphocytes from treated mice were stained for frequency of OVA-specific CTL on day 14 and day 21. As demonstrated in Figure 18, particles with a median size of 300 nm generated significantly more ($p < 0.05$) OVA-specific CTLs on day 14 as well as on day 21 when compared to all other groups. The frequency of OVA-specific CTL in all particle-treated groups, except for 300 nm sized particles, were found

to marginally, but not significantly, increase on day 21 (Figure 18 (ii)) as compared to day 14 (Figure 18 (i)) with mice treated with 1 μm sized particles being significantly different from naïve mice ($p < 0.05$) on day 21. These results demonstrate the significant potential of 300 nm sized particles in immunotherapy and cellular vaccines as they activate a significantly higher frequency of CTLs at a very early stage, day 14 in our studies, and maintain the level for a prolonged period of time, at least until day 21.

<div align="center">

IgG2a levels and IgG2a:IgG1 ratios are determined by

particle size

</div>

Mice were immunized as described in section, "Immunization of mice with different sizes of PLGA particles". Serum IgG antibodies were measured on day 28 using ELISA. Immunization of mice with PLGA particles co-loaded with OVA and CpG has been previously shown to induce OVA-specific IgG antibodies (77). Delivery of Ag and adjuvant induces mixed IgG subtype antibody responses that have significant therapeutic activity (151, 152). Higher proportions of IgG2a antibodies relative to IgG1 antibodies correlates with secretion of a set of cytokines that favor CTL proliferation (153). Thus, the IgG2a:IgG1 ratio reflects the phenotype of antigen-specific responses generated as a result of vaccination (174). Irrespective of size, all particulated groups demonstrated significantly greater levels ($p < 0.05$) of OVA-specific IgG2a antibodies than soluble OVA plus CpG, demonstrating the importance of particle-based vaccines and/or co-delivery of antigen and adjuvant for generation of systemic immunity. However, there were dramatic differences between particle sizes in their efficiencies at generating OVA-specific IgG2a responses. Figure 19 (i) shows the IgG2a antibody response of treated groups on day 28 which was significantly higher ($p < 0.05$) in mice vaccinated with 300 nm sized PLGA particles relative to all other groups. The 300 nm sized particles also gave more than a 50-fold increase in the IgG2a:IgG1 ratio (Figure 19 (ii)) suggesting polarization of a Th1 type immune response that has been reported to be correlated with

anti-tumor activity (176). As the particle size used for vaccination increased, the ratio of IgG2a:IgG1 was found to decrease with 1 μm particles generating approximately equal proportions of IgG2a and IgG1 antibodies on day 28.

Discussion

PLGA particles show a size dependent release of encapsulated molecules. Three hundred nm sized particles released 70 % of their cargo within 2 hours and 100 % release of encapsulated molecules was observed within 40 hours. On the contrary, as the size of particles increased, the percentage release of encapsulated molecules decreased. The enhanced immunogenicity observed with 300 nm PLGA particles encapsulating OVA and CpG is possibly due to a combinatorial effect of the size of PLGA particles as well as the rate of release of encapsulated molecules. The degree of particle internalization by DCs was dependent on size and increased with decreasing particle size. Particles of 300 nm diameter showed maximum internalization which when accompanied by their quick delivery of encapsulated antigen and adjuvant resulted in maximum activation of BMDCs in an *in vitro* 48 hour treatment. For other particulated groups, the ability of activating BMDCs decreased as the particle size increased. This may be due to a combination of the aforementioned low level of cargo release and low numbers of particles being taken up by the BMDCs.

Mice vaccinated with 300 nm sized particles generated the highest fraction of OVA-specific CTLs on day 14 and day 21, demonstrating that 300 nm sized particles can rapidly stimulate cell-mediated immunity. This is particularly important in therapeutic treatments of fast growing diseases which are difficult to control at later stages of illness. All particle based treatment groups generated higher OVA specific IgG2a antibodies by day 28 relative to soluble antigen. Particles that were 300 nm in size generated the highest ratio of IgG2a:IgG1 OVA-specific antibodies by day 28. This suggests that the systemic milieu is biased towards the maintenance and proliferation of OVA specific

CTLs which is particularly important for the eradication of intracellular diseases and cancer. Figure 20 represents the correlation between the ratio of IgG2a: IgG1 antibodies on day 28 on the y-axis with percentage OVA-specific CTL responses measured on day 21 on the x-axis. The ratio of IgG2a: IgG1 correlated well with the level of CTL response generated. Thus, the ratio of IgG2a to IgG1 antibodies in serum can indicate the level of CTL activation after vaccination. This study showed that the smaller the particle size used to vaccinate mice, the greater the magnitude of the antigen-specific immune response generated.
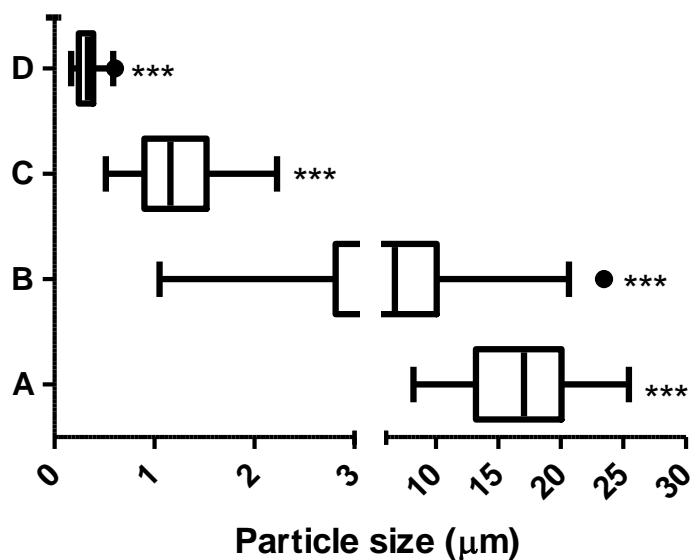
Figure 12 : Box plot of size distribution of different groups of particles as assimilated using Image J software. Each box represents first quartile, median and third quartile of size distribution with whiskers representing 1.5 times the interquartile distance. Particles collected at (A) 7xg; (B) 164xg; (C) 2880xg; (D) 6790xg show significantly distinct distribution in size as analyzed by Kruskal-Wallis one-way analysis of variance followed by Dunns post-hoc analysis. Group B showed highest polydispersity with a substantial tail of larger sized particles. ***$p < 0.001$.
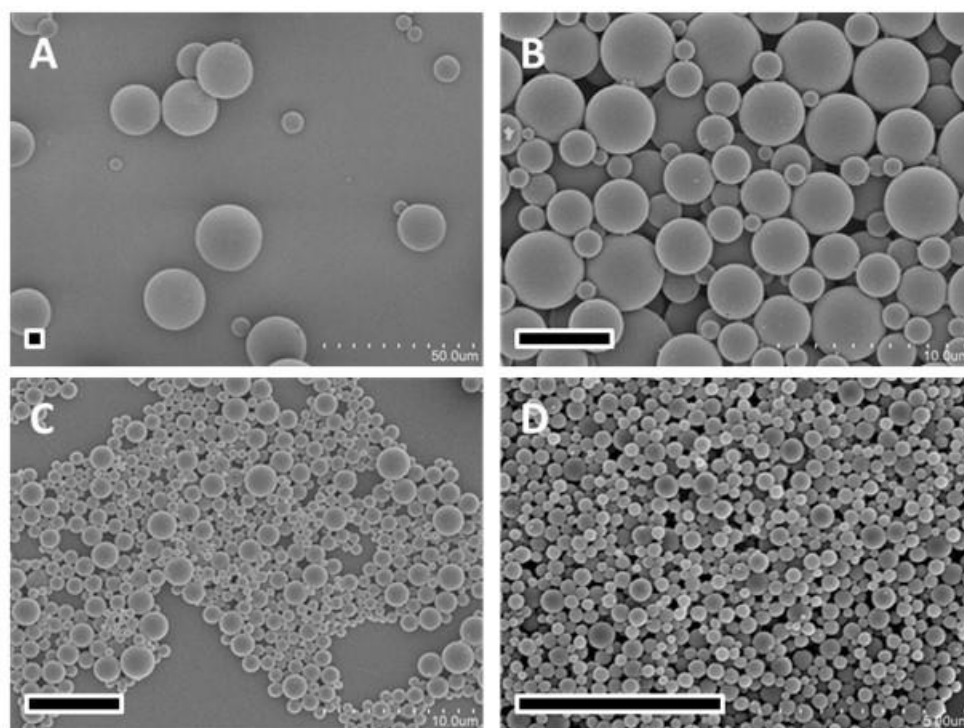
Figure 13: SEM images of each group of PLGA particles showing smooth morphology and distinct size distribution. Rectangle on the bottom left represents 5 µm scale bar.
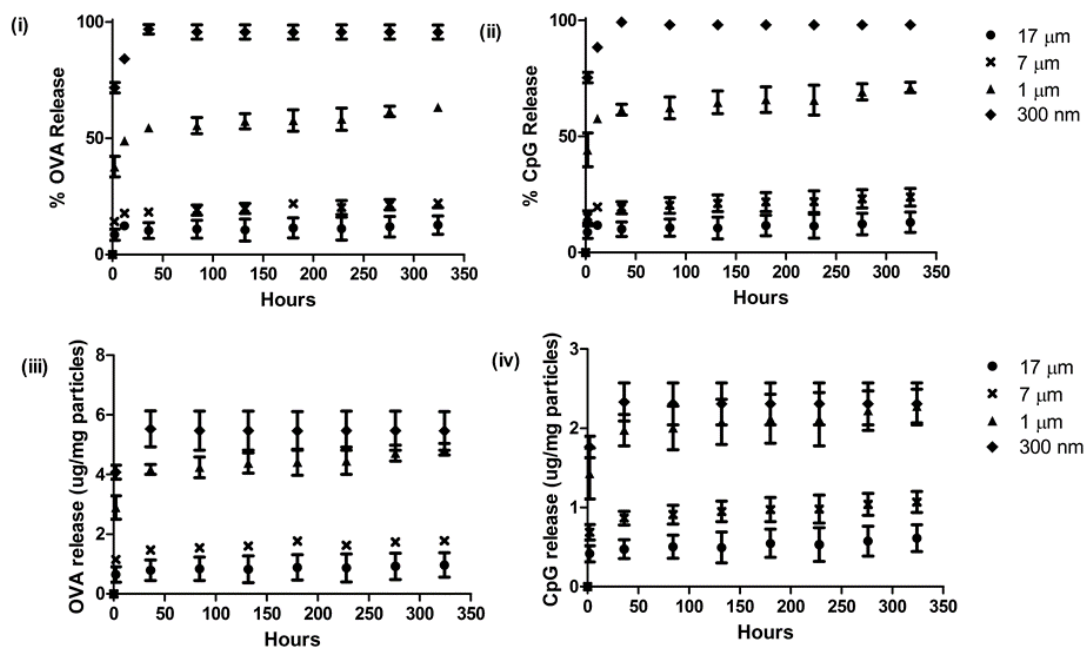
Figure 14: Release of OVA and CpG fromPLGA particles of different sizes. (i)
Percentage OVA,(ii) percentage CpG, (iii) amount of OVA and (iv) amount of
CpG released in PBS (pH 7.4) at 37°C from OVA and CpG co-loaded PLGA
particles of different sizes. All sizes demonstrated burst release of a fraction of
encapsulated molecules except in 300 nm where near 100% release was
observed within a few hours. Groups were compared using paired t-test (*p <
0.05). Each bar represents mean ± SEM (n = 3).
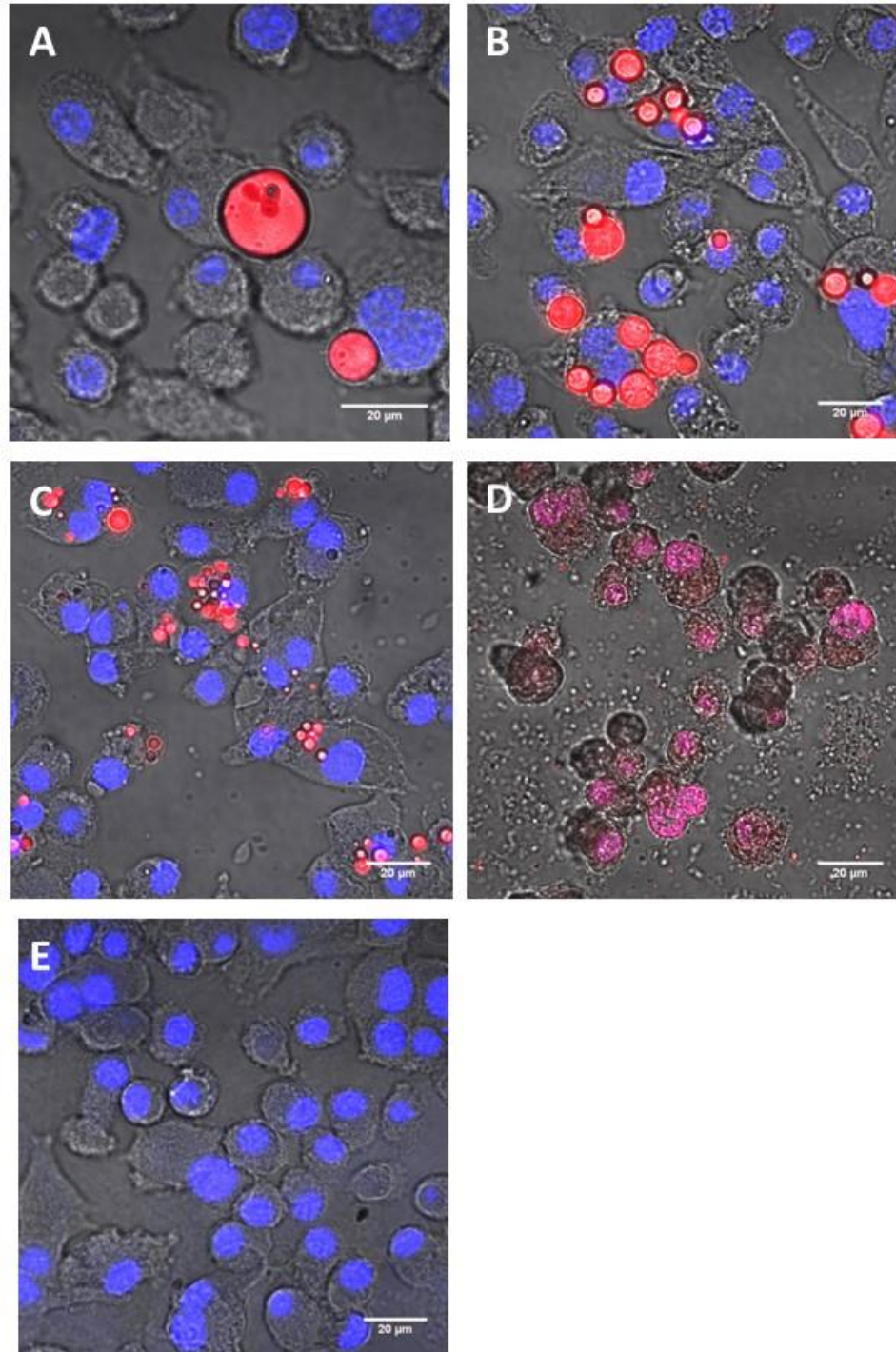
Figure 15: Internalization of rhodamine B loaded PLGA particles of (A) 17 μm, (B) 7 μm, (C) 1 μm and (D) 300 nm sizes were compared with (E) cells treated with soluble rhodamine B in JAWS II cells using confocal microscopy. Scale bar 20 μm.
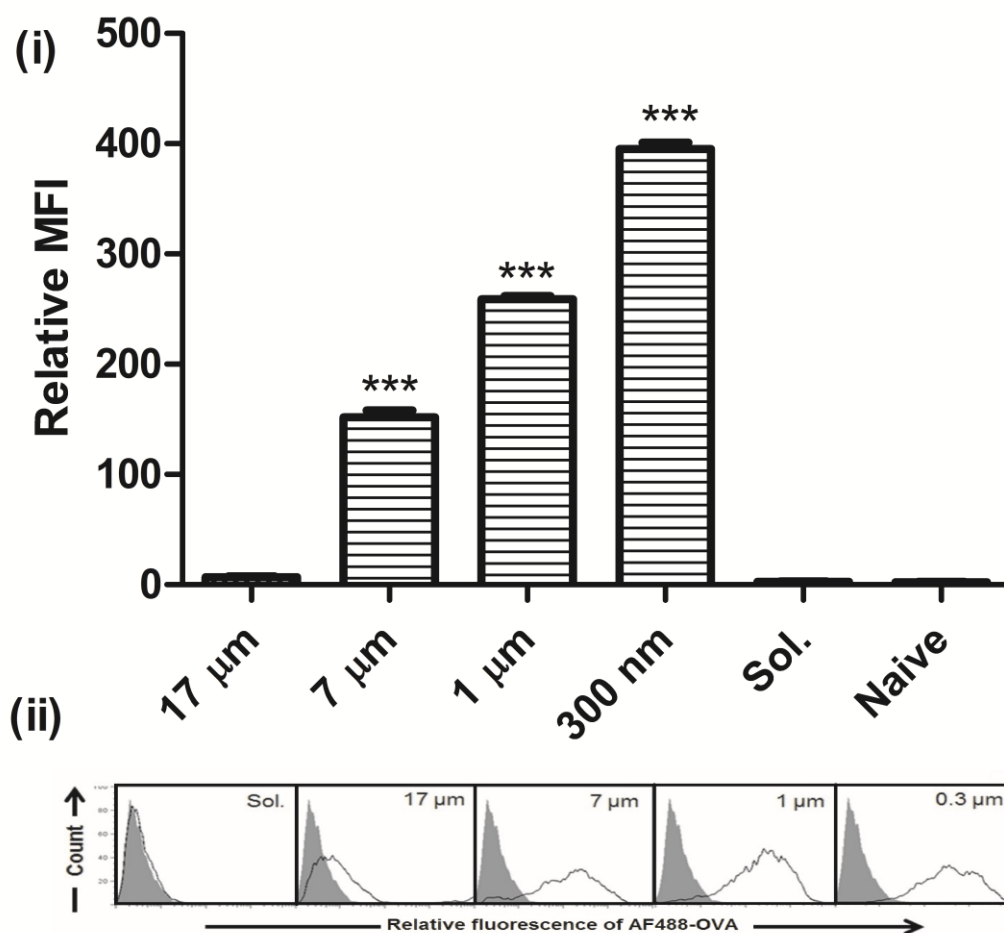
Figure 16: Efficiency of different sizes of particles to deliver Alexa Fluor® 488 conjugated OVA (AF488-OVA) was studied in JAWS II cells using flow cytometry. (i) Relative median fluorescent intensity (relative MFI ± SEM) of AF488-OVA signal upon incubation of different sizes of particles with JAWS II cells (n = 3). Statistical significance was determined using ANOVA followed by Tukey post-hoc analysis (***p < 0.001). (ii) Representative flow cytometry histograms showing uptake of AF488-OVA in different treatment group.
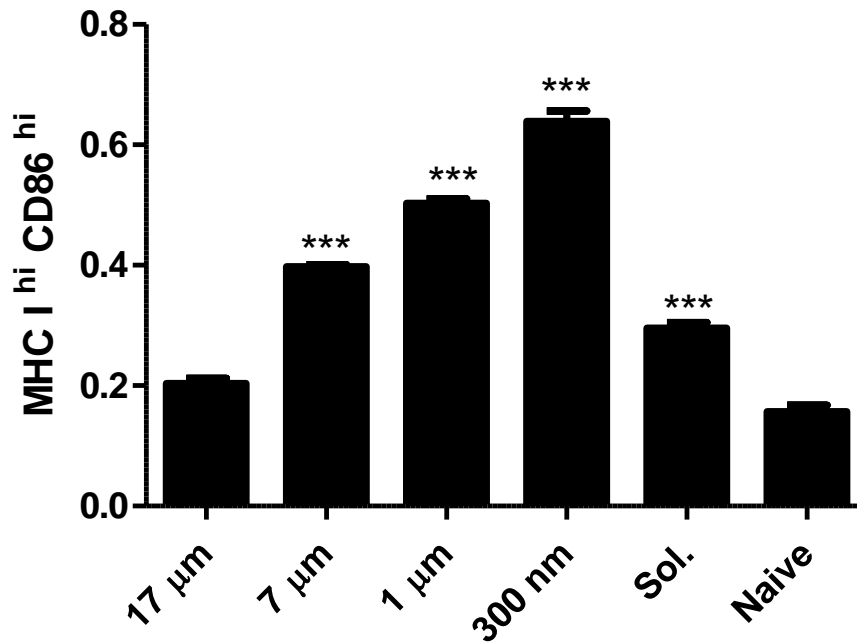
Figure 17: Up-regulation of MHC class I and CD86 expression on BMDCs is dependent on particle size. Flow cytometry analysis showing the fraction of BMDCs with high expression of both MHC class I (MHC I hi) and CD86 (CD86 hi) surface molecules. BMDCs were incubated with equivalent amounts of soluble and particulated forms of OVA (4 µg) and CpG (2 µg) for 48 hours at 37°C. Experiments were performed in triplicate (mean ± SEM).). Statistical significance was determined using ANOVA followed by Tukey post-hoc analysis (***p < 0.001).
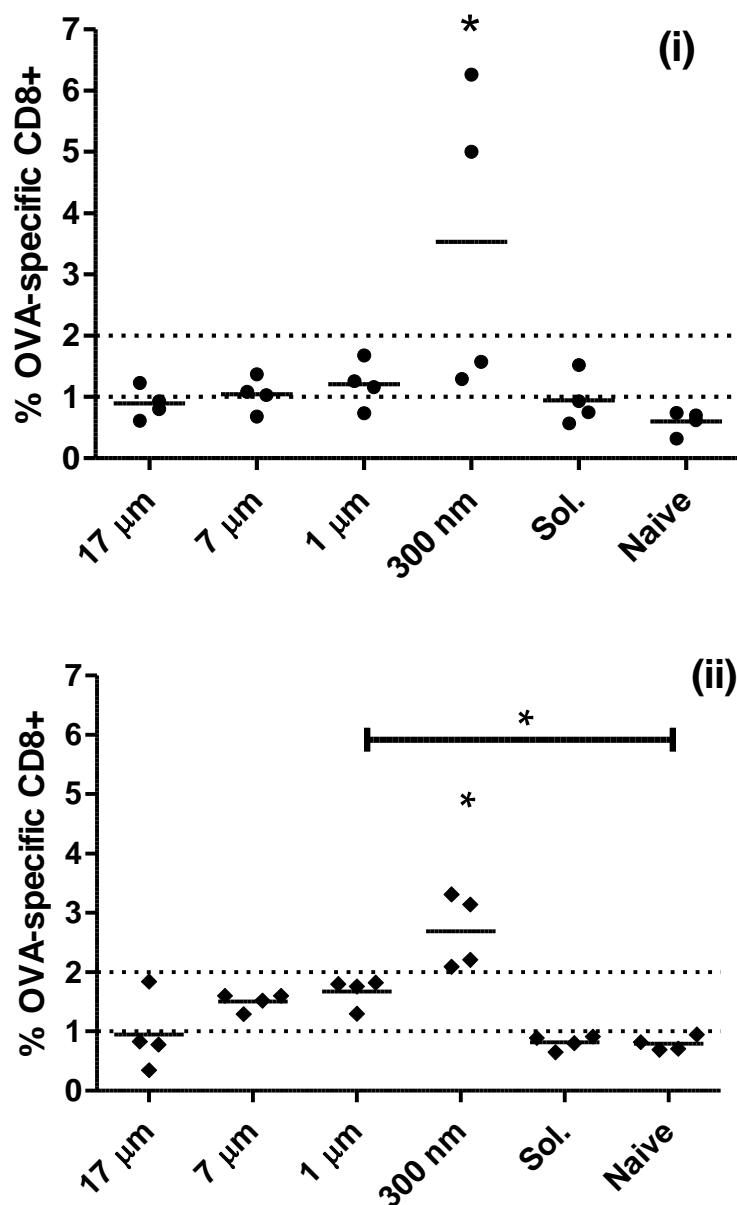
Figure 18: Analysis of OVA specific T-cell frequency in mouse PBLs after delivery of OVA and CpG in different particulate and soluble groups was analyzed by tetramer staining. PBLs were obtained from submandibular bleeding of mice (n = 4) vaccinated with OVA (100 µg) and CpG (50 µg) on day 0 and day 7. OVA specific T-cell frequency was measured on (i) day 14 and (ii) day 21. The value of 2 % and 1 % OVA specific T-cells are indicated with top and bottom horizontal dashed lines across each graph, respectively. The mean values of % OVA specific T-cells in each group are indicated by the solid horizontal line across the data points. All groups were compared using ANOVA followed by Tukey post-hoc analysis (*p < 0.05).
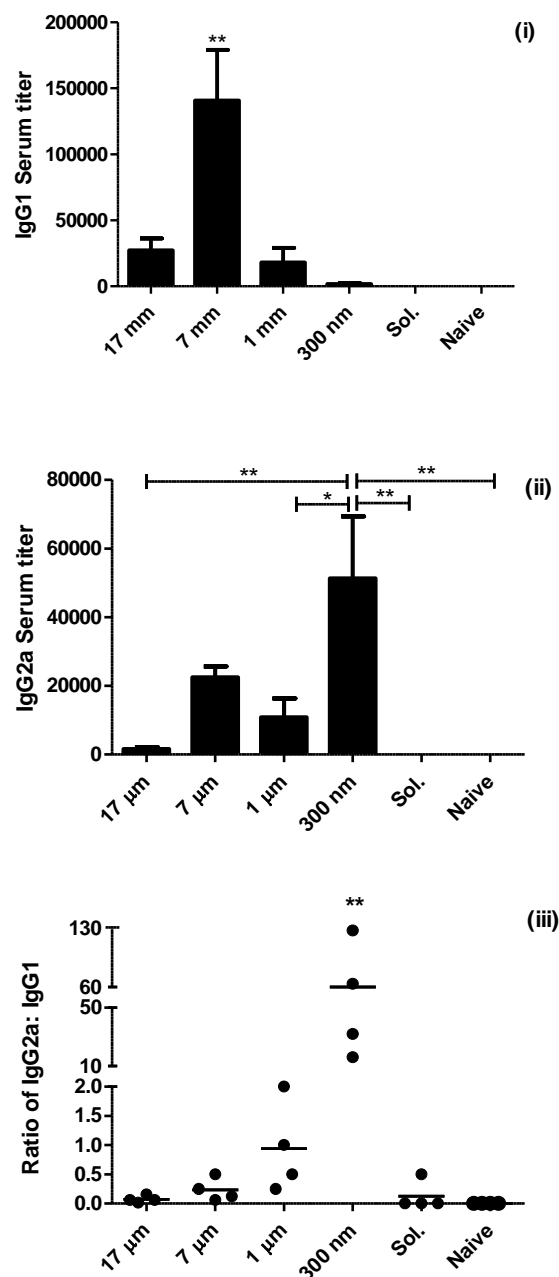
Figure 19: Anti-OVA IgG antibodies levels were measured in mouse serum on day 28. Highest dilution of serum displaying OVA specific (i) IgG1 antibody and (ii) IgG2a antibody responses as measured by ELISA assay. Bar graph represents mean + SEM of serum titers (n = 4). (*$p < 0.05$, **$p < 0.01$). (iii) Ratio of IgG2a:IgG1 antibodies in serum samples of different treatment groups on day 28. The mean values of the ratio of IgG2a:IgG1 antibodies in each group are indicated by the solid horizontal line across the data points. Statistical significance was determined using ANOVA followed by Tukey post-hoc analysis (**$p < 0.01$).
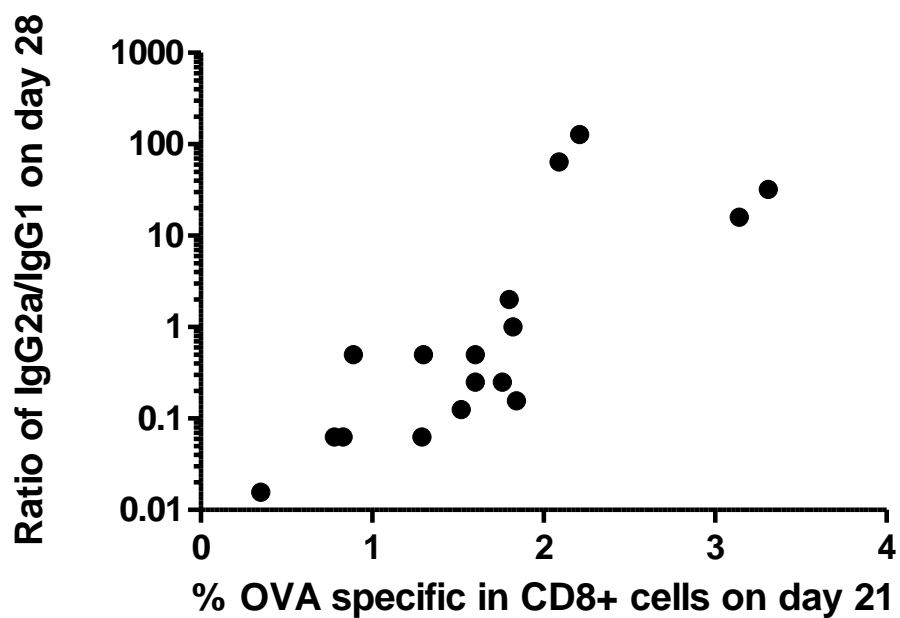
Figure 20: Correlation between ratio of IgG2a: IgG1 and cytotoxic T-cells response. IgG2a: IgG1 antibodies ratio was measured on day 28 and percentage OVA specific CTL response measured on day 21.

Table 3 : Mean and median size of different groups of PLGA particles.

Group Name	Sizes (Mean ± St. Dev.) (µm)	Median size (µm)
A	15.9 ± 3.7	17.4
B	5.5 ± 3.8	6.7
C	1.1 ± 0.3	1.2
D	0.3 ± 0.1	0.3

Table 4 : Influence of the secondary emulsification process on the size of PLGA particles (n = 3). The secondary emulsion was prepared using homogenization in method - 1 and sonication in method - 2.

	Method - 1	Method - 2
17 µm [a]	39.2 ± 0.6	0.0
7 µm [a]	60.8 ± 0.6	13.4 ± 1.2
1 µm [a]	0.0	63.2 ± 1.5
300 nm [a]	0.0	23.4 ± 2.7
Recovery [b]	89.8 ± 5.1	75.5 ± 5.3

a: Weight percent from the total weight of recovered particles. b: Weight percentage of polymer particles recovered with respect to starting material

Table 5 : Encapsulation efficiencies of two methods employed for the fabrication of PLGA particles (n = 3).

	Percentage Encapsulation Efficiency	
	OVA	CpG
Method - 1	37.7 ± 0.3	30.2 ± 2.0
Method - 2	38.0 ± 1.6	21.9 ± 1.8

Table 6 : Loading of OVA and CpG in different sizes of PLGA particles (n = 3).

Group Name	OVA (µg/mg PLGA particles)	CpG (µg/mg PLGA particles)
17 µm	7.4 ± 1.3	4.8 ± 0.4
7 µm	8.1 ± 0.7	4.5 ± 0.2
1 µm	7.6 ± 0.2	3.2 ± 0.3
300 nm	5.7 ± 0.7	2.4 ± 0.4

CHAPTER 4: DEVELOPMENT OF A PLGA PARTICLE VACCINE TO PROTECT AGAINST HOUSE DUST MITE INDUCED ALLERGY

Introduction

In the United States, 84 % of residences have detectable levels of house dust mite (HDM) allergens and a quarter of these houses have higher levels of allergens than the proposed limit for asthma (177). Chronic exposure to HDM allergens can lead to lung inflammation characterized by lung eosinophilia and airway obstructions which can trigger asthma attacks in sensitized individuals (178). It has been reported that prolonged exposure to HDM allergens activates dendritic cells (DCs) present in the lungs, priming T-helper 2 (Th2) immune responses (179), which consequently promotes secretion of proinflammatory cytokines, recruitment of eosinophils, and B cell stimulation to produce immunoglobulin IgE antibodies (180). Most current therapeutic treatments for asthma involve neutralization of inflammatory mediators and relieve local symptoms for only a short period (181, 182). Recently developed subcutaneous immunotherapy and sublingual immunotherapy to induce HDM-specific long-term tolerance has shown promising results in adults and children but such treatment requires regular administration of high doses of HDM allergens for at least 3 years to show satisfactory clinical efficacy (183-185). Absence of a long-term solution to HDM-induced asthma in combination with the dangerous levels of HDM allergens present in households necessitates the development of a prophylactic vaccine that would switch the inflammatory immune response induced by HDM allergen to a protective immunity. This vaccine should induce T-helper 1 (Th1) immunity that results in production of interferon-gamma (IFN- γ), interleukin (IL)-12, and IgG2a antibodies (186, 187). This negative regulation of Th2-orchestrated airway inflammation and induction of protective immunity by Th1 cells can reduce pathogenic symptoms associated with allergy (188-190).

Amongst the various allergen-producing HDM, *Dermatophagoides pteronyssinus* (Der p) is the most prevalent allergy-causing mite (191, 192). These HDMs produce Der p2, a highly potent allergen that has structural and functional similarity with the immunostimulatory lipopolysaccharide binding protein, MD2 (193). Serum samples of 79 % of patients suffering from asthma, wheezing and/or rhinitis possessed positive titers for anti-Der p2 IgE antibodies, making it a potential allergen for development of vaccines against HMD allergies (194). However, in an attempt to generate HDM vaccines, subcutaneous injections of Der p2 allergen to mice caused increases in the production of IgE antibodies and Th2-skewed immune responses (195). This necessitated the formulation of a vaccine that involved co-administration of the allergen with Th1 adjuvants that promote Th1-biased immune responses in order to effectively induce Der p2-specific Th1 antibodies that would alleviate lung damage associated with exposure to allergen (196, 197). Unmethylated cytosine-phosphate-guanine motifs–1826 (CpG) is used as an adjuvant for polarization of immune responses to the Th1 type (198-200). It is an agonist to Toll-like receptor–9 which activates DCs and B cells to produce Th1-specific cytokines and suppresses Th2 modulated allergic responses (197). Co-administration of CpG-containing immunostimulatory oligodeoxynucleotide (ISS-ODN) with HDM allergen has been shown to decrease eosinophilia and IL-5 production while increasing the production of IFN–γ in nasal lavage fluid (201). In the same study, these responses were significantly improved when ISS-ODN was chemically conjugated with HDM allergen. In a clinical trial for ragweed allergy, peripheral DCs isolated from healthy individuals vaccinated with ragweed allergen conjugated to immunostimulatory oligodeoxyribonucleotide 1018 (Dynavax Technologies, Berkeley, CA) expressed increased levels of Th1 cytokines and decreased levels of Th2 cytokines (202). In a similar murine study, subcutaneous immunization of Balb/c mice with CpG conjugated to cedar pollen allergen was shown to increase the production of allergen-specific IgG2a and secretion of IFN-γ by CD4+ T-cells isolated from spleens (203). With the clear

demonstration of the importance of CpG at inducing a robust immunity against allergens, these studies also demonstrated that co-delivery of allergen with CpG is essential for stimulating an active Th1 response (204). Chemical conjugation of CpG with allergen, although often successful, is expensive and can lead to structural modification of the conjugated molecules and changing of their immunostimulatory properties. In addition, *in-vivo* spontaneous cleavage of the conjugating bridge between allergen and adjuvant can prevent co-delivery of molecules to the same cell. An alternative co-delivery method is to administer CpG and Der p2 in biodegradable poly(lactic-co-glycolic acid) (PLGA) polymer particles. In addition to co-delivering multiple molecules, many studies have recognized the significance of PLGA particulate vaccines in stimulating robust Th1 type responses as characterized by secretion of IgG2a antibodies (205, 206). Vaccination of mice with antigen-loaded PLGA microparticles and CpG, either co-loaded with antigen or injected as a solution, showed enhanced secretion of IgG2a antibodies with a greater ratio of IgG2a:IgG1 antibodies when compared to mice vaccinated with a mixture of antigen and aluminium hydroxide (207). We have previously reported that PLGA particles encapsulating antigen and CpG can stimulate robust immune responses compared to vaccination of antigen and CpG in solution (80). Additionally, in Chapter 3, it was shown that the magnitude of immune responses generated directly depends on the size of PLGA particles used for immunization. While large particles encapsulating antigen with CpG are known to produce high levels of total IgG1 titers, submicron sized particles containing antigen with CpG have been shown to induce higher ratios of IgG2a to IgG1. To develop prophylactic therapies against allergy-associated lung disorders, induction of high IgG titers and Th1 type immune response is highly desirable. Th1 polarized immunity could decrease the secretion of IgE antibody and inflammatory damage to lungs upon exposure to allergen (196). In this study, the aim was therefore to determine the effects of the size of PLGA particle vaccines and the influence of CpG in the overall immune response to Der p2-coated PLGA particle vaccines.

<u>Materials and Methods</u>

Fabrication of different sizes of PLGA particles loaded

with CpG

Different sizes of particles were prepared using a modified method described in

Chapter 3, section "Fabrication of different sizes of PLGA particles loaded with OVA

and CpG". Briefly, 3 mg of CpG (Integrated DNA Technologies, Coralville, IA) was

dissolved in 75 µl of 1 % poly(vinyl alcohol) (PVA; Mowiol® 8–88; MW: ~67000;

Sigma, Allentown, PA). A primary emulsion was prepared by sonication of this solution

at 60 % output power for 30 seconds in 2 mL of dichloromethane (DCM) containing

200 mg of PLGA (Resomer® RG 503; PLGA 50:50 with viscosity: 0.32 – 0.44 dl/g;

MW: 24,000–38,000; Boehringer Ingelheim KG, Germany) using a sonic dismembrator

(Model FB 120 equipped with an ultrasonic converter probe CL-18; Fisher Scientific,

Pittsburgh, PA). To prepare different sizes of PLGA particles, two independent methods

were used for the preparation of the secondary emulsion. In method 1, the primary

emulsion was emulsified in 1 % PVA for 30 seconds using a sonic dismembrator at 60 %

output power. In method 2, an Ultra Turrax homogenizer (T 25 basic with 12.7 mm rotor;

IKA-werke; Wilmington, NC) at 13,500 rpm/min was used for 30 seconds to emulsify

the primary emulsion in 1% PVA. These secondary emulsions were stirred in a fume

hood for 2 hours for complete evaporation of DCM. Different sizes of suspended

particles were collected by sequential centrifugation of particles at 200 rpm (7 xg),

700 rpm (75 xg), 4000 rpm (2880 xg), and 7000 rpm (6790 xg) for 5 minutes. Particles

were washed with distilled water and lyophilized using FreeZone 4.5 (Labconco

Corporation, Kansas City, MO) at -53 ˚C collector temperature and 0.08 mBar pressure.

Particles collected at 700 rpm, 4000 rpm, and 7000 rpm were used for further

experiments.

Characterization of PLGA particles

The morphology of the particles was examined using scanning electron microscopy (SEM) as described in Chapter 2, section, "Scanning electron microscopy (SEM)". Particle sizes of different batches were calculated as described in Chapter 3 section, "Measurnment of PLGA particles sizes".

Estimation of *in-vitro* release of CpG from PLGA particles

Time-dependent release of CpG from different sizes of PLGA particles were studied in PBS at pH 7.4. In a glass vial 50 mg of particles were added to 3 mL of PBS heated to 37 ˚C. The vials were transferred to a 37˚C incubator shaker set at 200 rpm/min. Samples were collected at predetermined time points and the volumes removed were replaced by fresh PBS maintaining sink conditions for CpG. Solubility of CpG is more than 40 mg/mL in PBS. Samples were analyzed using OliGreen® assay kits to quantify CpG release using a procedure described in Chapter 2, section "Quantification of CpG"

Quantification of CpG encapsulated in PLGA particles

Loading of CpG into PLGA particles was estimated by degrading 20 mg of PLGA particles in 1 mL of 0.2 N NaOH for 12 hours or until a clear solution was obtained. This solution was neutralized with 1 N HCl. CpG was quantified using a fluorescence OliGreen® assay kit (Molecular Probes, Eugene, OR) as described in Chapter 2, section "Quantification of CpG" . Loading and encapsulation efficiency was calculated according to equation 1 and equation 2, respectively.

Equation 4 : Loading (µg/mg PLGA particles) = [Calculated conc. (µg/mL) x Volume of neutralized solution of degraded PLGA particles (mL)]/Initial weight of PLGA particles (mg)

Equation 5 : Percentage encapsulation efficiency = [Loading of CpG (µg/mg) x amount of PLGA particle recovered (mg)]/ Initial amount of CpG (µg)

where, Loading = μg CpG encapsulated per mg of particles, Calculated conc. = calculated concentration of Dox or CpG from standard curve (μg/mL).

Animal models of Der p2-induced asthma and immunization protocol

In-vivo efficacy of differently sized PLGA particles encapsulating CpG and coated with Der p2 were evaluated using an allergy model developed and optimized by Dr. Andrea Adamcakov Dodd and Dr. Xuefang Jing of the Department of Occupational and Environmental Health, College of Public Health, University of Iowa (personal communication). Male C3H/HeBFeJ mice (5-6 weeks old) were obtained from Jackson Laboratories (Bar Harbor, ME) and provided standard laboratory rodent chow and water *ad libitum* (208). All animal care, housing and procedure requirements of the National Institutes of Health Committee on Care and Use of Laboratory Animals were followed. Ninety six mice were acclimatized for 7 days prior to first vaccination and divided randomly into nine experimental groups as described in Table 8. Untreated (sentinels) and PBS-treated (shams) control mice were used as unsensitized controls. Twelve mice per group were used in each experiment, except for the sentinel group (n = 4). A solution of 10 μg LoTox Natural Der p2 (LTN-DP2-1, Indoor Biotechnologists, endotoxin<0.03 EU/μg) in 100 μl PBS was incubated with PLGA particles for 30 minutes to coat Der p2 on PLGA particles. Mice were vaccinated by subcutaneous (S.c.) injection into the loose skin over the interscapular region (area around the neck) on day 0 and day 7, under isoflurane anesthesia (using a precision Fortec vaporizer, Cyprane, Keighley, UK) with Der p2 coated on PLGA particles loaded with or without 5 μg CpG. On each of days 14 to 23 (10 doses), mice were exposed to 2.5 μg Der p2 in 50 μl PBS by intranasal instillation during isoflurane anesthesia to induce airway inflammation and hyperresponsiveness. Mice were weighed on day 0, 7, 14 and 24, and observed for any behavioral changes or clinical symptoms. All mice were euthanized on day 24.

Collection and processing of serum and bronchoalvelolar

lavage fluid

Mice were euthanized with an overdose of isoflurane on day 24 and blood for Igs analysis was collected through cardiac puncture. Bronchoalveolar lavage (BAL) fluid was collected and processed as described by George et. al with minor modifications (209). This protocol was developed and optimized by Dr. Andrea Adamcakov Dodd and Dr. Xuefang Jing of the Department of Occupational and Environmental Health, College of Public Health, University of Iowa (personal communication). Briefly, the trachea was exposed and BAL was performed using three doses of 1 mL of sterile saline (0.9 % sodium chloride solution; Baxter, Deerfield, IL). BAL fluid was centrifuged at 800 xg for 5 min at 4 °C and the supernatant was stored at -80 °C for determination of cytokines. Cells in the pellet were re-suspended in Hank's balanced salt solution (Life Technologies, Grand Island, NY) for total cell counts using a hemocytometer. For differential cell counts, cells were spun onto microscope slides at 800 xg for 3 min using a Cytospin 4 (Thermo Shandon, Thermo Scientific, Waltham, MA), air-dried and stained using Protocol® HEMA 3 stain set (Fisher Diagnostics, Pittsburgh, PA), and then 400 cells per slide were counted to enumerate macrophages, neutrophils, eosinophils and lymphocytes under an optical microscope (Olympus, Center Valley, PA).

Estimation of tumor necrosis factor-alpha (TNF-α) and

interferon-gamma (IFN-γ) secretion in bronchoalvelolar

lavage fluid using the enzyme-linked immuno-sorbent

assay (ELISA)

TNF-α and IFN-γ were measured in BAL fluid by enzyme-linked immunosorbent assay (ELISA) using the specific antibody pairs according to manufacturer's instructions (BD OptEIATM, BD Biosciences Pharmingen, San Diego, CA and Novex®, Life Technologies Corp., Frederick, MD, respectively). This protocol was developed and

optimized by Dr. Andrea Adamcakov Dodd and Dr. Xuefang Jing of the Department of Occupational and Environmental Health, College of Public Health, University of Iowa (personal communication).

For the estimation of IFN- γ, ELISA microwell plates (Nunc-Immuno ™, (Thermo Scientific, Waltham, MA) were incubated overnight at 4 °C with 100 µL of anti-INF- γ capture antibody (provided in the kit). Plates were washed 5 times with 300 µL of PBS-Tween buffer (0.05 % v/v Tween-20 in PBS). After washing, plates were blocked with 200 µL of assay diluent buffer (10 % FBS in PBS) for 1 hour. Plates were then washed 5 times with 300 µL of PBS-Tween buffer. BAL supernatants were not diluted. Dilutions of known concentration of recombinant IFN-γ standard antibody were also prepared for standard curve. One hundred microliters of samples and standards were added to the plate and incubated for 2 hours at RT. Plates were then washed 5 times with 300 µL of PBS-Tween buffer. This was followed by addition of 100 µL biotinylated anti-INF-γ detection antibody and streptavidin conjugated horseradish peroxidase (provided in the kit). After 1 hour of incubation, the plates were washed 10 times with 300 µL of PBS-Tween buffer. This was followed by addition of 100 µL of substrate solution (Tetramethyl benzidine and hydrogen peroxide; BD OptEIA™ TMB Substrate Reagent Set; BD Biosciences) to each well. The plates were incubated in the dark for 30 minutes then the reaction was terminated by addition of 50 µL of stop solution (1 M H_3PO_4 and 2 N H_2SO_4). Absorbance was measured at 450 nm using a SpectraMax® Plus384 microplate reader (Molecular Devices LLC,Sunnyvale, California). Samples were compared with a standard curve to calculate the concentration of the cytokine in BAL supernatants. A similar procedure was employed to estimate levels of TNF-α where known concentrations of recombinant TNF-α were used to prepare a standard curve. Samples were treated with biotinylated anti-TNF-α detection antibody and streptavidin conjugated horseradish peroxidase for the measurement of TNF-α levels in BAL samples.

Estimation of cytokine/chemokine secretion in

bronchoalveolar lavage fluid using multiplexed fluorescent

bead-based immunoassays

Multiplexed magnetic fluorescent bead-based immunoassays (Bio-Plex Pro Mouse Cytokine, Chemokine, and Growth Factor Multiplex Assays, Bio-Rad Laboratories, Inc., Hercules, CA) was used to measure IL-4, IL-5, IL-6, IL-1β, keratinocyte-derived cytokine (KC), and macrophage inflammatory protein (MIP)-1α. This protocol was developed and optimized by Dr. Andrea Adamcakov Dodd and Dr. Xuefang Jing of the Department of Occupational and Environmental Health, College of Public Health, University of Iowa (personal communication). In a 96-well plate, 50 µL of assay buffer containing cytokine conjugated beads were transferred to each well. Plates were then washed twice with 100 µL of Bio-Plex® wash buffer with magnetic washer. Fifty microliter of samples and diluted standards were added to the wells containing conjugated beads. The plate was covered with aluminum foil and incubated at RT for 1 hour on a shaker at 300 rpm. After the incubation, the plate was washed 3x with 100 µL of wash buffer followed by the addition of 25 µL of detection antibodies provided in the kit. The plate was incubated again at RT for 30 minutes on a shaker at 300 rpm followed by washing 3x with 100 µL of wash buffer. After that 50 µl of streptavidin-phycoerythrin in assay buffer was added to each well followed by a 10 minute incubation at RT on a shaker at 300 rpm. The plate was then washed again 3x with 100 µL of wash buffer. Beads were re-suspended in 125 µL of assay buffer and the plate was analyzed using the Bio-Plex® multiplex system (Luminex 100, Bio-Rad Laboratories, Inc., Hercules, CA).

Estimation of anti-Der p2 IgE, IgG1 and IgG2a antibodies
in peripheral blood using the enzyme-linked
immunosorbent assay (ELISA)

The presence of anti-Der p2 IgG1, IgE and IgG2a antibodies in sera were evaluated by ELISA. This protocol was developed and optimized by Dr. Andrea Adamcakov Dodd and Dr. Xuefang Jing of the Department of Occupational and Environmental Health, College of Public Health, University of Iowa (personal communication). Corning® 96-well EIA/RIA Microplates (Corning, Lowell, MA) were coated with 100 μl of LoTox Natural Der p2 (2.5 μg/mL for IgG1 or 5μg/mL for IgE and IgG2a) in 0.05 M sodium-potassium carbonate buffer (pH 9.6) and incubated overnight at 4 °C. After three washes with PBS containing 0.05 % v/v Tween® 20 (PBS-Tween), the plates were blocked with 150 μl of 1 % w/v BSA in PBS-Tween for 1 hour at RT. Serum samples were serially diluted in blocking buffer at ranges from 1:10 to 1:80 for IgE, 1:25 to 1:25600 for IgG2a and 1:100 to 1:102400 for IgG1 assay. Diluted sera were added to the plates (100 μl/well) and incubated for 2 hours at RT. Plates were washed 3x and incubated with 100 μl 1/4000 dilution of HRP conjugated rat anti-mouse IgG1 or IgG2a or goat anti-mouse IgE (Southern Biotech, Birmingham, AL) for 2 hours at RT. Plates were then washed 6x with PBS-Tween followed by addition of 100 μl/ well of TMB substrate (Thermo Scientific, Waltham, MA) and after a 15 min incubation at RT the reaction was stopped by addition of 0.17 N sulfuric acid (100 μl/well). The absorbance (optical density, OD) was measured at 450 nm in a microplate spectrophotometer (SpectraMax plus 384, Molecular Devices, Sunnyvale, CA). Because there are no commercially available standard mouse anti-hDer p2 antibodies, the equivalent concentrations of specific-Der p2 IgG1, IgG2a were calculated by comparison with a reference curve generated with a known serum. Results for IgG1 and IgG2a were expressed as ELISA units (U/mL). 1 U/mL was defined as the reciprocal value of the serum dilution that gave an optical density value of 1. This was always within the linear

part of the dilution curve. To ensure reproducibility, a serum sample of known titer was run with each test as a standard.

Histological analysis of lung tissues

Lungs that were not lavaged were rinsed with saline solution through the heart, perfused via the cannulated trachea and fixed in 10% zinc formalin (Fisher Scientific, Kalamazoo, MI). Tissues were paraffin-embedded and 5 μm thick sections were stained with hematoxylin and eosin (H&E). Lung tissues were evaluated for allergic airway inflammation using light microscopy to study the presence of inflammatory cell infiltrates and perivascular and peribronchiolar inflammation. Severity of perivascular inflammation was quantified by a 4-point scoring system as follows: 0 = absence of cell cuffs, 1 = rare to few scattered perivascular inflammatory cell cuffs, 2 = multifocal to moderate numbers of perivascular inflammatory cell cuffs, 3 = large number of diffuse perivascular inflammatory cell cuffs. Total lung inflammation was defined as the sum of perivascular cuffing scores across all slides. This procedure was performed by Dr. Katherine N. Gibson-Corley of the Department of Pathology, Carver College of Medicine, University of Iowa.

Evaluation of airway hyperresponsiveness

Airway hyperresponsiveness (AHR) was assessed on day 24, which was 24 hour after the final intranasal instillation of Der p2, using a forced oscillation technique (FlexiVent System, SCIREQ, Montreal, QC, Canada). This procedure was performed by Dr. Andrea Adamcakov Dodd of the Department of Occupational and Environmental Health, College of Public Health, University of Iowa. Mice were anaesthetized by an intraperitoneal injection of 90 mg/kg of sodium pentobarbital (Ovation Pharmaceuticals, Inc. Deerfield, IL) and tracheotomy was performed using a tracheal cannula with a luer adapter (1.3 mm, length 20 mm, Harvard Apparatus, Holliston, MA). Animals were connected to a small animal ventilator set at a frequency of 150 breaths/min, a tidal

volume of 10 mL/kg and a positive end-expiratory pressure of 2 to 3 cm H_2O. Each mouse was challenged with increasing concentrations (3, 10, 30, and 100 mg/mL) of methacholine chloride (ICN Biomedicals, Inc. Solon, OH) aerosol that were generated for 10 s with an in-line nebulizer. Airway resistance was measured using a "snapshot" protocol each 20 s for 5 min, ensuring that measured parameters were stabilized. The mean of these 15 values was calculated for each methacholine dose. At the end of the experiment the animal was disconnected from the ventilator and were euthanized by an overdose of sodium pentobarbital.

Statistical analysis

Values given are means ± SEM from at least six animals in each group unless otherwise noted. All assays were compared by one-way analysis of variance (ANOVA) to analyze if the mean values of treatment groups were different. This was followed by Tukey post-hoc analysis to compare all pairs of treatments and identify pairs of the treatment groups that showed significant differences in their mean values. Differences were considered significant at p-values that were less than or equal to 0.05. All statistical analysis was performed using statistical and graphing software Prism 5 (GraphPad Prism, La Jolla, CA)

Results

Preparation of CpG-loaded PLGA particles

The double emulsion solvent evaporation method was used to fabricate CpG-loaded PLGA particles. A modified procedure was used for the preparation of the secondary emulsions. Method 1 and method 2 generated different sizes of PLGA particles which were segregated at different centrifugation speeds into batches of large, medium and small sized PLGA particles as described in Table 7. Method 1, using an Ultra Turrax homogenizer to prepare secondary emulsions, gave a greater fraction of

larger sized particles as compared to the sonic dismembrator used in method 2. SEM images in Figure 21 show that each batch of particles had a distinct size distribution and smooth morphology. Particle sizes for each batch were calculated using SEM images and are described in Table 7. Particle sizes for medium and small sized particles were confirmed with dynamic light scattering.

<div align="center">Loading and release kinetics of PLGA particles</div>
<div align="center">encapsulating CpG depends on particle size</div>

The loading capacity of CpG was directly proportional to the size of the PLGA particles (see Table 7). Encapsulation efficiency for CpG was 22 % for method 1 and 22.5 % for method 2 as calculated from equation 2. Release kinetics of CpG from PLGA particle matrices were assessed in PBS using a 37°C shaking water incubator. All particle sizes demonstrated an initial burst release of CpG. The percentage of CpG released during the initial phase depended on the size of the particles. Smaller particles, probably due to a larger surface area to volume ratio, showed a higher percentage burst release of CpG which decreased with increasing particle size as demonstrated in Figure 22.

<div align="center">Accumulation of inflammatory cells depends on the size of</div>
<div align="center">PLGA particles and presence of CpG</div>

Upon allergen challenge, inflammatory cells can accumulate in the lungs activating downstream inflammatory pathways which can lead to asthma (210). Here, the accumulation of leukocytes was evaluated by studying the phenotype of cells collected from BAL fluids of vaccinated mice on day 24. These mice were intranasally exposed to Der p2 antigen from day 14 to day 23 to induce allergic airway inflammation and hyperresponsiveness.This is an established model for human allergic asthma (211, 212). As shown in Figure 23, accumulation of the total number of cells, chiefly eosinophils and lymphocytes, in BAL fluids of mice vaccinated with Der p2 coated on PLGA particles were found to increase with increasing size of PLGA particles. Mice vaccinated with

small-sized particles displayed minimal eosinophilia which was similar to shams and sentinels (mice unexposed to Der p2). Figure 23 also demonstrates that the presence of CpG in PLGA particles used for vaccination consistently dampened the eosinophilia and accumulation of lymphocytes in lung tissues of vaccinated mice. When mice were vaccinated with small or medium-sized microparticles, inclusion of CpG also reduced recruitment of macrophages compared with the mice without CpG (Figure 23 (v)). Mice vaccinated with large particles without CpG exhibited a significantly higher influx of eosinophils and lymphocytes into airways (*$p < 0.05$, **$p < 0.01$) as compared to other treatment groups as shown in Figure 23. This showed that it fails to prevent lung damage after Der p2 exposures. There was no significant difference in the numbers of neutrophils collected from BAL fluids. Figure 23 (vi) compared the fraction of each cell phenotype accumulated in the lungs of vaccinated mice. The fractions of eosinophils collected in lungs were significantly decreased in the presence of CpG and smaller PLGA particles.

<div align="center">

Der p2-coated PLGA particles induces IgG responses and

the presence of CpG favors production of IgG2a antibodies

</div>

Serum samples from mice vaccinated with different sizes of PLGA particles with or without CpG were collected on day 24 and measured for the induction of humoral immune responses by evaluating the levels of IgG1, IgG2a and IgE antibodies specific for Der p2 using ELISA. Mice vaccinated with large particles without CpG showed significantly higher levels of IgG1 antibody (**$p < 0.01$) than those vaccinated similarly but with CpG as shown in Figure 24 (i). This group of mice had comparatively low levels of IgG2a antibodies compared to PLGA particles with smaller sizes. The presence of CpG enhanced the induction of IgG2a antibodies in sera of mice vaccinated with small and medium sized particles as shown in Figure 24 (ii). It has been shown that the generation of IgG2a antibody is dependent on cytokines such as IFN-γ which favor the switch from Th2 to Th1 type responses (186). In contrast, secretion of IgG1 and IgE

antibodies is supported by IL-4 and IL-5 which primarily promotes Th2 type immune responses (196). Thus, the ratio of IgG2a:IgG1 antibodies measured in serum samples of each treatment group was evaluated in Figure 24 (iii). It was found that the presence of CpG in particles used in vaccinations resulted in increased proportions of IgG2a antibodies compared to mice vaccinated with the corresponding sized particles in the absence of CpG. In addition, ratios of IgG2a:IgG1 antibodies in mice vaccinated with Der p2 coated on small and medium sized particles encapsulating CpG were significantly higher (*p < 0.05, **p < 0.01) compared to other treatment groups. This would be expected to induce a blunting of airway inflammation and hyperresponsiveness associated with Der p2 lung exposure. Mice vaccinated with small and medium sized PLGA particles showed low levels of IgE secretion which was not significantly different from mice not exposed to Der p2 (Figure 24 (iv)). In contrast, mice vaccinated with large particles showed significant increases in the levels of IgE antibody detected in the serum (*p < 0.05, **p < 0.01). This clearly demonstrates that decreasing the size of PLGA particles used for vaccination decreases the induction of Th2 polarized antibody responses. This can be enhanced by the inclusion of CpG but it is the size of the PLGA particles that has the major role in determining the type of Th response.

<div align="center">Local cytokine/chemokine responses after Der p2 exposure

to vaccinated mice</div>

Cytokines/chemokines are extracellular proteins involved in triggering cell proliferation and chemotaxis of leukocytes. Inflammation caused by eosinophilic influx during asthma and secretion of IgE antibody is mediated by local levels of cytokines (213). Mice vaccinated with large particles without CpG showed detectable levels of IL-4, IL-5 and IL-6 suggesting the activation of a Th2 dominant response. Levels of these cytokines were under the limit of detection for other treated groups as shown in Figure 25. Levels of macrophage inflammatory protein (MIP)-1α, keratinocyte-derived cytokine

and Interferon-gamma (IFN-γ) were also highest in mice vaccinated with large particles without CpG. Titers of IFN-γ decrease with a decrease in the size of particles. Also, surprisingly, in the presence of CpG the secretion of IFN-γ was further decreased, although not significantly. The presence of IFN-γ and absence of IL-4 during antigen presentation favors the development of a Th1 dominant response. Thus, high levels of IFN-γ and IL-4 in mice vaccinated with large particles without CpG cannot be inferred to conclude if the response is Th1 or Th2 dominant. In all other groups the lack of detectable levels of IL-4, IL-5 and IL-6 in combination with the demonstration of a slight increase in the levels of IFN-γ might indicate the activation of Th1 responses. All treatment and control groups showed similar levels of TNF-α.

<div align="center">Presence of CpG in vaccines diminishes airway

hyperresponsiveness</div>

Allergic asthma is characterized by an increase in airway hyperresponsiveness (AHR) to non-specific bronchoconstrictors like methacholine (214). The ability of PLGA particle vaccines to suppress the induction of AHR was evaluated 24 hours after ten daily intranasal exposures of Der p2 to vaccinated mice. Mean baseline lung function (in the absence of methacholine challenge) did not differ among all experimental groups. As demonstrated in Figure 26, mice vaccinated with small sized particles showed no significant increase in AHR from baseline after increasing doses of methacholine challenge. In contrast, mice vaccinated with Der p2-coated on large PLGA particles demonstrated the greatest increase in airway resistance after methacholine challenge (10, 30, and 100 mg/mL) which was significantly different from shams and sentinels (**p < 0.01, ***p < 0.001). AHR was also significantly different in mice vaccinated with Der p2-coated medium sized particles after methacholine challenge at 30 mg/mL and 100 mg/mL, compared to sentinels and shams (*p < 0.05, ***p < 0.001). Vaccination of mice with CpG encapsulated in PLGA particles significantly suppressed AHR when

compared to Der p2-coated medium and large sized empty PLGA particles (*p < 0.05, **p < 0.01, ***p < 0.001).

Presence of CpG reduces perivascular cuffing

Allergy can cause infiltration of inflammatory cells into the peribronchiolar and perivascular connective tissues, both of which were examined by histological analysis. Experimental groups that showed inflammatory cell infiltrates were predominately perivascular in nature with adjacent airways showing a similar, although less intense, inflammatory cell response. As shown in Figure 27 and consistent with BAL data, the primary lesions caused by perivascular inflammation were predominantly composed of macrophages and eosinophils with fewer neutrophils. Mice vaccinated with Der p2 coated onto large and medium sized blank PLGA particles showed the most severe perivascular cuffing which were reduced in mice vaccinated with PLGA particles encapsulating CpG (Figure 28). Mice vaccinated with Der p2 coated onto small PLGA particles were also free from primary lesions caused by inflammatory cells. These mice, along with the mice vaccinated with medium sized particles containing CpG, had only a mild increase in the cellularity of the alveolar septa that was primarily due to increased numbers of mononuclear cells. Overall, using small-sized particles or CpG-containing particles for vaccination can significantly reduce the perivascular cuffing as shown in the graphical insert of Figure 28.

Discussion

Asthma caused by HDM leads to inflammatory damage of lungs that is associated with secretion of Th2-dependent anti-Der p2 IgE antibodies, eosinophilic influx into the lungs and airway hyperactivity (180). Currently there is no permanent treatment for pathological symptoms caused by asthma and most clinicians prescribe temporary therapies for alleviating the inflammatory responses caused by repeated exposure to allergen. The absence of an optimal therapeutic treatment and a high prevalence of

asthma in the United States (215) emphasize the need for the stimulation of allergen-specific Th1 biased responses to suppress the activation of Th2 driven inflammation. This can be achieved by the careful design of a vaccine system which can stimulate DC, an important modulator for the polarization of Th responses to favor Th1 activation (216). Recent studies have shown that vaccination of mice using polymer particles encapsulating antigen can stimulate an antigen-specific effector T-cell response which is characterized by an increase in cytotoxic T-lymphocyte (CTL) activity, IgG2a production and reduction in IgE secretion (217, 218). Particle-based vaccines are proposed to mimic bacterial or viral infections which are readily phagocytosed by DCs for antigen presentation to T-cells (219). PLGA particles are well characterized delivery systems which can be used for the co-delivery of allergic antigen and adjuvant to the same DC which, in turn, can steer immune responses toward a Th1 type (206, 220). To test this hypothesis, Der p2 allergen coated onto CpG-loaded or empty PLGA particles were used to develop a prophylactic treatment for allergy which can prevent AHR associated with pulmonary inflammation on exposure to allergen. In Chapter 3, it was shown that particle size in a PLGA vaccine system can affect the magnitude of stimulated effector responses. This study demonstrated that particle uptake and activation of DCs were increased with decreasing size of PLGA particles encapsulating OVA and CpG. It was also shown that the magnitude of the IgG2a response was highest in mice vaccinated with 300 nm PLGA particles compared to larger particles thereby demonstrating the importance of particle size in generating an appropriate immune response. In the study presented here, the effect of the size of PLGA particles on generating protective immune responses against Der p2 was investigated. Vaccinated mice were dosed with 10 daily intranasal instillations of Der p2 followed by various diagnostic and immunological assays to determine the efficacy of each vaccination formulation. It was shown that mice vaccinated with Der p2 coated onto small sized particles encapsulating CpG caused no increase in IgE and IgG1 serum levels after daily Der p2 exposures (Figure 24). In

addition, levels of Th2 cytokines, IL-4 and IL-5 in BAL fluid in this exposure group were below the limit of detection (Figure 25), confirming the absence of inflammatory Th2 responses. This was further validated by the discovery that the ratios of IgG2a:IgG1 antibodies were remarkably high for small sized PLGA particles containing CpG. These immunological responses generated by CpG-loaded PLGA particles coated with Der p2 were in agreement with data shown in Chapter 3 that PLGA particles of sizes smaller than 1 μm encapsulating OVA and CpG resulted in increased levels of IgG2a antibodies, a higher ratio of IgG2a:IgG1 and enhanced numbers of OVA-specific CD8+ T-cells. These studies combined suggest that a successful vaccine may be designed by either encapsulating the antigen inside of the particle or by adsorbing the antigen on to the surface of the particle.

Analysis of BAL fluids (Figure 23) and lung histopathology (Figure 27) of vaccinated mice exposed to Der p2 antigen demonstrated that antigen-specific immunity generated in mice vaccinated with small PLGA particles coated with Der p2 prevented pulmonary influx of leukocytes. Similarly, no significant increase in airway resistance was observed with small PLGA particles when challenged with increasing doses of methacholine. These results showed that small sized particles encapsulating CpG generate a robust immune response which can prevent strong allergic responses to Der p2 exposures. Mice vaccinated with medium and large sized empty PLGA particles coated with Der p2 exhibited airway remodeling and increased AHR on Der p2 exposures when compared to sentinels. Upon encapsulation of CpG into these particles, AHR (Figure 26) and eosinophilia (Figure 23) was significantly reduced compared to medium and large sized empty PLGA particles. These results demonstrate that incorporation of CpG can significantly improve the efficacy of the vaccine.
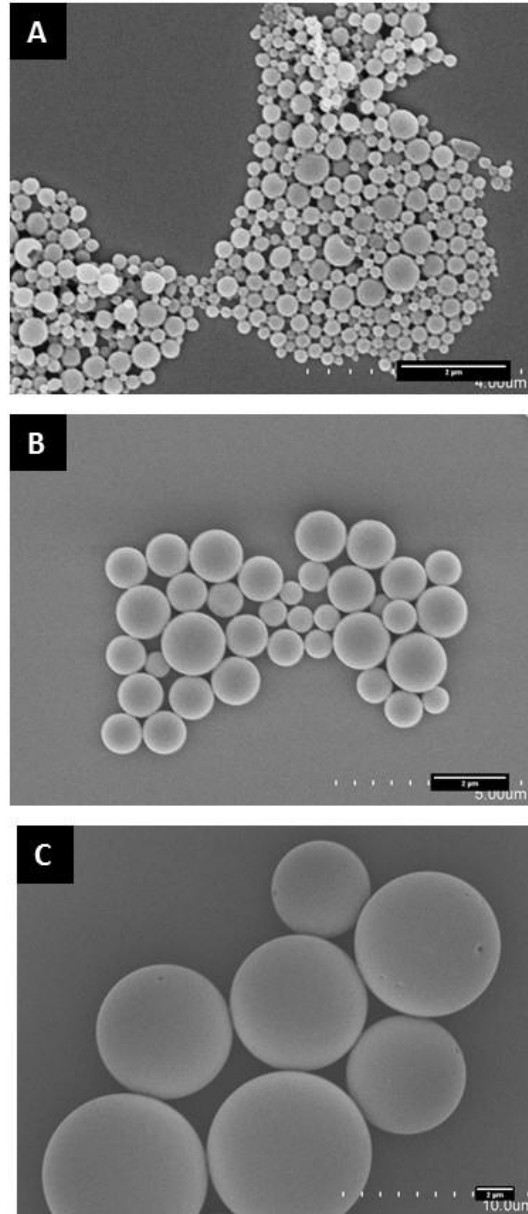
Figure 21 : Scanning electron micrographs of CpG loaded (A) Small, (B) Medium, and (C) Large sized PLGA particles. Scale bar on lower right of each micrograph represents 2 μm length.
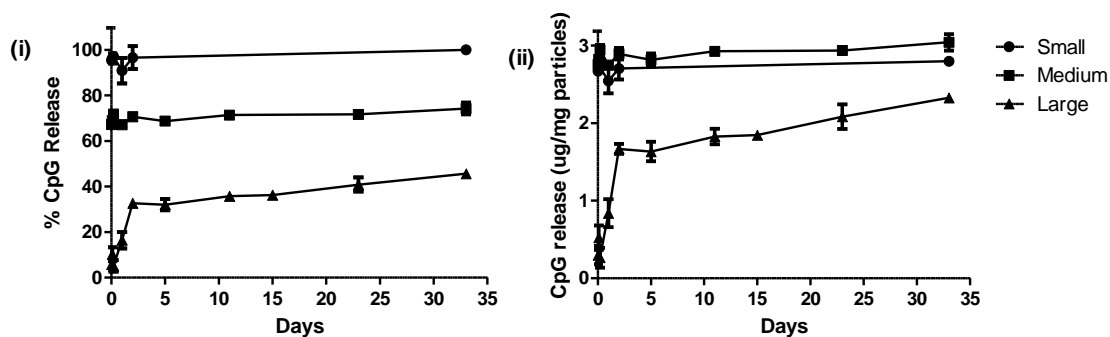
Figure 22 : Release of CpG from different sizes of PLGA particles. (i) Percentage release and (ii) amount release of CpG from different sizes of PLGA particles. Particles were incubated at 37 ˚C in an incubator shaker in PBS. Values are expressed as mean ± SEM (n = 3).
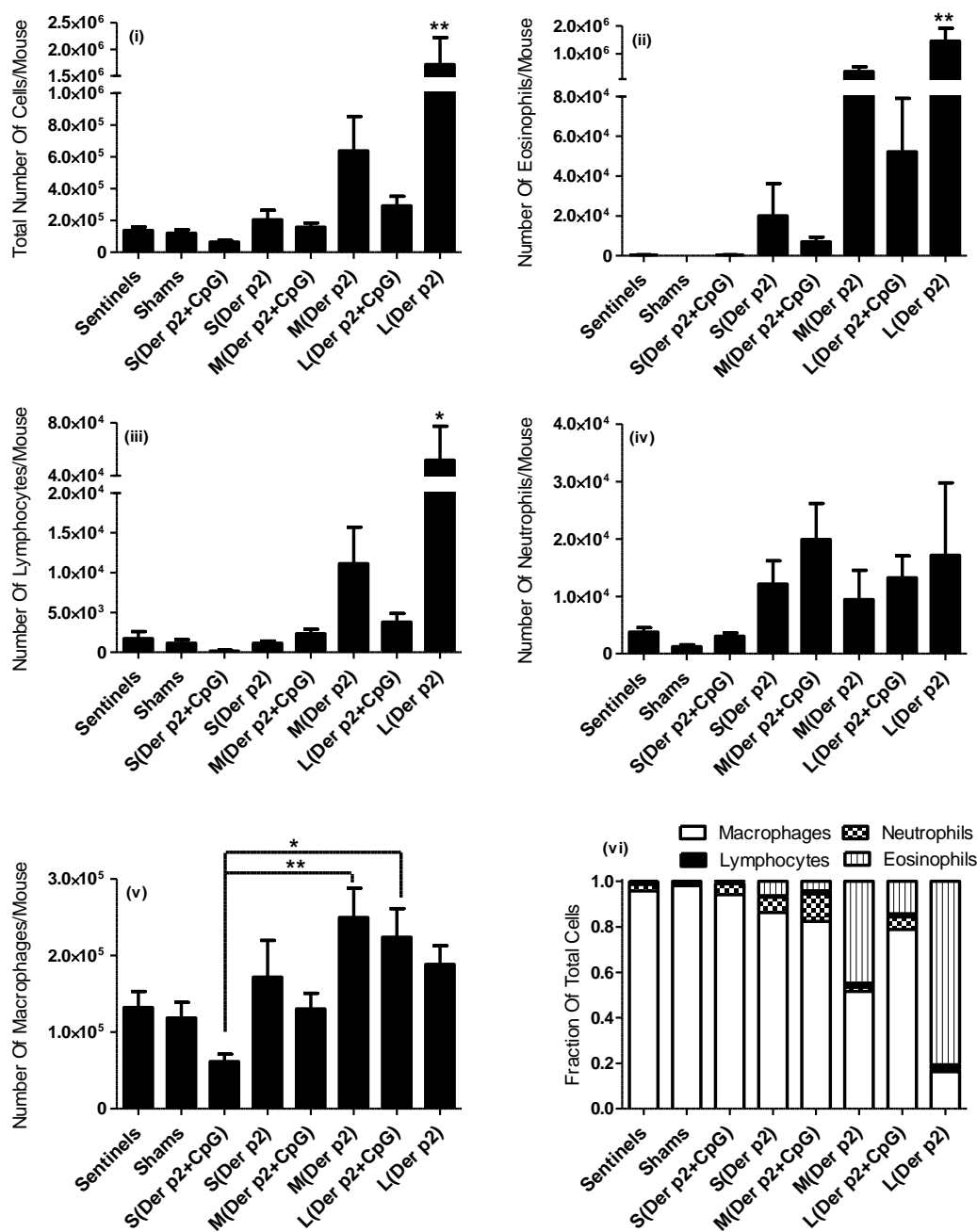
Figure 23 : Number of (i) total cells; (ii) eosinophils; (iii) lymphocytes; (iv) neutrophils and (v) macrophages in BAL fluids of vaccinated mice collected on day 24 (n = 6). (vi) Relative proportions of the different cell types in the BAL fluids of vaccinated mice on day 24. Significant differences were evaluated using one-way ANOVA followed by Tukey's post-hoc analysis. (*p < 0.05, **p < 0.01). Values are expressed as mean + SEM.
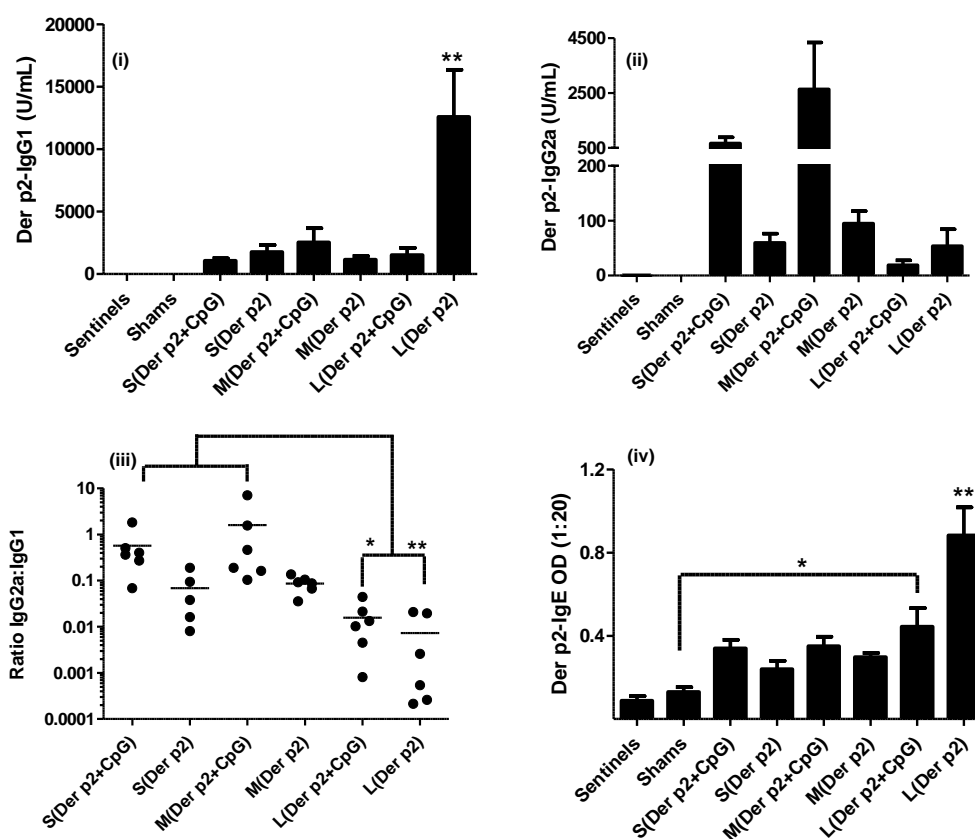
Figure 24 : Antibody levels in sera of vaccinated mice. (i) Anti-Der p2 IgG1, (ii) anti-Der p2 IgG2a, (iii) ratio of IgG2a:IgG1antibodies and (iv) anti-Der p2 IgE antibody titers were estimated in serum samples of mice collected through cardiac puncture on day 24 (n = 6). Significant differences were evaluated using one-way ANOVA followed by Tukey's post-hoc analysis. (*p < 0.05, **p < 0.01). Values are expressed as mean + SEM except in (iii) where the mean values of the ratio of IgG2a:IgG1 antibodies in each group are indicated by the solid horizontal line across the data points.
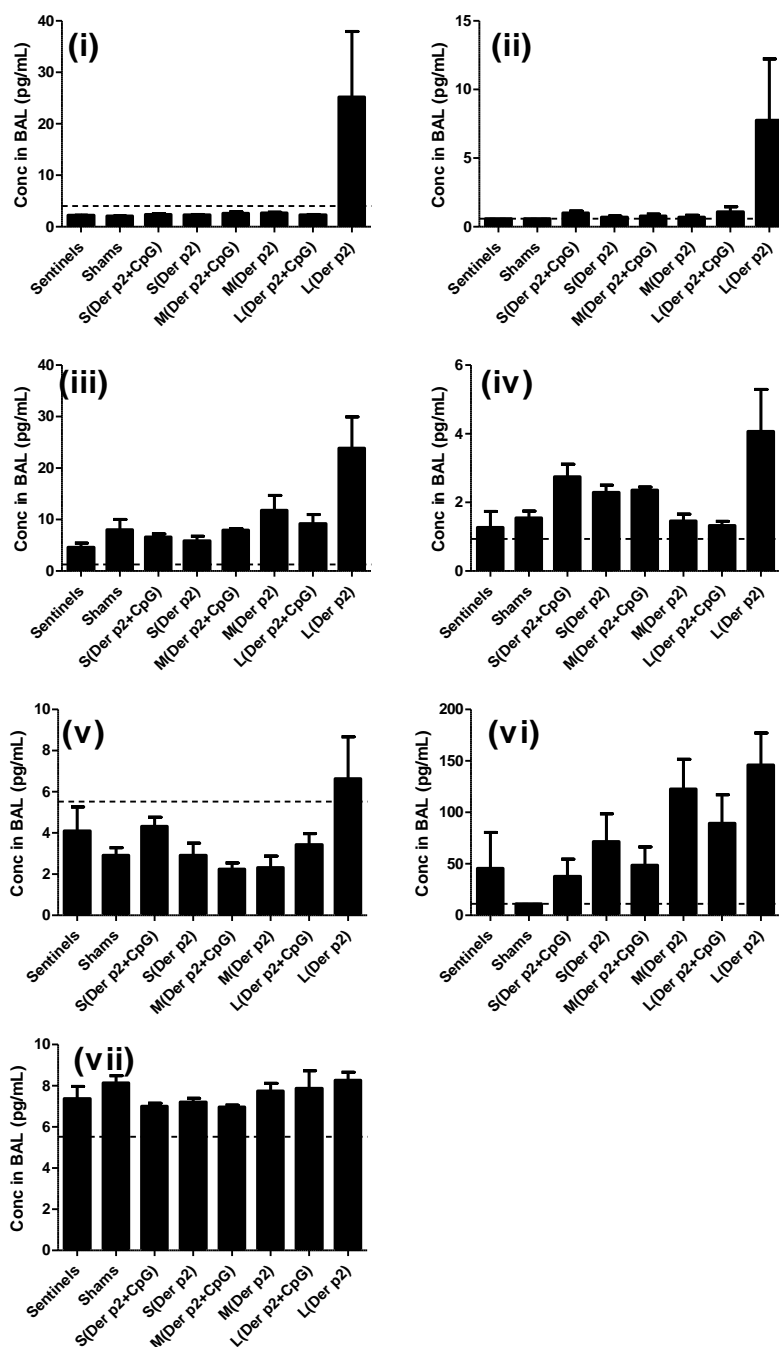
Figure 25 : The concentration of (i) IL-4, (ii) IL-5, (iii) keratinocyte-derived cytokine (KC), (iv) macrophage inflammatory protein (MIP)-1α, (v) IL-6, (vi) IFN-γ and (vii) tumor necrosis factor-alpha (TNF-α) detected in BAL fluid on Day 24. The horizontal dashed line in each graph represents limit of detection of each assay.
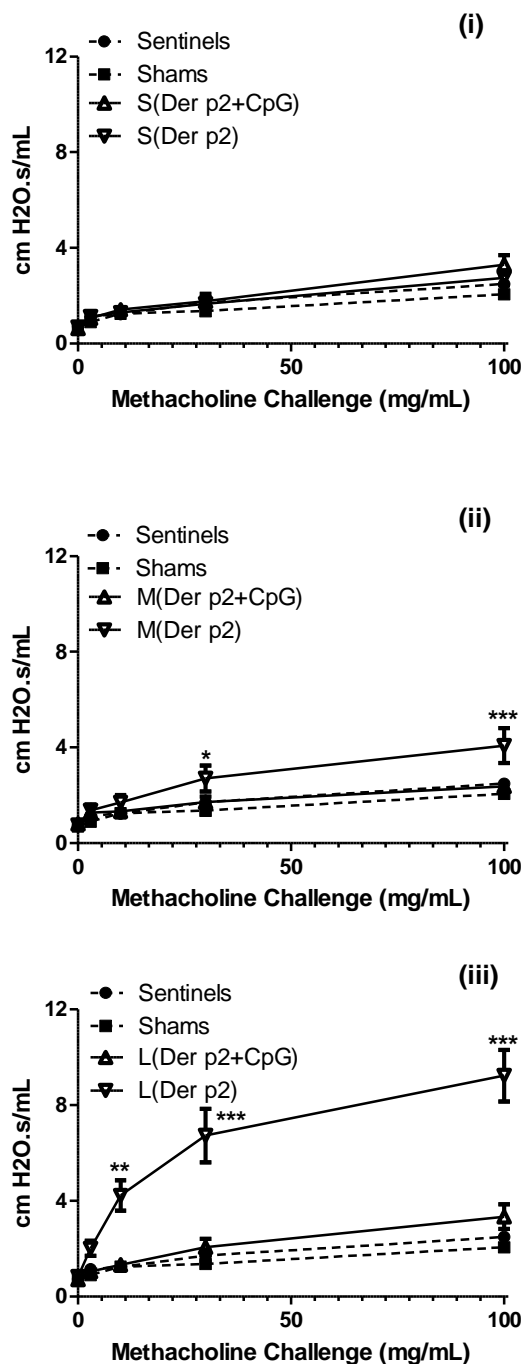
Figure 26 : Airway hyperresponsiveness (AHR) of mice vaccinated with Der p2 coated (i) small, (ii) medium and (iii) large sized PLGA particles with or without CpG (n = 6). Mice were challenged with increasing doses of methacholine on day 24. Significant differences were evaluated using one-way ANOVA followed by Tukey's post-hoc analysis (*p < 0.05, **p < 0.01, ***p < 0.001). Data represent mean ± SEM.
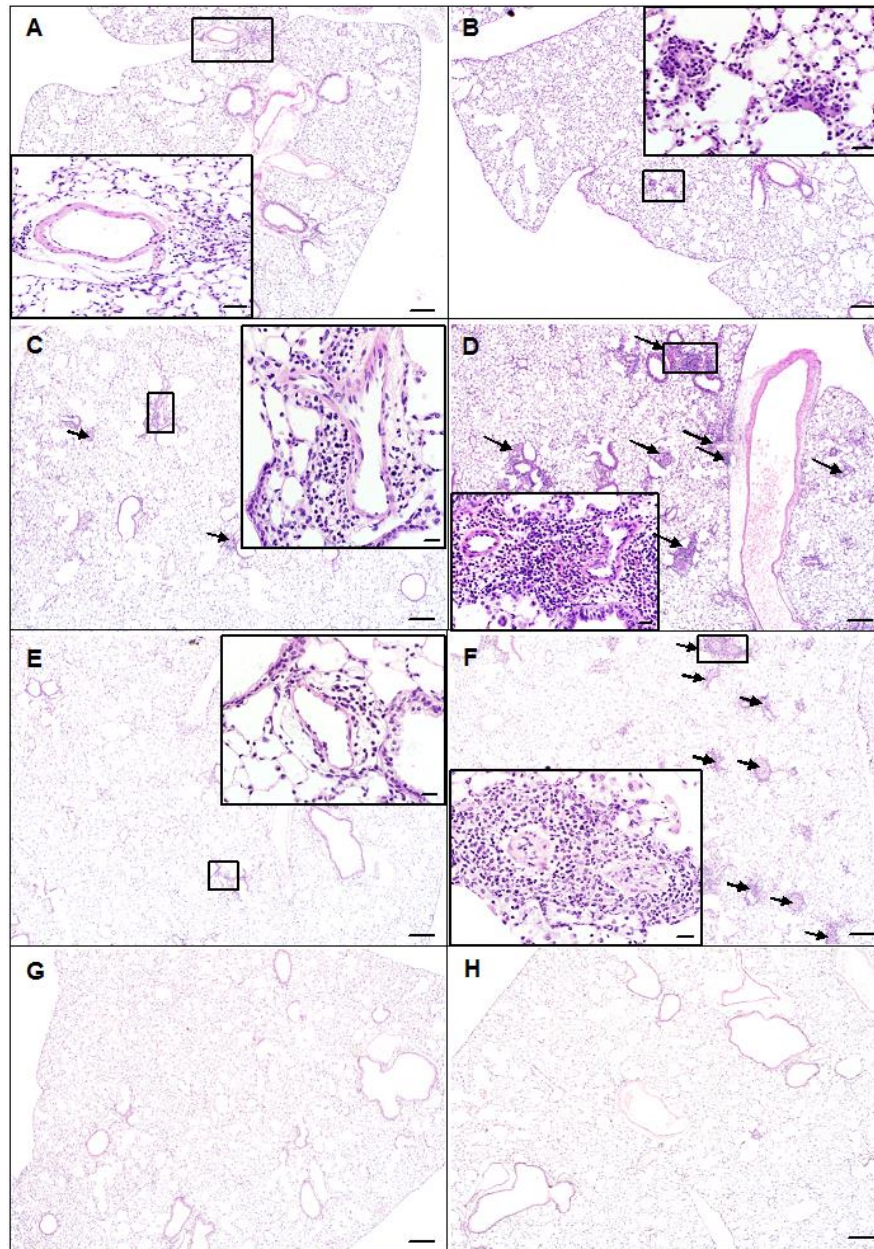
Figure 27 : Representative H&E stained lung sections of mice vaccinated with Der p2-coated on (A) small, (C) medium and (E) large sized CpG containing PLGA particles; (B) small, (D) medium and (F) large sized empty PLGA particles; (G) sentinels and (H) shams. Lung sections were collected on day 24. Arrows indicate key areas of pathology which were almost exclusively perivascular inflammatory cell infiltrates composed of macrophages and eosinophils and fewer neutrophils which are highlighted in the high resolution image inserts. Scale bar at the lower right corner of each image is 200 μm. Scale bars for high resolution image inserts are 20 μm in length.
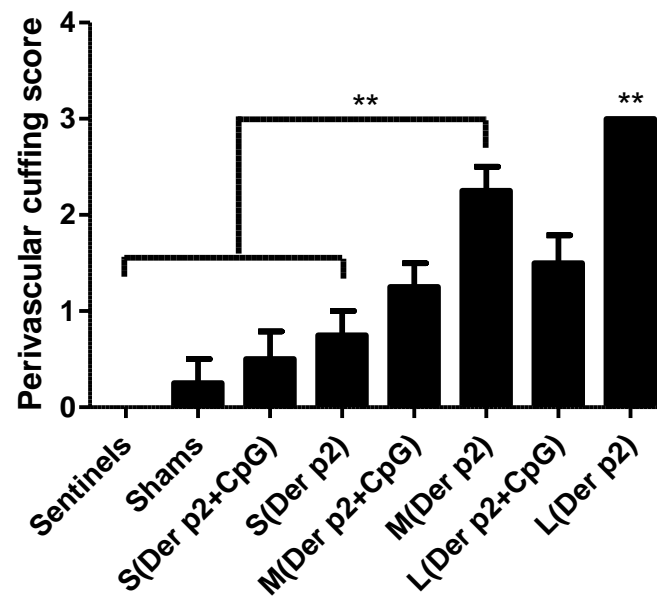
Figure 28 : Perivascular cuffing lesions (PCL) were scored in lung sections from all mice (n = 6) Significant differences were evaluated using one-way ANOVA followed by Tukey's post-hoc analysis (**p < 0.01). Values are expressed as mean + SEM.

Table 7 : Characterization of a representative batch of PLGA particles prepared using methods 1 and 2. Particles were separated into 3 different batches. The table enumerates the mean size of each batch of particles and the corresponding loading of CpG.

Batch name	Percentage weight recovered		Collection G force (xg)	Size (µm)	Loading of CpG (µg/mg particles)
	Method 1	Method 2			
Small	0.0	29.6	7000	0.3 ± 0.1	2.8
Medium	4.2	62.2	4000	1.0 ± 0.2	4.1
Large	58.4	0.0	700	9.2 ± 2.1	5.1

Table 8 : Treatment groups and experimental timeline for investigating effects of size of PLGA particles and presence of CpG in inducing protective immunity against Der p2 allergy. On day 0 and day 7 mice were vaccinated (s.c. injection) with Der p2-coated blank or CpG loaded microparticles. From day 14 to day 23, mice received 10 doses of Der p2 via intranasal instillation.

Treatment groups	Day 0 and Day 7		Day 14 to Day 23	Day 24
1. S(Der p2+CpG) Small sized PLGA particle containing CpG coated with Der p2 2. S(Der p 2) Small sized PLGA particle coated with Der p2 3. M(Der p 2 +CpG) Medium sized PLGA particle containing CpG coated with Der p2 4. M(Der p 2) Medium sized PLGA particle coated with Der p2 5. L(Der p 2 +CpG) Large sized PLGA particle containing CpG coated with Der p2 6. L(Der p 2) Large sized PLGA particle coated with Der p2	s.c. administration of 10μg Der p2 w/ or w/o 5μg CpG		Intranasal instillation of 2.5μg Der p2	(6 mice from each group were sacrificed for BAL, blood and lung histology.) Necropsy
7. Shams	s.c. administration of PBS		Intranasal instillation of PBS	
8. Sentinels	No treatment		No treatment	

CHAPTER 5: A THERAPEUTIC ANTI-CANCER VACCINE:
DOXORUBICIN AND CpG LOADED PLGA PARTICLES

Introduction

As discussed in Chapter 2, cancer is responsible for one in every four deaths in the United States (221) and is still not effectively managed therapeutically. Current conventional anti-cancer treatments include surgery, chemotherapy, and radiation administered either singly or in combination (129). Advancement in cancer therapeutics and early diagnosis have significantly improved the overall life expectancy of cancer patients in the last two decades (5). However, increasing numbers of recurrences highlight the inability of current therapies to provide complete eradication of tumors (8, 9, 222, 223). These recurrences can be potentially avoided through therapies designed to activate adaptive tumor-specific immune responses. As discussed in Chapter 1, section: "Immune response to vaccines", dendritic cell (DC)-mediated TAA-specific cytotoxic T-lymphocytes (CTL) responses are stimulated when an immunoadjuvant is co-delivered with TAA. However, it has been reported that a tumor mass contains a heterogeneous population of cells that may not all express the same TAAs (224). Therefore, stimulation of the immune system against a specific TAA may not lead to the eradication of all tumor cells from cancer patients. Thus, for therapeutic immunotherapy, it is required to stimulate T-cell immunity against multiple TAAs associated with the cancer, and this can be achieved by using a more novel approach of in-situ immunization where the tumor is induced to undergo an immunogenic cell death (225). Significant improvement in cancer patient survival has been reported with the combinatorial treatment of chemotherapy and DC-based vaccines (226-228). In another clinical trial, administration of Bacillus Calmette-Guerin (BCG vaccine) significantly reduces the progression of cancer and distant metastasis in high-risk and intermediate-risk bladder cancer patients (229). CpG, as discussed in Chapter 1, section "Adjuvants", is potent synthetic Toll-like receptor–9

agonist that promotes the activation of DCs and the generation of Th1-type immune responses (230). Administration of CpG as a cancer vaccine adjuvant has been shown to enhance protective and therapeutic immune responses against tumors in preclinical studies and has shown promising results in clinical trials (138, 231).

In a more novel approach some researchers have investigated the anti-tumor effect of combining chemotherapy with CpG administration. It has been recognized that certain chemotherapeutic drugs are independently capable of triggering an immunogenic cell death (228). Dying tumors could serve as the pool of multiple TAAs and the presence of CpG within dying tumors could stimulate tumor-specific immunity (Figure 29). Moreover, patients undergoing highly cytotoxic chemotherapy may often have compromised immune systems that fail to generate a robust anti-tumor immune response (232). Thus, the potential of combination chemo-immunotherapy could be exploited by co-administration of CpG and chemotherapeutic drug to the local environment of tumor. Combinatorial treatment of mice bearing the PC-3 human prostate carcinoma with once a week oral dose of topotecan and every third/fourth day intraperitoneal dose of CpG showed increased anti-tumor effects compared to the treatment with topotecan alone (233). Also, in a phase I/II study in lymphoma patients, intratumoral injection of CpG with low-dose radiotherapy showed enhanced anti-tumor responses at distant untreated tumor sites when compared to conventionally used therapies (234).

In the studies performed here, the aim was to develop a co-delivery system for CpG and the chemotherapeutic drug, doxorubicin (Dox). Studies have shown that tumor cells treated with Dox undergo an immunogenic cell death (235, 236). The immunogenicity of dying tumor cells can further be increased by the presence of CpG within the tumor. A recent attempt at developing formulation for co-delivery of Dox and CpG include complexation of Dox with the plasmid containing CpG motifs (237). In another attempt, Dox was complexed with bioconjugates of CpG (238, 239). In such formulation designs, Dox complexes with the phosphate backbone of CpG and is released

via decomplexation. However, these complexes could easily degrade in blood leading to uncontrolled the release of Dox systemically. Additionally, multiple intratumoral injections of these complexes were required to improve survival in a mouse tumor model (238, 239). Other recently developed formulation strategies include hydrogels and nanogels that have shown to provide sustained delivery of Dox and could potentially be used to co-entrap CpG (240, 241). In the study presented here, PLGA particles co-encapsulating Dox and CpG were designed. PLGA particle are promising delivery systems that can form depots when injected at the site of tumors and provide sustained release of Dox and CpG for long duration.

Specific aims for this study are:

1. To investigate the anti-tumor effect of Dox solution and CpG solution in a therapeutic tumor mouse model

2. To design and characterize different formulations of PLGA particles encapsulating Dox and CpG

3. To study the anti-tumor effect of different formulations of PLGA particles encapsulating Dox and CpG in a therapeutic tumor mouse model.

Materials and Methods

A therapeutic tumor model to investigate the anti-tumor
activity of Dox solution and CpG solution

A therapeutic tumor model was established using the protocol developed and optimized by Dr. Sean Geary and Dr. Caitlin Lemke of the Division of Pharmaceutics, College of Pharmacy, University of Iowa (personal communication). C57BL/6 mouse thymoma cell line, EL4 cells (American Type Culture Collection, Manassas, VA) , were maintained in RPMI 1640 media (Gibco Life Technologies, Inc., Grand Island, NY) supplemented with 10% fetal bovine serum, 1% sodium pyruvate and 0.05 mg/mL gentamycin sulphate in a humidified chamber with 5 % carbon dioxide at 37 °C.

C57BL/6 male mice, 6 to 8 weeks old, were obtained from Jackson Laboratories (Bar Harbor, ME). All animal care, housing and experimental procedures were carried out according to the requirements of the National Institutes of Health Committee on Care and Use of Laboratory Animals. Mice were challenged with tumor by subcutaneously injecting 5×10^6 EL4 cells into the right flank of the mouse on day 0. Beginning on day 4 these mice were given the following treatments (n = 4):

Dox and CpG: Each mouse received intratumoral (i.t.) injections of 25 µg of Dox solution in PBS on days 4, 6 and 8 and then 50 µg of Dox on subsequent even numbered days. Ten micrograms of CpG were administered i.t. to each mouse on odd numbered days starting from day 5.

Dox: Each mouse received i.t. injections of 25 µg of Dox on day 4, 6 and 8 and then 50 µg of Dox on subsequent even numbered days.

CpG: Ten micrograms of CpG were administered i.t. to each mouse on odd numbered days starting from day 5.

Naïve: No treatment

Tumor growth was monitored by measuring tumor dimensions every 2 – 3 days and calculating tumor volume using equation 1. Mice were sacrificed if they became morbid, developed open sores or excessive redness on the tumor surface, or if the tumor had grown more than 20 mm in one or more dimensions.

Equation 1: Tumor Volume = π/6 x [Diameter 1(mm) × Diameter 2 (mm) × Height (mm)] (138)

Fabrication of PLGA microparticles loaded with Dox and CpG

Three prototype of PLGA particles (A, B and C) described in Figure 13 were designed for co-delivery of Dox and CpG. The initial amounts of Dox and CpG used were adapted from research studies executed by Dr. Yogita Krishnamachari (personal

communication). All batches of particles were prepared using the double emulsion solvent evaporation method with a few modifications described below.

1. Admixture of PLGA particles encapsulating Dox or CpG

Three milligrams of Dox wwere dissolved in 75 µL of of 1 % poly(vinyl alcohol) (PVA; Mowiol®; Sigma, Allentown, PA) solution. A primary emulsion was prepared by emulsifying this solution in 1.5 mL of dichloromethane (DCM) containing 200 mg of PLGA 50:50 (Resomer® RG 503; PLGA 50:50 with viscosity: 0.32 – 0.44 dl/g; Boehringer Ingelheim KG, Germany) using a Sonic Dismembrator (Model FB 120 equipped with an ultrasonic converter probe CL-18; Fisher Scientific, Pittsburgh, PA) at 40 % amplitude for 30 seconds. The primary emulsion was formed using the same settings for the Sonic Dismembrator in 8 mL of 1 % PVA. This secondary emulsion was added to 22 mL of 1 % PVA which was stirred in a fume hood for 2 hours to allow the DCM to evaporate. Particles were collected by centrifugation using Eppendorf centrifuge 5804 R (Eppendorf, Westbury, NY) at 5000 rpm (4500 xg) for 5 minutes. The pellet was resuspended in 30 mL of distilled water and washed twice with 30 mL of Nanopure® water. Particles were then suspended in 5 mL of Nanopure® water and were frozen at -20 ˚C for 4 hours and lyophilized for 18 hours with a Labconco freeze dry system (FreeZone® 4.5 Liter, Model 7750020; Labconco Corporation, Kansas City, MO) at a collector temperature of -53˚C and 0.08 mBar pressure. For the preparation of CpG-loaded PLGA 50:50 ((CpG)PLGA$^{50/50}$) particles 2 mg of CpG was used instead of Dox. For the preparation of CpG-loaded PLGA 75:25 ((CpG)PLGA$^{75/25}$) particles, PLGA 75:25 (PLGA 75:25 with viscosity: 0.52 dL/g; Durect Corporation, Pelham, AL) was used.

2. (Dox/CpG)PLGA$^{50/50}$

In this formulation, Dox and CpG were co-encapsulated in the same PLGA particle matrix. However, Dox and CpG were physically separated during formation of

the w/o primary emulsion giving PLGA particles with Dox and CpG present in "different" phases, either separated or combined, within the PLGA particles (Figure 30). To prepare these particles, Dox was dissolved in 75 µL of 1 % PVA and sonicated into 100 mg of PLGA dissolved in 750 µL of DCM as described in the previous section. Similarly, CpG was dissolved in 75 µL of 1 % PVA which was sonicated in 750 µL of DCM containing 100 mg of PLGA. The two primary emulsions were combined to form a compound emulsion. PLGA particles were fabricated from this compound emulsion using the double emulsion solvent evaporation method as described previously.

3. (Dox::CpG)PLGA$^{50/50}$

In this formulation, Dox and CpG were complexed with each other and then encapsulated into PLGA particles (Figure 30). Dox (pK_a: 8.2; molecular weight: 579.98 g/mol) carries a positive charge at acidic to neutral pH. CpG (molecular weight: ~6365 g/mol) has a negative charge due to the presence of phosphate groups in the DNA backbone. Thus, complexes of Dox and CpG were prepared and encapsulated in PLGA particles. For the preparation of complexes, equal volumes of Dox and CpG solutions in 0.9 % saline were mixed and vortexed for 30 seconds. This solution was allowed to sit at RT for 30 minutes to stabilize the complexes. An optimum ratio of Dox to CpG for complexation was identified by preparation of complexes with decreasing concentrations of Dox and with increasing concentrations of CpG solutions. After identifying the optimum ratio, a concentrated solution of PVA was added to the complexes to achieve a 1% PVA solution containing complexes of Dox and CpG. Two hundred microliters of this solution was used to prepare PLGA particles using the double emulsion solvent evaporation process as described above.

Optimization of Dox and CpG loading

The encapsulation efficiency of the double emulsion solvent evaporation method was reduced due to diffusion of encapsulated molecules from solidifying particles into

the continuous external aqueous phase during the evaporation of the organic solvent. The diffusion can be reduced by adding buffer or salts in the external water phase. The use of 1% PVA in 0.1 M ammonium acetate (NH_4Ac) solution as the external water phase was used in an attempt to increase the efficiency of the double emulsion solvent evaporation process. Dox (pK_a 8.2) has a relatively low solubility at higher pH as there are more unionized molecules. Therefore, NH_4Ac solution (pH 8.4) was used as the external phase during the preparation of Dox particles. DNA from herring sperm DNA (hsDNA; Sigma, Allentown, PA) was used to optimize the formulation procedure for CpG. PLGA particles encapsulating hsDNA were prepared using the double emulsion solvent evaporation method described above with 1 % PVA in NH_4Ac solution at pH 8.4 and 1 % PVA in NH_4Ac solution at pH 4.2 as the external aqueous phase.

Preparation of NH_4Ac solutions

A stock solution of 0.2 M acetic acid was prepared by adding 11.4 mL of concentrated acetic acid to 1L water; 0.2 M NH_4OH was prepared by adding 14.92 mL of concentrated NH_4OH solution (56.6 % w/w with density 0.9 g/mL) to 1L of water; and 0.2 M NH4Ac was prepared by dissolving 15.4 g of salt in 1L water. NH_4Ac solution (pH 4.2) was prepared by dissolving 75 mL of 0.2 M NH_4Ac solution in 425 mL 0.2 M acetic acid. The final pH of the solution was achieved using acetic acid followed by the addition of water to make up the volume to 1 L. NH_4Ac solution (pH 8.4) was prepared by dissolving 26.6 mL of 0.2 M NH_4Ac solution in 473.4 mL 0.2 M NH_4OH solution. The final pH of the solution was adjusted using NH_4OH followed by the addition of water to make up the volume to 1 L.

Characterization of particles

The morphology of the particles was examined using scanning electron microscopy. Presence of crystals in the final formulations was examined using powder X-

ray diffraction. Differential scanning calorimetry (DSC) was used to study any change in the glass transition temperature of the lyophilized particles encapsulating Dox and CpG.

Scanning Electron Microscopy (SEM)

SEM micrographs were obtained as described in Chapter 2, section "Scanning electron microscopy (SEM)". Briefly, particles suspensions were placed on a silicon wafer mounted on SEM stubs. They were then coated with the gold-palladium by an argon beam K550 sputter coater (Emitech Ltd., Kent, England). Images were captured using the Hitachi S-4800 SEM at 8 kV accelerating voltage. Size and charge of particles were measured using a Zetasizer Nano ZS particle analyzer (Malvern Instrument Ltd., MA) using the protocol described in Chapter 2, section "Particle size and zeta potential".

Powder X-ray diffraction (XRD) patterns

Powder XRD patterns for $(Dox/CpG)PLGA^{50/50}$, $(Dox)PLGA^{50/50}$, and blank PLGA particles were obtained using a Bruker D-5000 diffractometer equipped with a Kevex energy-sensitive detector. Patterns were recorded starting from a 2θ angle of $10.0°$ to $49.9°$ with an increment of $0.059°$ at every step. All analyses were performed at RT.

Differential scanning calorimetry (DSC)

One to three milligrams of sample were sealed in an aluminum sample pan using a Perkin-Elmer pan sealing tool. A reference pan was sealed without sample. The sample pan was placed on the left-side base and reference pan on the right side base of the furnace in the DSC apparatus. Samples were scanned at a rate of 10 °C/min under a nitrogen atmosphere using Perkin Elmer DSC 7 (Perkin Elmer, Alameda, CA) and analyzed using Pyris™ software.

Estimation of *in-vitro* release of Dox and CpG from PLGA

particles

Time dependent release of Dox and CpG from PLGA particles was studied in phosphate buffered saline (PBS) at pH 7.4. In a glass vial, 50 mg of particles was added to 3 mL of PBS which was previously heated to 37 ˚C. The vials were covered with aluminum foil and transferred to a 37 ˚C incubator shaker set at the speed of 200 rpm/min. Samples were collected at predetermined time points and the volumes removed were replaced by fresh PBS maintaining the sink condition for Dox and CpG. Concentrations of Dox and CpG in samples were estimated as described below. Percentage cumulative release of Dox and CpG were plotted with respective to time.

Quantification of Dox and CpG encapsulated in PLGA

particles

For estimation of Dox loading, 10 mg of particles from each batch was dissolved in 1 mL of dimethyl sulfoxide (DMSO). Dox was quantified as described in the next section. For estimation of CpG loading, 20 mg of particles from each batch was treated with 0.2 N NaOH for 12 hours. Once the particles had degraded (i.e. a clear solution was obtained), they were neutralized using 0.2 N HCl and loading was calculated using Equation 2. Encapsulation efficiency of Dox and CpG were calculated using Equation 3.

Equation 2: Loading (µg/mg PLGA particles) = [Calculated conc. (µg/mL) x Volume of neutralized solution of degraded PLGA particles (mL)]/Initial weight of PLGA particles (mg)

Equation 3: EE = [Loading of drug (µg/mg) x amount of PLGA particle recovered (mg)]/ Initial weight of drug (µg)

where, Loading = µg Dox or CpG encapsulated per mg of particles, Calculated conc. = calculated concentration of Dox or CpG from standard curve (µg/mL).

Quantification of Doxorubicin (Dox)

Quantification of Dox was performed using fluorescence spectroscopy. Known concentrations of Dox were prepared in DMSO (Fisher Scientific, Pittsburgh, PA) or PBS (pH 7.4, Gibco Life Technologies Inc., Grand Island, NY). These standard solutions and samples were added to a 96-well plate (100 μl/well). Fluorescence was measured at λ_{ex} 444 nm and λ_{em} 585 nm using a SpectraMax® M5 multi-mode microplate reader (Molecular Devices, Sunnyvale, CA). A standard curve was generated with solutions of known concentration of Dox.

Loss of Dox fluorescence in phosphate buffered saline

Dox showed time dependent loss of fluorescence in PBS at 37 ˚C (242). To quantify the degradation rate, solutions of Dox at known concentration (30 μg/mL, 20 μg/mL and 15 μg/mL) were incubated in PBS at pH 7.4 in a 37 ˚C incubator shaker. The concentration of Dox in the solution was quantified at different time points. Estimated concentration (C_t) at different time points were normalized by the initial concentration of the solution to obtain the fraction of Dox remaining in the solution at each time point. A log-plot was graphed for fraction of Dox remaining vs time. The slope of the regression lines were used to correct for the concentration of Dox in released samples.

Quantification of CpG

Quant-iT™ OliGreen® ssDNA Assay Kit (Invitrogen, Carlsbad, CA) was used according to the manufacturer's protocol to quantify CpG concentrations. Concentrations of CpG in samples from loading and release studies were determined using the procedure described in Chapter 2, section "Quantification of CpG".

Evaluation of the in vitro cytotoxicity of Dox and CpG complexes

CellTiter 96® Aqueous One solution Reagent (Promega Corporation, WI) was used to estimate the cytotoxicity of Dox-CpG complexes in EL4 cells. Ten thousand cells per well were plated into 96-well plates for 24 hours. Cells were treated with 1.33 µg/ mL dose of Dox in the form of Dox-CpG complexes prepared with different ratios of Dox and CpG. Cells treated with Dox solution and untreated cells were used as controls for the experiment. The plate was incubated at 37°C with 5% CO_2 for 12 hours followed by centrifugation of cells at 230 xg for 5 minutes. Supernatants from each well were discarded and replaced with 100 µL of fresh media containing 20% v/v of the MTS tetrazolium compound included in CellTiter 96® kit. After 4 h of incubation of cells with the MTS reagent at 37°C with 5% CO_2, the absorbance was recorded at 490 nm using a Spectra Max® plus 384 Microplate Spectrophotometer (Molecular Devices, CA). Relative cell viability values are expressed as the percentage of absolute absorbance from wells containing treated cells compared to the control wells containing untreated cells.

Therapeutic tumor model to investigate anti-tumor activity of PLGA particles encapsulating Dox and CpG

A murine therapeutic tumor model was established as mentioned above with a few modifications. C57BL/6 mice were subcutaneously injected with 10^6 EL4 cells on day 0. Two independent studies were conducted to evaluate the effect of PLGA particles encapsulating Dox and CpG on tumor growth and mouse survival as described in Table 13. In study 1, mice were treated on day 7 with i.t. injections of 100 µg of Dox and 50 µg of CpG encapsulated in PLGA particles. In study 2, mice were treated on day 3 with i.t. injections of 100 µg of Dox and 100 µg of CpG encapsulated in PLGA particles. The following treatment groups were included in each study (n = 4):

1. (Dox)PLGA$^{50/50}$: PLGA 50:50 particles encapsulating Dox

2. $(Dox/CpG)PLGA^{50/50}$: PLGA 50:50 particles co-encapsulating Dox and CpG

3. $(Dox)PLGA^{50/50}(CpG)PLGA^{50/50}$: Admixture of PLGA 50:50 particles encapsulating Dox and PLGA 50:50 particles encapsulating CpG

4. $(Dox)PLGA^{50/50}(CpG)PLGA^{75/25}$: Admixture of PLGA 50:50 particles encapsulating Dox and PLGA 75:25 particles encapsulating CpG

5. Naïve: No treatment

Tumor progression was monitored with respect to time using equation 1. Mice were sacrificed if the tumor became inflamed or blistered or grew more than 20 mm in at least one dimension.

Statistical Analysis

Groups were compared by one-way analysis of variance (ANOVA) to analyze if the mean values of treatment groups were different. This was followed by Tukey post-hoc analysis to compare all pairs of treatments and identify pairs of the treatment groups that showed significant differences ($p<0.05$) in their mean values. Survival curves of treatment groups follow a right skewed distribution. Thus, analysis of survival curves was performed using a non-parametric log-rank (Mantel-Cox) test. All statistical analyses were performed using Prism 5 (GraphPad Prism, La Jolla, CA). P-values < 0.05 were considered statistically significant.

Results

Combination of Dox and CpG treatment decreases tumor progression

EL4 tumor bearing mice were treated with intratumoral injections of Dox and CpG on alternating days. Untreated mice and mice treated with CpG possessed rapidly growing tumors and were sacrificed by day 10. Mice treated with Dox and Dox-CpG

combination exhibited slower growth of tumors by comparison as shown in Figure 31. As shown in the survival curve (Figure 32), treatment with CpG alone did not enhance survival whilst the combination of CpG with Dox resulted in enhanced survival. Median survival of mice treated with the Dox-CpG combination was found to be 28.5 days as compared to Dox treatment which was only 20 days. This confirms that the anti-tumor activity of Dox is enhanced by the combinatorial treatment.

Preparation of PLGA particles encapsulating Dox and CpG

Ammonium acetate solution enhances the loading of Dox
and CpG in PLGA particles

     PLGA particles were prepared using the double emulsion solvent evaporation process. NH_4Ac solution (0.1 M) was used as the external water phase to enhance the loading of Dox and CpG into PLGA particles. Dox is a weak base (pK_a: 8.25). As pH levels increase, the fraction of unprotonated species of Dox increases which decreases the total solubility of Dox. Also, the presence of dissolved NH_4Ac salts increases the osmotic pressure of the external water phase further preventing the diffusion of Dox out of the solidifying PLGA particles during the evaporation of organic solvents. Similarly, oligodeoxynucleotides (ODNs) have phosphate backbones that have a greater number of unprotonated molecules at an acidic pH. Thus, NH_4Ac solution with pH 4 was evaluated to improve loading of ODNs in PLGA particles. The combination of increasing the osmotic pressure and decreasing the solubility of encapsulated molecules can increase the loading of Dox and CpG in PLGA particles. As shown in Table 9, loading of Dox was improved when particles were prepared with NH_4Ac solution (pH 8). Loading of hsDNA also increased in NH_4Ac solution (pH 8) due to increased osmotic pressure in the external water phase. Using NH_4Ac solution (pH 4) further enhanced the loading of hsDNA in PLGA particles. For the preparation of Dox and CpG co-loaded particles, 0.1 M NH_4Ac solution (pH 8) was chosen as the external water phase. As shown in Table 9,

using NH_4Ac (pH 8) as the external phase resulted in higher loading of CpG when compared to particles prepared in the absence of NH_4Ac solution. PLGA particles encapsulating Dox or CpG were prepared using 1% PVA solution in 0.1 M NH_4Ac solution (pH 8) as the external phase during the double emulsion solvent evaporation.

Preparation of admixtures of particles encapsulating Dox or
CpG

PLGA particles encapsulating Dox or CpG were successfully prepared using the double emulsion solvent evaporation method. These particles had a smooth morphology (Figure 33). The final formulation was a physical mixture of lyophilized powder of Dox-loaded PLGA particles and lyophilized powder of CpG-loaded PLGA particles.

Preparation of (Dox/CpG)PLGA$^{50/50}$

As mentioned in the previous section, a modified procedure of the double emulsion solvent evaporation process was utilized to prepare (Dox/CpG)PLGA$^{50/50}$ particles. Dox and CpG solutions were independently emulsified in PLGA solution in DCM that generated a water-in-oil primary emulsion with Dox and CpG droplets suspended independently in PLGA solution. During further processing of this emulsion to form PLGA particles, Dox and CpG droplets were fused together giving compartment of water phase with Dox and CpG. Hence, in this formulation, Dox and CpG are suspended either independently or in same compartment within a PLGA particle matrix.

As shown in Figure 34, PLGA particles co-encapsulating Dox and CpG were amorphous when analyzed with PXRD confirming the absence of any crystal structure of Dox or CpG. These particles showed smooth morphology (Figure 33). Table 10 shows the loading and percentage encapsulation efficiency of Dox and CpG in these particles. It was found that loading, but not the encapsulation efficiency, of these molecules was affected by the initial amount of Dox and CpG used for the preparation. Particles with different loading of Dox and CpG were mixed to achieve the required ratio of Dox to

CpG dose for animal experiments. DSC thermograms in Figure 34 (a) confirmed that presence of Dox in the particle does not change the glass transition temperature (T_g) of the formulation. However, (Dox/CpG)PLGA$^{50/50}$ showed a shoulder in DSC thermograms before the T_g peak which suggests that encapsulated molecules had physical interactions with the polymer. This can change the *in-vitro* or *in-vivo* characteristics of the formulation. The PXRD pattern displayed in Figure 34 (b) indicate the amorphous nature of all particle formulations.

Preparation of (Dox::CpG)PLGA$^{50/50}$

Dox was complexed with CpG for the preparation of this formulation. As shown in Table 11, complexes were prepared using different ratios of Dox and CpG to achieve the optimum size required for the preparation of PLGA particles. It was found that particles size and PDI of prepared complexes decreased with decreasing ratios of Dox:CpG with 4:1 giving complexes of size 454 nm and PDI of 0.6. This ratio was chosen for further experiments as it resulted in the smallest size of complexes with minimum polydispersity. PLGA particles could be prepared by adding 1 - 3 mg of Dox or CpG to the internal water phase, which typically had a volume between 75 μl to 200 μl. Thus, a concentrated solution of Dox-CpG complexes was required to prepare (Dox::CpG)PLGA$^{50/50}$ particles. As shown in Figure 35, the sizes of the complexes were found to increase by increasing the concentration of Dox and CpG solution to prepare complexes. Also, adding excess water to the complexes resulted in decomplexation of Dox and CpG suggesting that the complexes were unstable. An *in-vitro* treatment of EL4 tumor cells with Dox-CpG complexes showed that Dox was reduced in potency when complexed with CpG (Figure 36). In this experiment 1.33 μg/mL of Dox solution was complexed with decreasing concentrations of CpG (2.66 μg/mL to 0.04 μg/mL). Higher amounts of CpG complexes greater amounts of Dox, thereby reducing its potency, which in turn led to an increase in the cell viability of EL4 cells. Cells treated with CpG alone

showed the same viability as cells with no treatment. As complexation of CpG reduces cytotoxic activity of Dox, this formulation strategy was not developed for any further experiments.

Release of Dox and CpG from PLGA particles

<u>Incubation of Dox in PBS at 37 ˚C showed time</u>

<u>dependentloss in fluorescence</u>

Solutions of Dox with known concentrations were kept at 37 ˚C incubator shaker in glass vials covered with aluminum foil. As shown in Figure 37, different concentrations of Dox showed time-dependent decreases in fluorescence. The ecreasing value of the y-intercept in regression equations (Figure 37 (ii)) suggest that, though small in value, the initial concentration might have a contribution to the rate of loss of the fluorescence. Assuming a first-order decrease in fluorescence, an average rate of loss of fluorescence, k, was calculated with the slope of the regression lines from Figure 37 (ii). Samples of Dox solution which were collected during the release study of Dox from PLGA particles were corrected to obtain a more accurate determination of the Dox concentration released using the following equation.

Equation 4: $\log(C_t/C_o) = kt$

where, C_t = concentration of Dox solution calculated at time t; C_o = true Dox concentration; k = rate of loss of fluorescence(25.3×10^{-4}); t = time.

<u>Dox and CpG encapsulated in PLGA particles showed</u>

<u>burst release followed by sustained release</u>

PLGA particles encapsulating Dox and CpG exhibited burst release followed by sustained release of encapsulated molecules. Dox showed time dependent loss of fluorescence when incubated in PBS at 37 ˚C. The concentration of Dox in samples

collected from the release studies was corrected using equation 3 with an assumption that Dox in the PLGA particles was in contact with PBS solution during the *in vitro* release studies. As shown in Figure 38 (i), Dox encapsulated in PLGA particles showed a significantly higher percentage release as compared to Dox released from $(Dox/CpG)PLGA^{50/50}$. This may be due to the interaction of encapsulated Dox and CpG with PLGA polymer that was also observed in DSC thermograms in Figure 34 (a). The presence of Dox and CpG in PLGA particles showed a thermal event around $35°C$, before reaching the T_g at approximately $42 °C$. This can lead to the conversion of PLGA particles into a partially glassy state at $37°C$ leading to decreased diffusion of encapsulated molecules from $(Dox/CpG)PLGA^{50/50}$. Also, CpG present in $(Dox/CpG)PLGA^{50/50}$ can from complexes with Dox molecules causing reduced release of Dox from $(Dox/CpG)PLGA^{50/50}$ with no significant effect in the release rate of CpG from $(Dox/CpG)PLGA^{50/50}$ when compared to release of CpG from $(CpG)PLGA^{50/50}$. Further studies, are required to better understand the reason for the decreased release of Dox from $(Dox/CpG)PLGA^{50/50}$. The release rate of CpG from $(Dox/CpG)PLGA^{50/50}$ particles and CpG particles encapsulated in PLGA 50:50 were similar. The percentage release of CpG from PLGA 75:25 particles was marginally and insignificantly less than from PLGA 50:50 (Figure 38 (ii)).

<div align="center">

PLGA particles co-encapsulating Dox and CpG decreased

tumor progression
</div>

PLGA particles encapsulating Dox and CpG, alone or in combination were successfully prepared and the results of the loading of Dox and CpG are described in Table 12. EL4 tumor bearing mice were treated with these PLGA particles encapsulating Dox and CpG. Treatments (described in Table 13) were initiated when tumors reached a palpable size. In study 1, tumors were treated on day 7 with different formulations of Dox and CpG. Wherever applicable, each mouse was treated with 100 µg of Dox and 50 µg of

CpG. As shown in Figure 39 (A), all naïve mice were sacrificed by day 13 whereas mice treated with admixtures of Dox and CpG particles as well as mice treated with only Dox particles showed improved survival. However, there was no significant difference between these treatments. Mice treated with (Dox/CpG)PLGA$^{50/50}$ particles showed enhanced survival (Figure 40 (A)) over other treatment groups suggesting that (Dox/CpG)PLGA$^{50/50}$ is the best formulation strategy among those tested to treat growing tumors. To evaluate any potential differences in the efficacy of the admixture of Dox and CpG particles versus Dox particles only, another experiment was conducted in which the dose of CpG was increased from 50 µg to 100 µg/mouse. The Dox dose was kept constant at a 100 µg/mouse. As shown in Figure 39 (B), all naïve mice needed to be sacrificed by day 9. Mice treated with (Dox/CpG)PLGA$^{50/50}$ or (Dox)PLGA$^{50/50}$ (CpG)PLGA$^{75/25}$ showed an initial reduction in tumor growth. However, all groups treated with either the admixture of Dox and CpG particles or Dox only particles showed no significant improvement in survival as shown in Figure 40 (B). In study 2, mice treated with (Dox/CpG)PLGA$^{50/50}$ showed enhanced survival compared to all other treatment groups (Figure 40 (B)). Both these studies confirmed that EL4 challenged mice had improved survival when therapeutically treated with (Dox/CpG)PLGA$^{50/50}$. Also, the admixture of Dox and CpG particles did not show any improvement in survival when compared to treatment with (Dox)PLGA$^{50/50}$.

<div align="center">Discussion</div>

Advanced combinatorial treatments with surgery, radiation and chemotherapy have led to improvements in the survival of cancer patients, but reoccurrences of tumor or metastases still remain the major concern (243-245). A prospective combination of chemo and immunotherapy has been tested in clinics where stimulation of immunity against cancer along with administration of chemotherapeutic drugs have shown significant enhancement in survival of cancer patients (246). In Figure 31 and Figure 32,

it was shown that i.t. injections of Dox with CpG on alternate days can enhance the survival in tumor bearing mice. However, frequent injections of Dox and CpG caused skin inflammation, redness and ulceration at the site of injection. Similar observations have been recorded in clinics where multiple administrations of adjuvants led to inflammation of local tissue (247, 248). To prevent this local inflammation caused by multiple injections of soluble doses of Dox and CpG, PLGA particles were desigened that provided sustained release of these molecules. One time administration of these particles can potentially deliver Dox and CpG in the tumor milieu for longer durations of time than soluble Dox and CpG. PLGA particles encapsulating the water soluble molecules were fabricated by a double emulsion solvent evaporation method. One major drawback of this method is that it reduces encapsulation efficiency of Dox and CpG due to the diffusion of encapsulated molecules into the external water phase during processing. In this study, it was shown that the encapsulation efficiency of these molecules can be improved by using 0.1 M NH_4Ac solution in the external water phase which decreased the solubility of these molecules in the external medium. This, in turn, decreased the concentration gradient of encapsulated molecules resulting in decreased diffusion of the encapsulated molecules to the external water phase. Thus, the use of 0.1 M NH_4Ac solution in the external water phase increased the loading and encapsulation efficiency of Dox and CpG into PLGA particles. One of the major challenges associated with developing delivery systems for co-delivery of Dox and CpG is the opposite charges of these molecules. The physical association of these molecules can influence their spatial organization in the particle matrix and can affect diffusion, the release kinetics and the *in-vivo* efficacy of the particles. In this study, it was discovered that complexation of Dox with CpG decreased the *in vitro* cytotoxicity of Dox (Figure 36). Thus, for co-delivery of Dox and CpG three PLGA-based formulation strategies were designed, characterized and and evaluated   as sustained delivery systems of Dox and CpG. In the first formulation, (Dox/CpG)PLGA$^{50/50}$, Dox and CpG molecules were

present in "different" sub-compartments within the PLGA particle matrix. To formulate these particles two independent emulsions of Dox and CpG were prepared in DCM solutions containing PLGA polymer. On combining these emulsions, a stable compound primary emulsion was formed that contained aqueous droplets of Dox and CpG suspended independently in the PLGA solution. Emulsification of Dox and CpG in two independent PLGA solutions limits any possible spatial interaction of Dox and CpG in the PLGA particle matrix. Particles prepared from this method showed smooth morphology and sustained release of Dox and CpG (Figure 33 and Figure 38). In the second formulation prototype, the aim was to encapsulate uniformly sized nanocomplexes of Dox and CpG in PLGA particles. However, it was found that varying ratios of Dox and CpG resulted in the formation of non-uniform complexes with large polydispersity. Also, increasing the concentration of Dox and CpG solution during complexation increased the size of complexes to the micron range and these complexes could not be encapsulated into PLGA particles. Unstable complexation of Dox with CpG in combination with a decrease in the potency of Dox when complexed with CpG could be the main reason for the failure of this formulation at later stages of development. Thus this strategy was not pursued further. A third formulation propotype included the admixture of PLGA particles independently encapsulating either Dox or CpG. In this formulation CpG particles were prepared with PLGA 50:50 and PLGA 75:25 to study if delayed release of CpG could enhance the *in-vivo* efficacy of this formulation. CpG encapsulated in PLGA 75:25 showed a decrease in the rate of release of CpG when compared to CpG encapsulated in PLGA 50:50. However, these particles showed similar results when used in an *in-vivo* therapeutic tumor mouse model.

The *in-vivo* activity of PLGA particles to enhance survival of tumor bearing mice was evaluated in a therapeutic tumor mouse model. Each mouse was treated with 100 µg of Dox and 100 µg or 50 µg of CpG in study 1 and study 2, respectively. In both independent studies, treatment of tumor bearing mice with (Dox/CpG)PLGA$^{50/50}$

significantly reduced tumor growth and increased survival of mice. Admixtures of Dox particles and CpG particles showed marginal improvement in survival of mice when compared to treatment with PLGA particles encapsulating Dox only. This study showed that enhanced survival can be achieved by a combination of chemotherapy and immunotherapy. The combination treatment is further improved with co-administration of Dox and CpG together in PLGA particles.
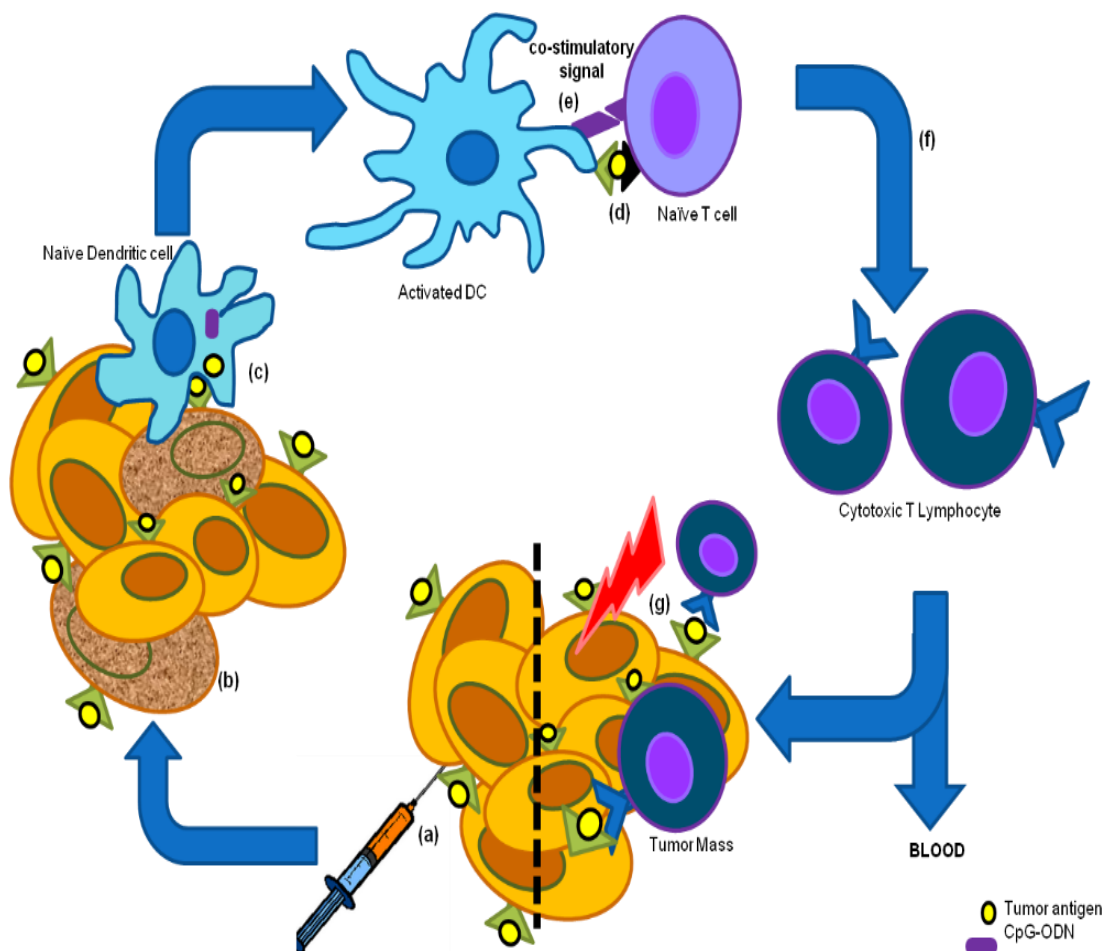
Figure 29 : Mechanism of induction of antigen-specific T-cell immunity by biodegradable particles: PLGA particles co-encapsulating Dox and CpG (a) are injected into the tumor mass. Dox released from PLGA particles induces immunogenic apoptotic tumor cell death (b). Tumor antigens released by dying tumor cells and CpG released from the particles are phagocytosed by naïve dendritic cells (DCs) (c). CpG induces activation of DCs that are characterized by enhanced antigen presentation (d) and upregulation of costimulatory molecules (e). Mature DCs travel to lymph node where they present tumor antigen with co-stimulatory signals to naïve tumor-specific CD8 cells resulting in their activation to cytotoxic T-lymphocytes (f) which circulate through peripheral blood and target cells (tumor) carrying the antigen inducing their death (g).

A: Admixture of Dox and CpG particles

B: (Dox/CpG)PLGA$^{50/50}$

C: (Dox::CpG)PLGA$^{50/50}$
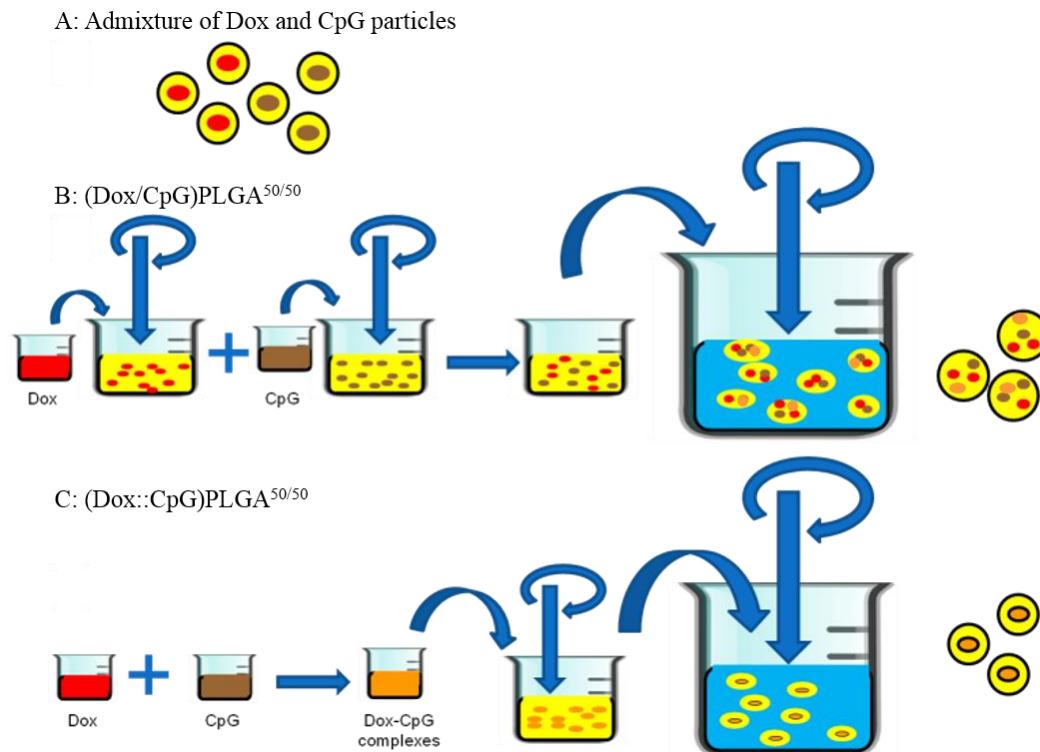
Figure 30 : Formulation prototypes of PLGA particles for co-delivery of Dox and CpG. (A) Admixture of Dox and CpG particles: Lyophilized powder of PLGA particles encapsulating Dox were mixed with lyophilized PLGA particles encapsulating CpG. These particles were prepared using double emulsion solvent evaporation. (B) (Dox/CpG)PLGA$^{50/50}$: Dox and CpG were encapsulated independently and in combination into PLGA particle matrices. To prepare these particles, Dox and CpG were emulsified independently in PLGA solution. These primary emulsions were combined to achieve the compound primary emulsion which was again emulsified in aqueous phase to prepare PLGA particles co-loaded with Dox and CpG. (C) (Dox::CpG)PLGA$^{50/50}$: Dox and CpG were encapsulated together in the PLGA particles matrix. To prepare these particles, complexes of Dox and CpG were encapsulated in PLGA particles using double emulsion solvent evaporation method.
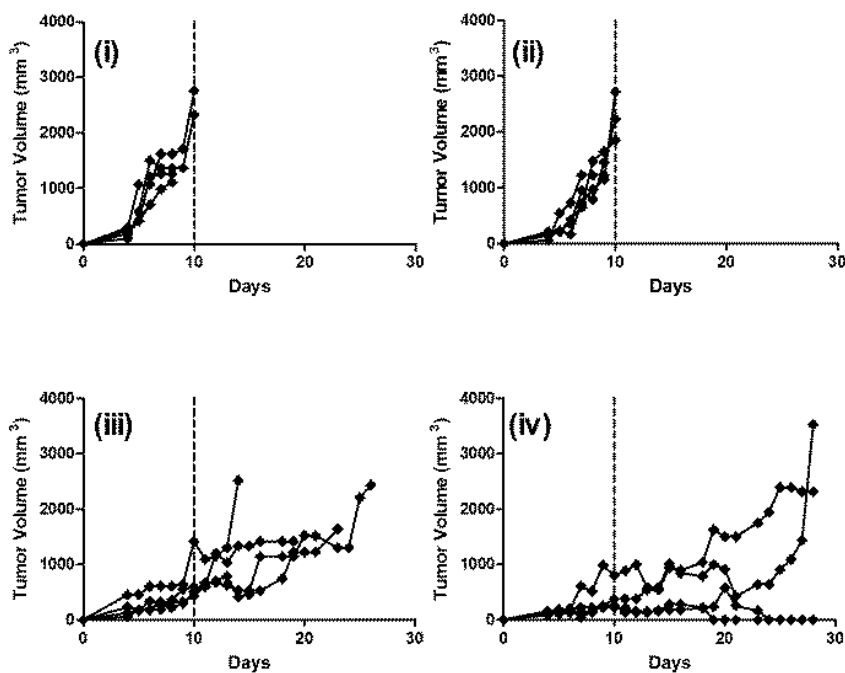
Figure 31 : Anti-tumor effect of Dox and CpG treatment in tumor bearing mice. Mice were challenged with EL4 cells and treated on alternate days with: (i) No treatment; (ii) CpG solution; (iii) Dox solution and (iv) Dox solution on day 1 and CpG solution on the other day. Vertical dashed line represents the time point at which all mice from the naïve group were euthanized due to large tumor size. Each curve represents tumor growth for each mouse of the group (n = 4).
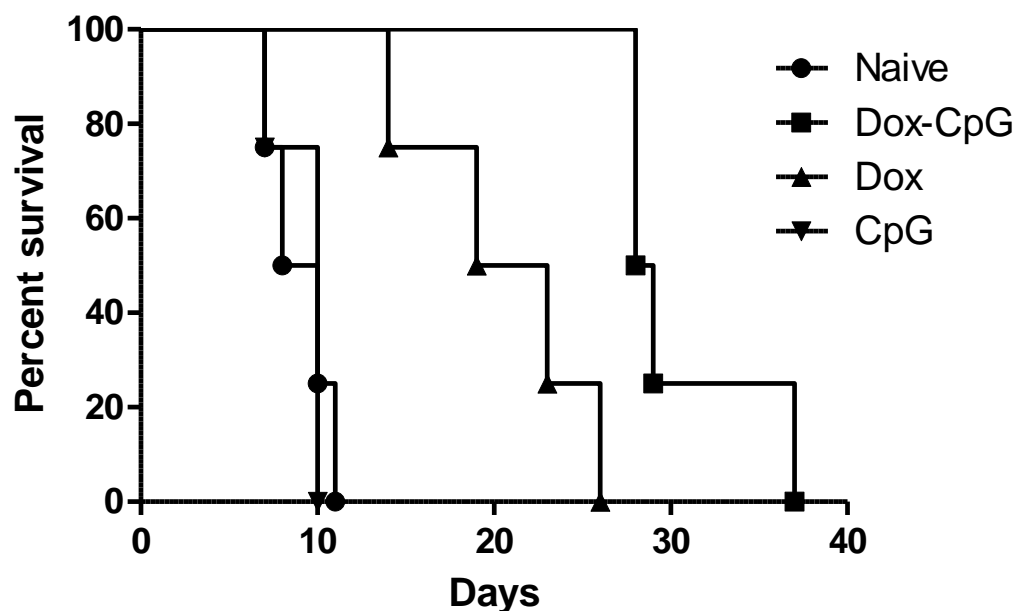
	Naive	Dox-CpG	Dox	CpG
Median Survival (days)	9	28.5	21	10
p value		0.0067	0.0067	0.9169

Figure 32 : Survival curves of mice bearing EL4 tumors. Mice were challenged with EL4 cells followed by treatment with solution of Dox or CpG (n = 4). Table represents median survival of each treatment group.
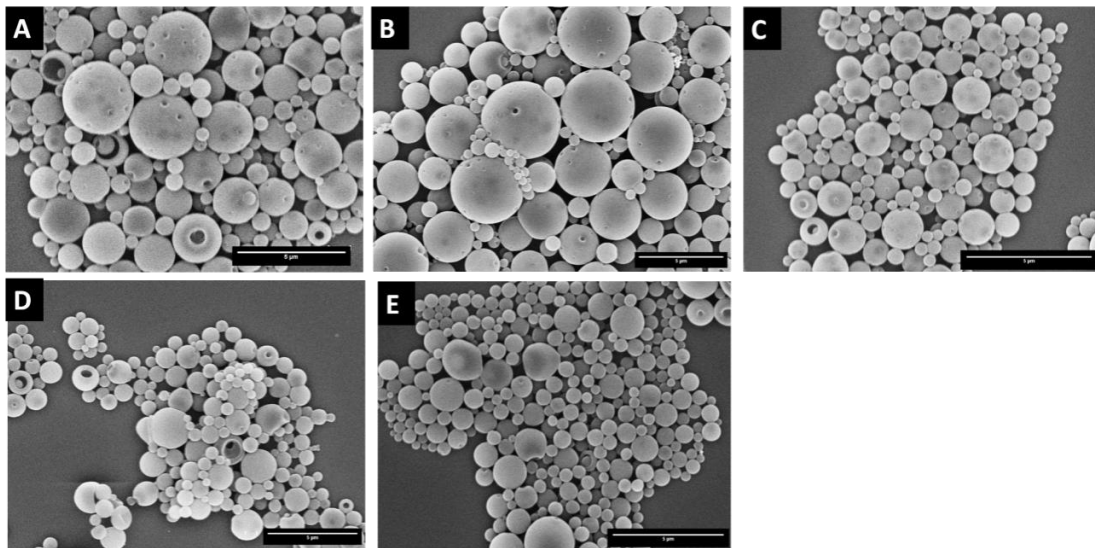
Figure 33 : SEM microphotographs of (A) (CpG)PLGA$^{50/50}$: CpG encapsulated in particles prepared from PLGA 50:50; (B) (CpG)PLGA$^{75/25}$: CpG encapsulated in particles prepared from PLGA 75:25; (C) (Dox)PLGA$^{50/50}$: Dox encapsulated in particles prepared from PLGA 50:50; (D) (Dox/CpG)PLGA$^{50/50}$: Dox and CpG co-encapsulated in particles prepared from PLGA 50:50; (E) empty PLGA 50:50 particles. The scale bar on lower right represents 5 µm length.
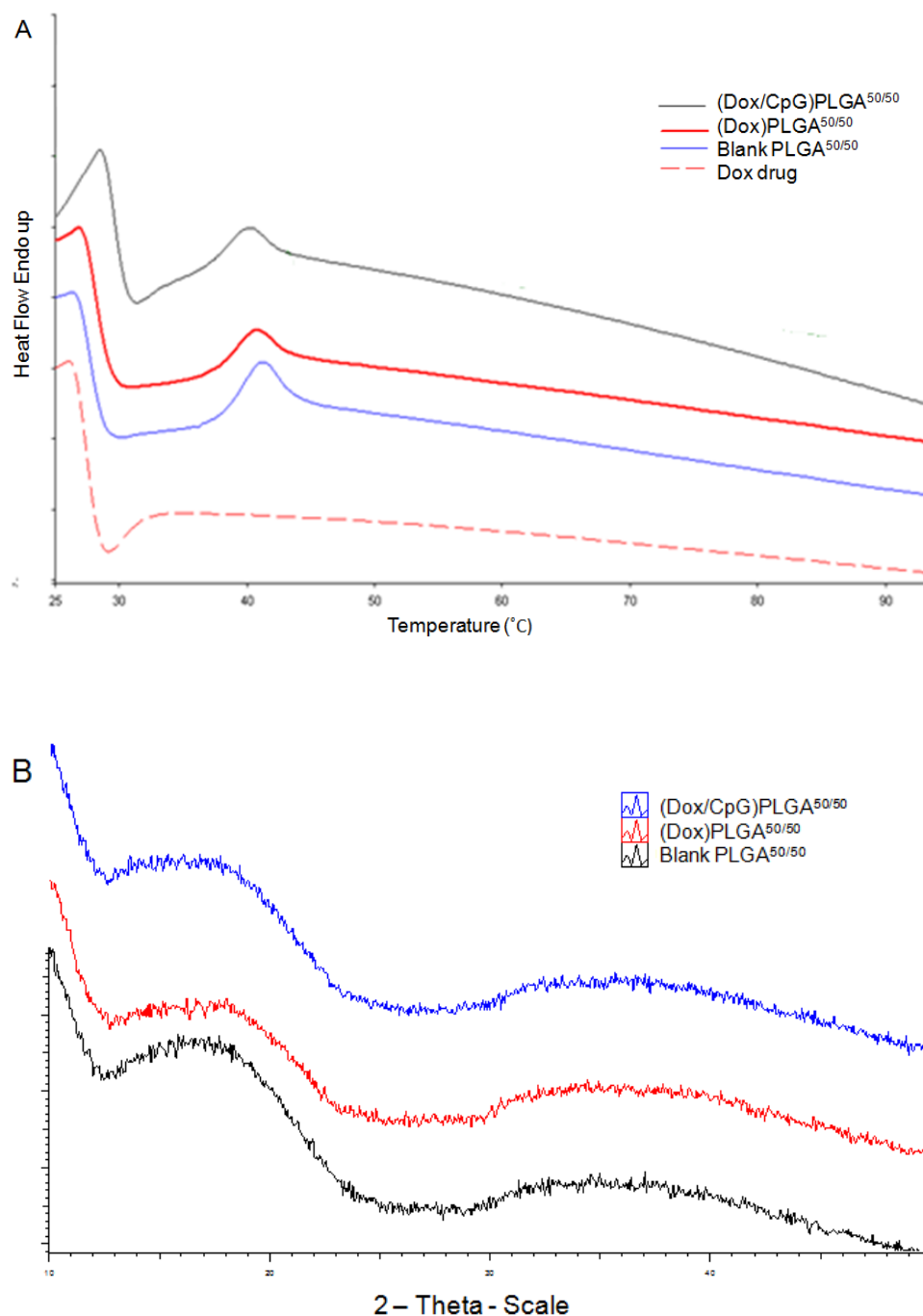
Figure 34 : PLGA particles were prepared using a double emulsion solvent evaporation method. Dried PLGA powders were achieved by lyophilization of the particle suspensions which were analyzed by (A) Differential scanning calorimetry thermograms obtained at a heating rate of 10˚C/minute and (b) X-ray diffraction patterns (2θ of 10º to 49.9º) showed the amorphous nature of PLGA particles encapsulating Dox and CpG.
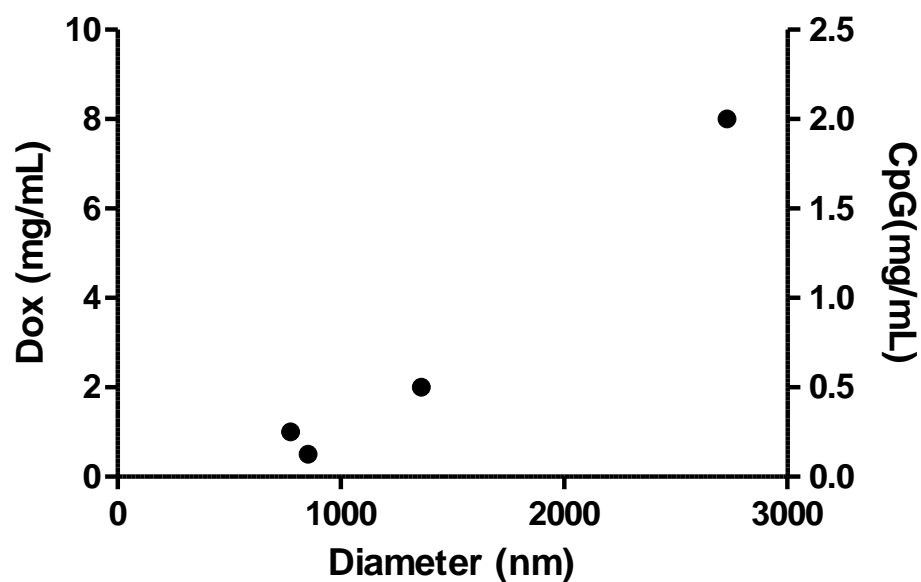
Dox (mg/ml)	CpG(mg/ml)	Diameter (nm)	PDI
8	2	2729	0.5
2	0.5	1360	0.9
1	0.25	774	0.5
0.5	0.12	853	0.5

Figure 35 : Size of Dox-CpG complexes prepared at increasing concentrations of Dox and CpG at weight ratio 4:1. The Table displays the size and polydispersity index (PDI) of Dox-CpG complexes. Increasing the initial concentration of Dox and CpG solutions showed increases in the size of prepared complexes.
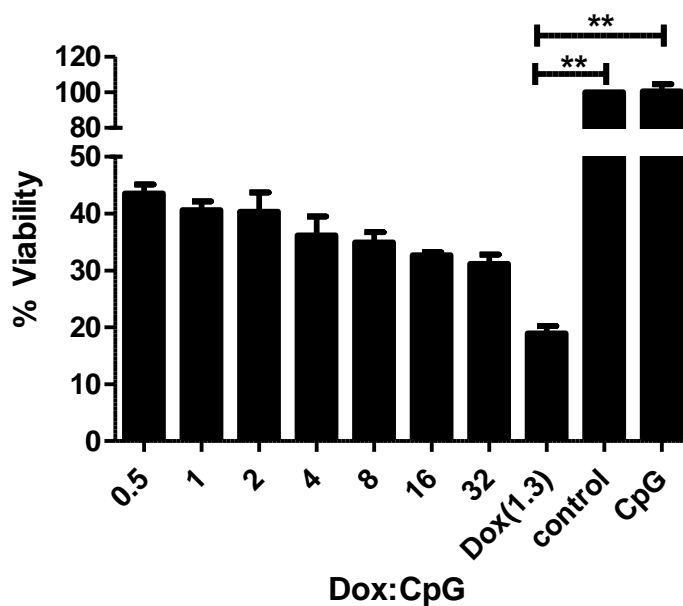
Dox:CpG ratio	1:2	1:1	2:1	4:1	8:1	16:1	32:1
Dox (µg/ml)	1.33	1.33	1.33	1.33	1.33	1.33	1.33
CpG (µg/ml)	2.66	1.33	0.67	0.33	0.17	0.08	0.04

Figure 36 : Percentage viability of EL4 cells treated with complexes of Dox and CpG. Cells were incubated for 12 hours with different ratio of Dox and CpG complexes. Percentage viability was estimated using MTS assay. All groups were compared using ANOVA followed by Tukey's post-hoc analysis (**p < 0.01). Each bar represents mean + SEM percentage viability (n = 3).
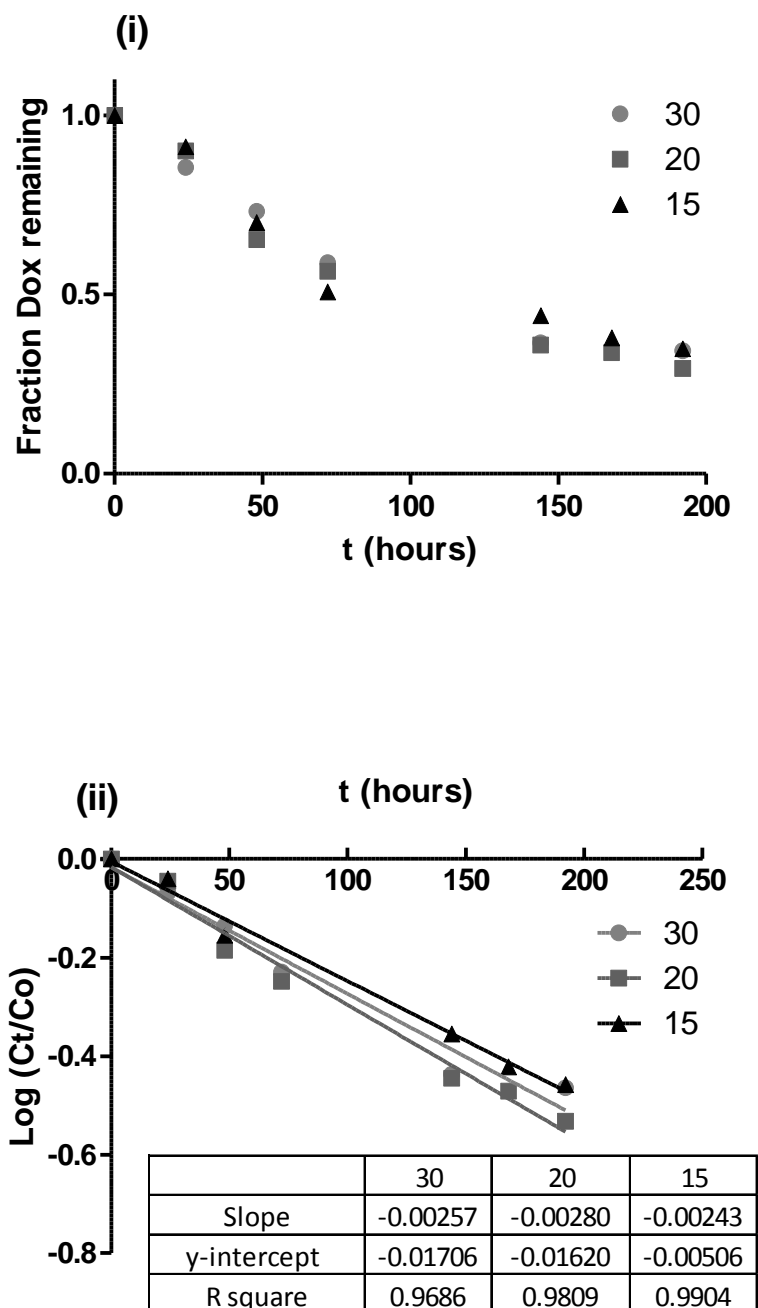
Figure 37 : Time dependent loss of fluorescence by Dox in PBS at 37 °C. (i) Time dependent decrease in the fraction of Dox. (ii) Log concentration at different times (C_t) normalized against the initial concentration (C_o) vs time plot for three different Dox concentrations. Loss of fluorescence from Dox followed first order kinetics with negligible y-intercept and similar slope across all three concentrations.
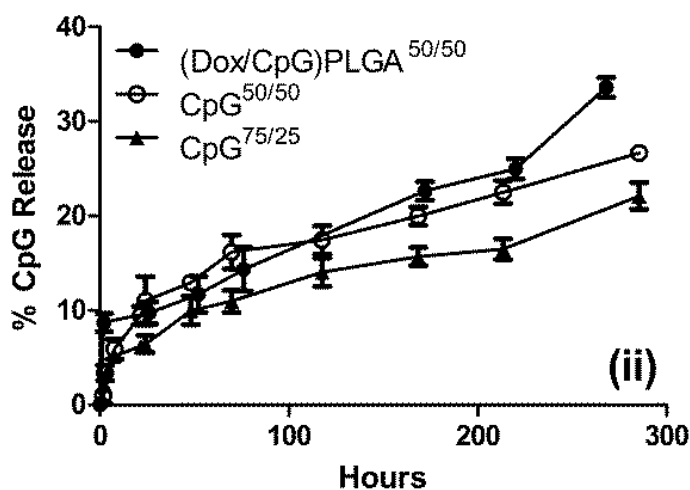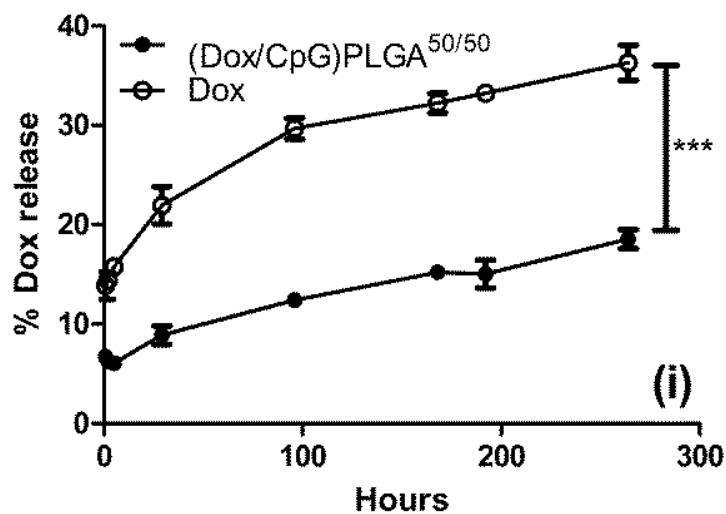
Figure 38 : (i) Dox and (ii) CpG release in PBS (pH 7.4) at 37°C from (Dox/CpG)PLGA[50/50], Dox loaded PLGA particles, CpG loaded PLGA 50:50 particles and CpG loaded PLGA 75:25 particles. All PLGA particles demonstrated burst release followed by sustained release of encapsulated molecules. Dox showed higher burst release from Dox loaded PLGA particles when compared to release of Dox from (Dox/CpG)PLGA[50/50] particles. Groups were compared using paired t-test (***$p < 0.001$). Each bar represents mean ± SEM (n = 3).
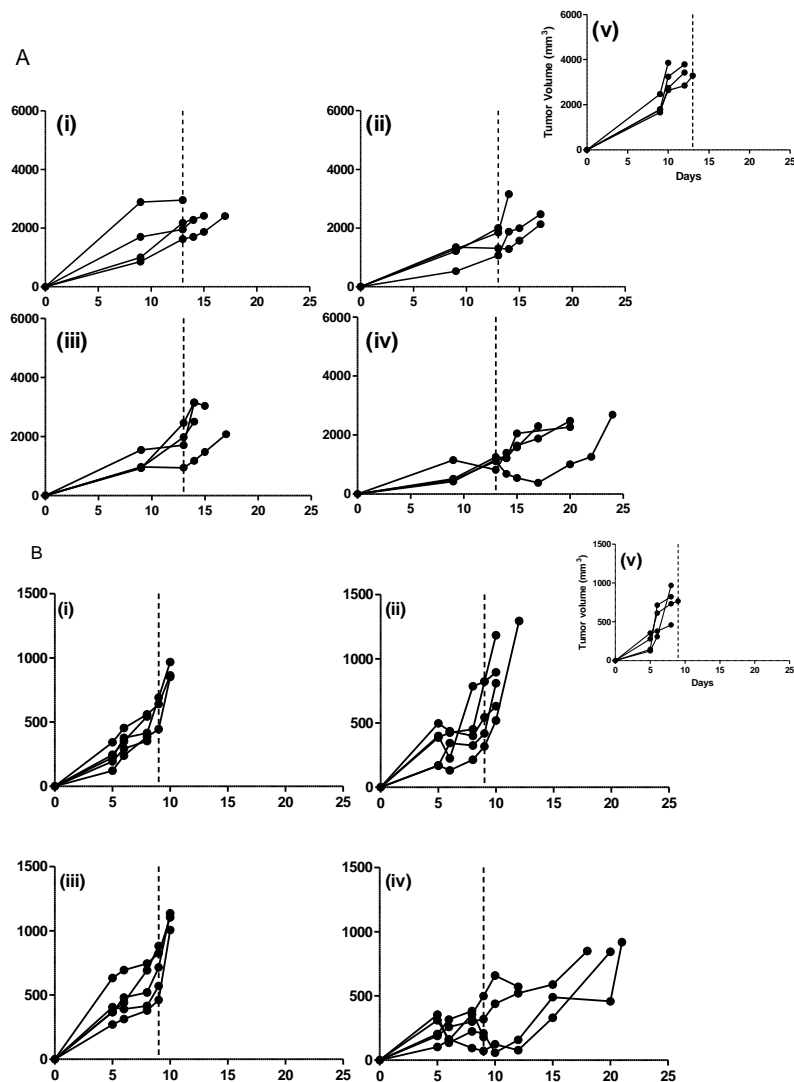
Figure 39 : Anti-tumor effect of PLGA particles encapsulating Dox and CpG in a therapeutic tumor mouse model. Mice were treated with (i) (Dox)PLGA$^{50/50}$(CpG)PLGA$^{50/50}$: admixture of PLGA particles encapsulating Dox and PLGA 50:50 particles encapsulating CpG; (ii) (Dox)PLGA$^{50/50}$(CpG)PLGA$^{75/25}$:admixture of PLGA particles encapsulating Dox and PLGA 75:25 particles encapsulating CpG; (iii) (Dox)PLGA$^{50/50}$: PLGA particles encapsulating Dox; (iv) (Dox/CpG)PLGA$^{50/50}$: PLGA 50:50 particles co-encapsulating Dox and CpG; and (v) No treatment. Two independent studies were performed in which each mouse was treated with (A) 100 µg Dox and 50 µg CpG, and (B) 100 µg Dox and 100 µg CpG, for required treatment groups. Each curve represents the tumor growth for each mouse of the respective group (n = 4). Vertical dashed line represents the time point at which all mice from the naïve group were euthanized due to large tumor size.

(i)

	Naive	(Dox/CpG)PLGA50/50	(Dox)PLGA50/50	(Dox)PLGA50/50 (CpG)PLGA50/50	(Dox)PLGA50/50 (CpG)PLGA75/25
Median Survival (Days)	12.0	20.5	14.5	14.5	15.5
p value		0.007	0.018	0.007	0.018

(ii)

	Naive	(Dox/CpG)PLGA50/50	(Dox)PLGA50/50	(Dox)PLGA50/50 (CpG)PLGA50/50	(Dox)PLGA50/50 (CpG)PLGA75/25
Median Survival (Days)	8	18	10	10	10
p value		0.008	0.089	0.014	0.003
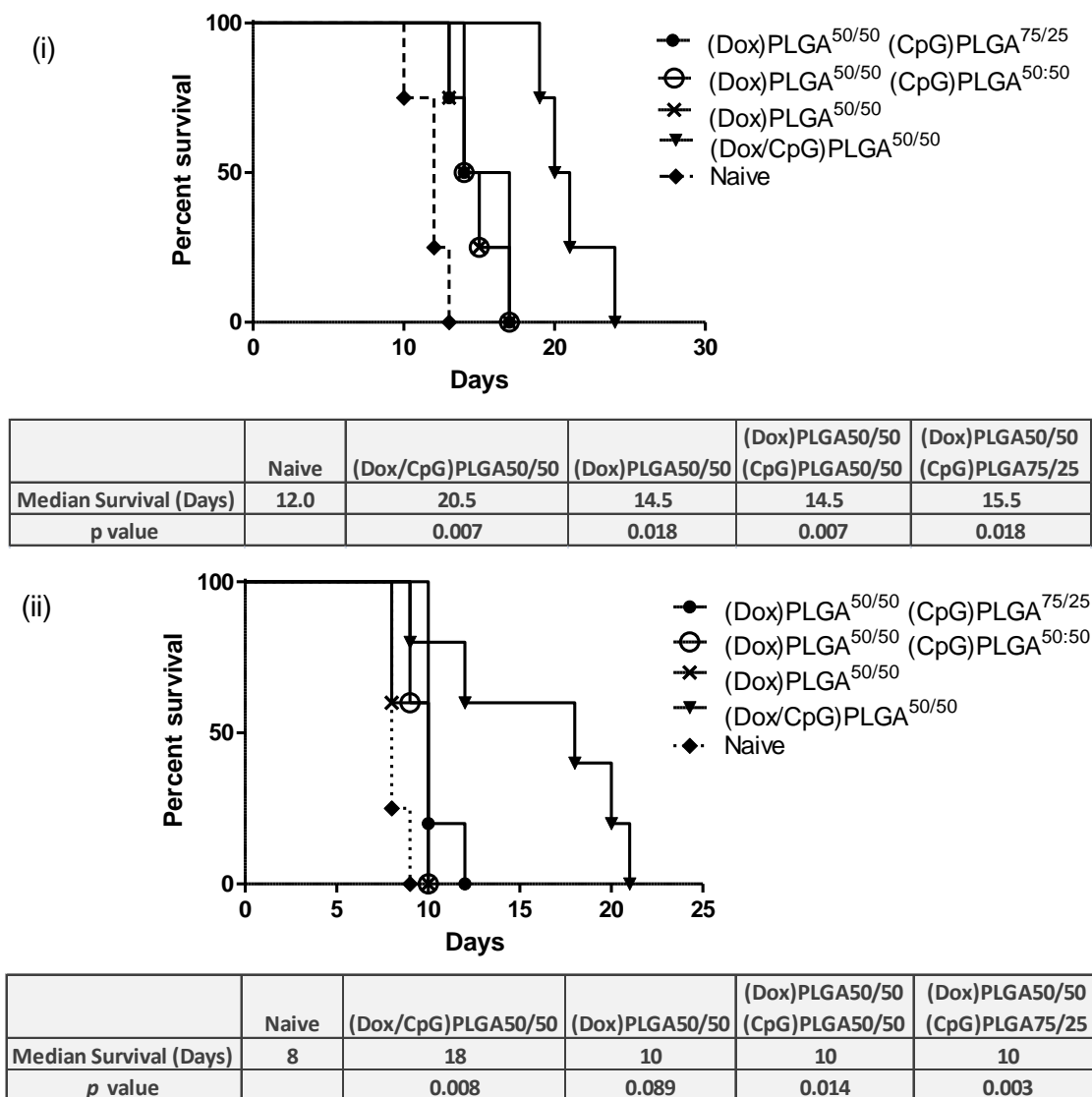
Figure 40 : Survival curves of tumor bearing mice treated with PLGA particles
encapsulating Dox and CpG. In respective treatment groups each mouse was
treated with (A) 100 µg Dox and 50 µg CpG, and (B) 100 µg Dox and 100 µg
CpG. Table represents median survival for each group. Survival curves were
analyzed using the Mantel–Cox test and significant differences of each
treatment group against naïve group were calculated using Chi-squared test.

Table 9 : Loading and percentage encapsulation efficiency (% EE) of Dox and oligos encapsulated in PLGA particles using the double emulsion solvent evaporation process. During the fabrication process the addition of ammonium acetate (NH4Ac) solution in the external water phase increased the loading and %EE of encapsulated molecules in PLGA particles.

External water phase	Loading (μg/mg particles)	% EE
Dox		
1% PVA	3.14	20.9
1% PVA in NH$_4$Ac solution (pH 8)	8.70	58.0
Herring sperm DNA		
1% PVA (pH ~5)	0.15	3.1
1% PVA in 0.1M NH$_4$Ac solution (pH 8)	0.33	6.4
1% PVA in 0.1M NH$_4$Ac solution (pH 4)	0.48	9.4
CpG		
1% PVA (pH ~5)	0.53	3.5
1% PVA in 0.1M NH$_4$Ac solution (pH 8)	4.50	30.2

Table 10 : Loading and percentage encapsulation efficiency (% EE) of Dox and CpG in (Dox/CpG)PLGA$^{50/50}$. A different initial amount of Dox and CpG were used in each preparation. A considerable change in loading and % EE was observed by changing the initial amount of Dox and CpG used during preparation. Loading was increased by using NH$_4$Ac solution.

	Without 0.1M NH$_4$Ac solution (pH 8)		With 0.1M NH$_4$Ac solution (pH 8)	
	Loading (µg/mg of PLGA particles)	% EE	Loading (µg/mg of PLGA particles)	% EE
Preparation 1: Dox: 1 mg and CpG 3 mg				
Dox	1.3 ± 0.5	27.3 ± 10.2	3.4 ± 0.2	64.5 ± 2.8
CpG	2.7 ± 0.7	18.0 ± 5.3	11.1 ± 0.5	71.5 ± 3.7
Preparation 2: Dox: 3 mg and CpG 2 mg				
Dox	3.5 ± 0.4	23.8 ± 2.7	8.5 ± 0.6	56.6 ± 4.2
CpG	2.4 ± 0.6	24.7 ± 4.0	5.6 ± 0.5	56.3 ± 5.0

Table 11 : Size (nm) and polydispersity index (PDI) of Dox-CpG complexes with varying ratios of Dox and CpG. Changing the ratio of Dox:CpG resulted in different sizes of prepared complexes as measured by NanoZS.

Ratio of Dox:CpG (w/w)	Molar ratio of Dox:CpG	Dox (µg/ml)	CpG(µg/ml)	Size (nm)	PDI
64:1	702:1	1000.00	15.62	2434;172;17	1.0
16:1	177:1	500.00	31.25	318; 20; 3	0.7
4:1	44:1	250.00	62.50	454	0.6
1:1	11:1	125.00	125.00	465	0.8
1:16	1:1	31.25	500.00	234	0.9

Table 12 : Loading of Dox and CpG encapsulated in PLGA particles.

Preparation	Loading (µg/mg of PLGA particles)
(Dox)PLGA$^{50/50}$	8.7
(CpG)PLGA$^{72/25}$	4.5
(CpG)PLGA$^{50/50}$	3.7
(Dox/CpG)PLGA$^{50/50}$ (study 1)	Dox: 11.8
	CpG: 5.2
(Dox/CpG)PLGA$^{50/50}$ (study 2)	Dox: 5.9
	CpG: 6.9

Table 13 : Study design of the therapeutic mouse model used for the evaluation of the anti-tumor activity of PLGA particles encapsulating Dox and CpG. Two independent studies were performed with different treatment day post tumor inoculation and different doses of CpG to study anti-tumor activity of PLGA particles encapsulating Dox and CpG.

	Tumor inoculation on Day 0	Treatment post tumor inoculation	Treatment dose
Study 1	10^6 EL4 cells	Day 7	100 µg of Dox and 50 µg of CpG
Study 2	10^6 EL4 cells	Day 3	100 µg of Dox and 100 µg of CpG

GLOSSARY

Adjuvant (Immunological): Molecules co-delivered with antigen in vaccine formulations in order to enhance the antigen-specific immune response.

Antigen (Ag): Molecules (usually protein/peptides) that generate fragments (known as epitopes) that are recognized by the T-cell receptor (presented in association with MHC molecules) on T-cells or by antibodies on, produced by B cells.

B7 protein (CD80 and CD86): Cell surface proteins expressed by dendritic cells. They are essential co-stimulatory molecules (during antigen presentation) that bind to CD28 receptors on the surface of T-cells.

CD4: A surface protein expressed by a subset of T-lymphocytes that often denotes T-helper lymphocyte phenotype.

CD8: A surface protein expressed by a subset of T-lymphocytes that often denotes cytotoxic T-lymphocyte phenotype.

Cytokine: Small proteins produced by a wide range of cells that can stimulate the activation, maturation, proliferation or chemotaxis of a variety of cell types.

Cytotoxic T-lymphocyte (CTL): An activated CD8+ T-cells that can kill other cells expressing specific antigen in association with MHC class I protein.

Dendritic cells: Bone marrow derived cells found in most tissues of the body. They internalize antigen in peripheral tissue and travel to closest lymph node for activation of T-cells.

Epitope: A specific amino acid sequence or structural motif that are recognized by antibody or T-cell receptors.

Interferon (IFN)-γ: A cytokine produced primarily by CD4+ and CD8+ T-cells that activates antigen presenting cells and stimulates antitumor activity.

Interleukin (IL)-2: Cytokine produced by T-cells that helps in their proliferation and differentiation.

Major Histocompatibility Complex (MHC): A cell surface membrane glycoprotein(s) involved in antigen presentation and fundamental to determining compatibility of transplant tissues.

MHC class I: These cell surface proteins are expressed by virtually all cell types in the human body and present epitopes derived from cytosolic antigens to CD8+ T-cells.

MHC class II: These cell surface proteins are expressed by antigen presenting cells and activated T-cells and present epitopes derived from exogenously acquired antigens to CD4 T-cells.

T-cell/lymphocyte: Lymphocytes that originates from bone marrow and undergo development in the thymus. They play critical role in development of cellular based adaptive immunity.

T-helper (Th): A subset of activated CD4 cells that are categorized into T-helper 1 (Th1) and T-helper 2 (Th2) based on the cytokines they produce. They can stimulate B cells to produce antigen specific antibodies, secrete cytokines for stimulation of antigen presenting cells and proliferation of CD8 T-cells.

Toll-like receptor (TLR): Receptors expressed by macrophages, dendritic cells and B cells that recognize microbial components such as CpG and trigger signaling cascades that stimulate innate and adaptive immune responses.

Tumor associated antigens (TAAs): Proteins that are aberrantly expressed by tumor cells, exclusively expressed by tumor cells, or expressed by tumor cells and other tissue that is considered non-vital or immune privileged.

(Dox)PLGA$^{50/50}$: Dox was encapsulated in PLGA 50:50 (Resomer® RG 503; PLGA 50:50 with viscosity: 0.32 – 0.44 dl/g; Boehringer Ingelheim KG, Germany) particles using double emulsion solvent evaporation method.

(Dox/CpG)PLGA$^{50/50}$: Dox and CpG were co-encapsulated in PLGA 50:50 (Resomer® RG 503; PLGA 50:50 with viscosity: 0.32 – 0.44 dl/g; Boehringer Ingelheim KG, Germany) particles using a modified double emulsion solvent evaporation method. This preparation contained Dox and CpG molecules encapsulated in the PLGA particle matrix. In this formulation Dox and CpG were independently emulsified in PLGA solution to form w/o emulsion. Two emulsion were then combined and emulsified again in water phase for preparation of w/o/w emulsion. When the primary emulsions of Dox and CpG were combined, Dox and CpG droplets can combine to give a complex primary emulsion with Dox and CpG suspended independently as well as in combined droplets. These particles have Dox and CpG suspended independently as well as in combination within PLGA particle matrix.

(Dox::CpG)PLGA$^{50/50}$: Complexes of Dox and CpG were encapsulated in PLGA 50:50 (Resomer® RG 503; Boehringer Ingelheim KG, Germany) particles using double emulsion solvent evaporation method.

REFERENCES

1.   Plotkin SA, Offit PA, editors. A short history of vaccination. 5th ed. New York: Elsevier; 2008.

2.   PhRMA. Vaccine fact book 2012 2012 [cited 2014 03/08]. Available from: http://www.phrma-jp.org/archives/pdf/vaccine_factbook_2012/en/vaccine_factbook_2012_en.pdf

3.   Zhang JY, Casiano CA, Peng XX, Koziol JA, Chan EKL, Tan EM. Enhancement ot antibody detection in cancer using panel of recombinant tumor-associated antigens. Cancer Epidem Biomar. 2003;12(2):136-43.

4.   Casiano CA, Mediavilla-Varela M, Tan EM. Tumor-associated antigen arrays for the serological diagnosis of cancer. Mol Cell Proteomics. 2006;5(10):1745-59.

5.   Siegel R, Naishadham D, Jemal A. Cancer statistics, 2013. Ca:a Cancer Journal for Clinicians. 2013;63(1):11-30.

6.   Hickey R, Vouche M, Sze DY, Hohlastos E, Collins J, Schirmang T, et al. Cancer concepts and principles: primer for the interventional oncologist-part II. Journal of vascular and interventional radiology : JVIR. 2013;24(8):1167-88.

7.   Gluer AM, Cocco N, Laurence JM, Johnston ES, Hollands MJ, Pleass HC, et al. Systematic review of actual 10-year survival following resection for hepatocellular carcinoma. HPB : the official journal of the International Hepato Pancreato Biliary Association. 2012;14(5):285-90.

8.   Lloyd Davies E. Metastatic disease of the breast and local recurrence of breast cancer. Surgery (Oxford). 2013;31(1):41-5.

9.   Yano T, Okamoto T, Haro A, Fukuyama S, Yoshida T, Kohno M, et al. Local treatment of oligometastatic recurrence in patients with resected non-small cell lung cancer. Lung Cancer. 2013;82(3):431-5.

10.   Buonaguro L, Petrizzo A, Tornesello ML, Buonaguro FM. Translating Tumor Antigens into Cancer Vaccines. Clin Vaccine Immunol. 2011;18(1):23-34.

11.   Scanlan MJ, Gure AO, Jungbluth AA, Old LJ, Chen YT. Cancer/testis antigens: an expanding family of targets for cancer immunotherapy. Immunol Rev. 2002;188:22-32.

12.   Vanderbruggen P, Traversari C, Chomez P, Lurquin C, Deplaen E, Vandeneynde B, et al. A Gene Encoding an Antigen Recognized by Cytolytic Lymphocytes-T on a Human-Melanoma. Science. 1991;254(5038):1643-7.

13.	Boon T, Cerottini JC, Vandeneynde B, Vanderbruggen P, Vanpel A. Tumor-Antigens Recognized by T-Lymphocytes. Annu Rev Immunol. 1994;12:337-65.

14.	Jager E, Chen YT, Drijfhout JW, Karbach J, Ringhoffer M, Jager D, et al. Simultaneous humoral and cellular immune response against cancer-testis antigen NY-ESO-1: definition of human histocompatibility leukocyte antigen (HLA)-A2-binding peptide epitopes. J Exp Med. 1998;187(2):265-70.

15.	Takahashi M, Chen W, Byrd DR, Disis ML, Huseby ES, Qin HL, et al. Antibody to ras proteins in patients with colon cancer. Clin Cancer Res. 1995;1(10):1071-7.

16.	Novellino L, Castelli C, Parmiani G. A listing of human tumor antigens recognized by T cells: March 2004 update. Cancer Immunol Immun. 2005;54(3):187-207.

17.	Bocchia M, Bronte V, Colombo MP, De Vincentiis A, Di Nicola M, Forni G, et al. Antitumor vaccination: where we stand. Haematologica. 2000;85(11):1172-206.

18.	Chi DD, Merchant RE, Rand R, Conrad AJ, Garrison D, Turner R, et al. Molecular detection of tumor-associated antigens shared by human cutaneous melanomas and gliomas. Am J Pathol. 1997;150(6):2143-52.

19.	Brower V. Approval of provenge seen as first step for cancer treatment vaccines. J Natl Cancer I. 2010;102(15):1108-10.

20.	Wood RA. Skin testing: making the most of every prick. Ann Allerg Asthma Im. 2002;88(4):347-9.

21.	Arbes SJ, Jr., Gergen PJ, Elliott L, Zeldin DC. Prevalences of positive skin test responses to 10 common allergens in the US population: results from the third National Health and Nutrition Examination Survey. J Allergy Clin Immunol. 2005;116(2):377-83.

22.	Williams CMM, Galli SJ. The diverse potential effector and immunoregulatory roles of mast cells in allergic disease. J Allergy Clin Immunol. 2000;105(5):847-59.

23.	Bousquet J, Jeffery PK, Busse WW, Johnson M, Vignola AM. Asthma. From bronchoconstriction to airways inflammation and remodeling. Am J Respir Crit Care Med. 2000;161(5):1720-45.

24.	Craig TJ, King TS, Lemanske RF, Jr., Wechsler ME, Icitovic N, Zimmerman RR, Jr., et al. Aeroallergen sensitization correlates with PC(20) and exhaled nitric oxide in subjects with mild-to-moderate asthma. J Allergy Clin Immunol. 2008;121(3):671-7.

25.	Custovic A, Taggart SC, Francis HC, Chapman MD, Woodcock A. Exposure to house dust mite allergens and the clinical activity of asthma. J Allergy Clin Immunol. 1996;98(1):64-72.

26.   Bousquet J, Lockey R, Malling HJ. Allergen immunotherapy: therapeutic vaccines for allergic diseases. A WHO position paper. J Allergy Clin Immunol. 1998;102(4 Pt 1):558-62.

27.   Muller UR. Recent developments and future strategies for immunotherapy of insect venom allergy. Current opinion in allergy and clinical immunology. 2003;3(4):299-303.

28.   Freyne B, Curtis N. Does neonatal BCG vaccination prevent allergic disease in later life? Arch Dis Child. 2014;99(2):182-4.

29.   Kaufmann SHE. Tuberculosis vaccines: Time to think about the next generation. Semin Immunol. 2013;25(2):172-81.

30.   Okuda M. [A long-term follow-up study after discontinuation of immunotherapy for Japanese cedar pollinosis]. Arerugi = [Allergy]. 2006;55(6):655-61.

31.   Durham SR, Emminger W, Kapp A, de Monchy JGR, Rak S, Scadding GK, et al. SQ-standardized sublingual grass immunotherapy: Confirmation of disease modification 2 years after 3 years of treatment in a randomized trial. J Allergy Clin Immunol. 2012;129(3):717-25.

32.   Calderon MA, Alves B, Jacobson M, Hurwitz B, Sheikh A, Durham S. Allergen injection immunotherapy for seasonal allergic rhinitis. Cochrane Db Syst Rev. 2007(1).

33.   Radulovic S, Calderon MA, Wilson D, Durham S. Sublingual immunotherapy for allergic rhinitis. Cochrane Db Syst Rev. 2010(12).

34.   Shishido SN, Varahan S, Yuan K, Li X, Fleming SD. Humoral innate immune response and disease. Clin Immunol. 2012;144(2):142-58.

35.   Amanna IJ, Slifka MK. Contributions of humoral and cellular immunity to vaccine-induced protection in humans. Virology. 2011;411(2):206-15.

36.   Cella M, Sallusto F, Lanzavecchia A. Origin, maturation and antigen presenting function of dendritic cells. Curr Opin Immunol. 1997;9(1):10-6.

37.   Maurer T, Heit A, Hochrein H, Ampenberger F, O'Keeffe M, Bauer S, et al. CpG-DNA aided cross-presentation of soluble antigens by dendritic cells. Eur J Immunol. 2002;32(8):2356-64.

38.   Gordon S. Pattern recognition receptors: doubling up for the innate immune response. Cell. 2002;111(7):927-30.

39.   Hubbell JA, Thomas SN, Swartz MA. Materials engineering for immunomodulation. Nature. 2009;462(7272):449-60.

40.   Schnurr M, Chen Q, Shin A, Chen W, Toy T, Jenderek C, et al. Tumor antigen processing and presentation depend critically on dendritic cell type and the mode of antigen delivery. Blood. 2005;105(6):2465-72.

41.   Aarntzen EH, De Vries IJ, Lesterhuis WJ, Schuurhuis D, Jacobs JF, Bol K, et al. Targeting CD4(+) T-helper cells improves the induction of antitumor responses in dendritic cell-based vaccination. Cancer Res. 2013;73(1):19-29.

42.   Huber VC, McKeon RM, Brackin MN, Miller LA, Keating R, Brown SA, et al. Distinct contributions of vaccine-induced immunoglobulin G1 (IgG1) and IgG2a antibodies to protective immunity against influenza. Clin Vaccine Immunol. 2006;13(9):981-90.

43.   Snapper CM, Paul WE. Interferon-gamma and B cell stimulatory factor-1 reciprocally regulate Ig isotype production. Science. 1987;236(4804):944-7.

44.   Karan D, Krieg AM, Lubaroff DM. Paradoxical enhancement of CD8 T cell-dependent anti-tumor protection despite reduced CD8 T cell responses with addition of a TLR9 agonist to a tumor vaccine. Int J Cancer. 2007;121(7):1520-8.

45.   Moore MW, Carbone FR, Bevan MJ. Introduction of soluble protein into the class I pathway of antigen processing and presentation. Cell. 1988;54(6):777-85.

46.   van den Boorn JG, Hartmann G. Turning tumors into vaccines: co-opting the innate immune system. Immunity. 2013;39(1):27-37.

47.   Chen W, Yu Y, Shao C, Zhang M, Wang W, Zhang L, et al. Enhancement of antigen-presenting ability of B lymphoma cells by immunostimulatory CpG-oligonucleotides and anti-CD40 antibody. Immunol Lett. 2001;77(1):17-23.

48.   Tada F, Abe M, Hirooka M, Ikeda Y, Hiasa Y, Lee Y, et al. Phase I/II study of immunotherapy using tumor antigen-pulsed dendritic cells in patients with hepatocellular carcinoma. International journal of oncology. 2012;41(5):1601-9.

49.   Einstein MH, Schiller JT, Viscidi RP, Strickler HD, Coursaget P, Tan T, et al. Clinician's guide to human papillomavirus immunology: knowns and unknowns. The Lancet infectious diseases. 2009;9(6):347-56.

50.   Coutant F, Perrin-Cocon L, Agaugue S, Delair T, Andre P, Lotteau V. Mature dendritic cell generation promoted by lysophosphatidylcholine. J Immunol. 2002;169(4):1688-95.

51.   Perrin-Cocon L, Agaugue S, Coutant F, Saint-Mezard P, Guironnet-Paquet A, Nicolas JF, et al. Lysophosphatidylcholine is a natural adjuvant that initiates cellular immune responses. Vaccine. 2006;24(9):1254-63.

52.   Hemmi H, Kaisho T, Takeuchi O, Sato S, Sanjo H, Hoshino K, et al. Small anti-viral compounds activate immune cells via the TLR7 MyD88-dependent signaling pathway. Nat Immunol. 2002;3(2):196-200.

53.   Pashine A, Valiante NM, Ulmer JB. Targeting the innate immune response with improved vaccine adjuvants. Nature Medicine. 2005;11(4):S63-S8.

54.   Krieg AM. CpG motifs in bacterial DNA and their immune effects. Annu Rev Immunol. 2002;20:709-60.

55.   Krieg AM. From A to Z on CpG. Trends Immunol. 2002;23(2):64-5.

56.   Bode C, Zhao G, Steinhagen F, Kinjo T, Klinman DM. CpG DNA as a vaccine adjuvant. Expert review of vaccines. 2011;10(4):499-511.

57.   Shirota H, Klinman DM. Recent progress concerning CpG DNA and its use as a vaccine adjuvant. Expert review of vaccines. 2014;13(2):299-312.

58.   Weeratna RD, McCluskie MJ, Xu Y, Davis HL. CpG DNA induces stronger immune responses with less toxicity than other adjuvants. Vaccine. 2000;18(17):1755-62.

59.   Obeid M, Tesniere A, Ghiringhelli F, Fimia GM, Apetoh L, Perfettini JL, et al. Calreticulin exposure dictates the immunogenicity of cancer cell death. Nat Med. 2007;13(1):54-61.

60.   Gardai SJ, McPhillips KA, Frasch SC, Janssen WJ, Starefeldt A, Murphy-Ullrich JE, et al. Cell-surface calreticulin initiates clearance of viable or apoptotic cells through trans-activation of LRP on the phagocyte. Cell. 2005;123(2):321-34.

61.   Casares N, Pequignot MO, Tesniere A, Ghiringhelli F, Roux S, Chaput N, et al. Caspase-dependent immunogenicity of doxorubicin-induced tumor cell death. J Exp Med. 2005;202(12):1691-701.

62.   Buttiglieri S, Galetto A, Forno S, De Andrea M, Matera L. Influence of drug-induced apoptotic death on processing and presentation of tumor antigens by dendritic cells. Int J Cancer. 2003;106(4):516-20.

63.   Tanaka H, Matsushima H, Mizumoto N, Takashima A. Classification of chemotherapeutic agents based on their differential in vitro effects on dendritic cells. Cancer Res. 2009;69(17):6978-86.

64.   Shurin GV, Tourkova IL, Kaneno R, Shurin MR. Chemotherapeutic agents in noncytotoxic concentrations increase antigen presentation by dendritic cells via an IL-12-dependent mechanism. J Immunol. 2009;183(1):137-44.

65.   Kim JE, Jang MJ, Lee JI, Chung YH, Jeong JH, Hung CF, et al. Cancer cells containing nanoscale chemotherapeutic drugs generate antiovarian cancer-specific CD4(+) T cells in peritoneal space. J Immunother. 2012;35(1):1-13.

66.   Mattarollo SR, Loi S, Duret H, Ma YT, Zitvogel L, Smyth MJ. Pivotal role of innate and adaptive immunity in anthracycline chemotherapy of established tumors. Cancer Res. 2011;71(14):4809-20.

67.   Hortobagyi GN. Anthracyclines in the treatment of cancer. An overview. Drugs. 1997;54 Suppl 4:1-7.

68.   Carvalho C, Santos RX, Cardoso S, Correia S, Oliveira PJ, Santos MS, et al. Doxorubicin: the good, the bad and the ugly effect. Curr Med Chem. 2009;16(25):3267-85.

69.   Vonhoff DD, Layard MW, Basa P, Davis HL, Vonhoff AL, Rozencweig M, et al. Risk-factors for doxorubicin-induced congestive heart-failure. Ann Intern Med. 1979;91(5):710-7.

70.   Weiss RB. The anthracyclines: will we ever find a better doxorubicin? Semin Oncol. 1992;19(6):670-86.

71.   Batist G, Ramakrishnan G, Rao CS, Chandrasekharan A, Gutheil J, Guthrie T, et al. Reduced cardiotoxicity and preserved antitumor efficacy of liposome-encapsulated doxorubicin and cyclophosphamide compared with conventional doxorubicin and cyclophosphamide in a randomized, multicenter trial of metastatic breast cancer. J Clin Oncol. 2001;19(5):1444-54.

72.   Safra T, Muggia F, Jeffers S, Tsao-Wei DD, Groshen S, Lyass O, et al. Pegylated liposomal doxorubicin (doxil): reduced clinical cardiotoxicity in patients reaching or exceeding cumulative doses of 500 mg/m2. Ann Oncol. 2000;11(8):1029-33.

73.   Zepp F. Principles of vaccine design-Lessons from nature. Vaccine. 2010;28 Suppl 3:C14-24.

74.   Sinha VR, Trehan A. Biodegradable microspheres for parenteral delivery. Crit Rev Ther Drug Carrier Syst. 2005;22(6):535-602.

75.   Abbas AO, Donovan MD, Salem AK. Formulating poly(lactide-co-glycolide) particles for plasmid DNA delivery. J Pharm Sci-Us. 2008;97(7):2448-61.

76.   Krishnamachari Y, Geary SM, Lemke CD, Salem AK. Nanoparticle delivery systems in cancer vaccines. Pharm Res. 2011;28(2):215-36.

77.   Krishnamachari Y, Salem AK. Innovative strategies for co-delivering antigens and CpG oligonucleotides. Adv Drug Deliver Rev. 2009;61(3):205-17.

78.   Elamanchili P, Lutsiak CM, Hamdy S, Diwan M, Samuel J. "Pathogen-mimicking" nanoparticles for vaccine delivery to dendritic cells. J Immunother. 2007;30(4):378-95.

79.   Elamanchili P, Diwan M, Cao M, Samuel J. Characterization of poly(D,L-lactic-co-glycolic acid) based nanoparticulate system for enhanced delivery of antigens to dendritic cells. Vaccine. 2004;22(19):2406-12.

80.   Zhang XQ, Dahle CE, Baman NK, Rich N, Weiner GJ, Salem AK. Potent antigen-specific immune responses stimulated by codelivery of CpG ODN and antigens in degradable microparticles. J Immunother. 2007;30(5):469-78.

81.   Ulery BD, Petersen LK, Phanse Y, Kong CS, Broderick SR, Kumar D, et al. Rational design of pathogen-mimicking amphiphilic materials as nanoadjuvants. Sci Rep. 2011;1.

82.   Yoshida M, Babensee JE. Poly(lactic-co-glycolic acid) enhances maturation of human monocyte-derived dendritic cells. J Biomed Mater Res A. 2004;71(1):45-54.

83.   Hamdy S, Molavi O, Ma Z, Haddadi A, Alshamsan A, Gobti Z, et al. Co-delivery of cancer-associated antigen and Toll-like receptor 4 ligand in PLGA nanoparticles induces potent CD8+ T cell-mediated anti-tumor immunity. Vaccine. 2008;26(39):5046-57.

84.   Shen H, Ackerman AL, Cody V, Giodini A, Hinson ER, Cresswell P, et al. Enhanced and prolonged cross-presentation following endosomal escape of exogenous antigens encapsulated in biodegradable nanoparticles. Immunology. 2006;117(1):78-88.

85.   Allen TM. Ligand-targeted therapeutics in anticancer therapy. Nature reviews Cancer. 2002;2(10):750-63.

86.   Carter PJ, Senter PD. Antibody-drug conjugates for cancer therapy. Cancer journal. 2008;14(3):154-69.

87.   Garnett MC. Targeted drug conjugates: principles and progress. Adv Drug Deliver Rev. 2001;53(2):171-216.

88.   Makadia HK, Siegel SJ. Poly lactic-co-glycolic acid (PLGA) as biodegradable controlled drug delivery carrier. Polymers-Basel. 2011;3(3):1377-97.

89.   Park J, Fong PM, Lu J, Russell KS, Booth CJ, Saltzman WM, et al. PEGylated PLGA nanoparticles for the improved delivery of doxorubicin. Nanomedicine. 2009;5(4):410-8.

90.   Hu CM, Aryal S, Zhang L. Nanoparticle-assisted combination therapies for effective cancer treatment. Ther Deliv. 2010;1(2):323-34.

91.   Blander JM, Medzhitov R. Toll-dependent selection of microbial antigens for presentation by dendritic cells. Nature. 2006;440(7085):808-12.

92.   Gnjatic S, Sawhney NB, Bhardwaj N. Toll-like receptor agonists: are they good adjuvants? Cancer journal. 2010;16(4):382-91.

93.   Foged C, Hansen J, Agger EM. License to kill: Formulation requirements for optimal priming of CD8(+) CTL responses with particulate vaccine delivery systems. Eur J Pharm Sci. 2012;45(4):482-91.

94.   Keijzer C, Slutter B, van der Zee R, Jiskoot W, van Eden W, Broere F. PLGA, PLGA-TMC and TMC-TPP nanoparticles differentially modulate the outcome of nasal vaccination by inducing tolerance or enhancing humoral immunity. PLoS ONE. 2011;6(11):e26684.

95.   Zhou SB, Deng XM, Li XH, Jia WX, Liu L. Synthesis and characterization of biodegradable low molecular weight aliphatic polyesters and their use in protein-delivery systems. J Appl Polym Sci. 2004;91(3):1848-56.

96.   Chung TW, Tsai YL, Hsieh JH, Tsai WJ. Different ratios of lactide and glycolide in PLGA affect the surface property and protein delivery characteristics of the PLGA microspheres with hydrophobic additives. J Microencapsul. 2006;23(1):15-27.

97.   Moon JJ, Suh H, Polhemus ME, Ockenhouse CF, Yadava A, Irvine DJ. Antigen-displaying lipid-enveloped PLGA nanoparticles as delivery agents for a Plasmodium vivax malaria vaccine. PLoS One. 2012;7(2):6.

98.   Demento SL, Eisenbarth SC, Foellmer HG, Platt C, Caplan MJ, Saltzman WM, et al. Inflammasome-activating nanoparticles as modular systems for optimizing vaccine efficacy. Vaccine. 2009;27(23):3013-21.

99.   Raghuwanshi D, Mishra V, Suresh MR, Kaur K. A simple approach for enhanced immune response using engineered dendritic cell targeted nanoparticles. Vaccine. 2012;30(50):7292-9.

100.   Diesner SC, Wang XY, Jensen-Jarolim E, Untersmayr E, Gabor F. Use of lectin-functionalized particles for oral immunotherapy. Ther Deliv. 2012;3(2):277-90.

101.   Zhang XQ, Intra J, Salem AK. Comparative study of poly (lactic-co-glycolic acid)-poly ethyleneimine-plasmid DNA microparticles prepared using double emulsion methods. J Microencapsul. 2008;25(1):1-12.

102.   Jiang W, Gupta RK, Deshpande MC, Schwendeman SP. Biodegradable poly(lactic-co-glycolic acid) microparticles for injectable delivery of vaccine antigens. Adv Drug Deliv Rev. 2005;57(3):391-410.

103.   Le Corre P, Rytting JH, Gajan V, Chevanne F, Le Verge R. In vitro controlled release kinetics of local anaesthetics from poly(D,L-lactide) and poly(lactide-co-glycolide) microspheres. J Microencapsul. 1997;14(2):243-55.

104.   Greenwald D, Shumway S, Albear P, Gottlieb L. Mechanical comparison of 10 suture materials before and after in vivo incubation. J Surg Res. 1994;56(4):372-7.

105. Blanco FC, Srinivasan P, Walk RM, Snyder JA, Behlke M, Salem AK, et al. Development of an siRNA delivery system targeting macrophage function in-vivo. J Am Coll Surgeons. 2012;215(3):S74-S.

106. Hong L, Krishnamachari Y, Seabold D, Joshi V, Schneider G, Salem AK. Intracellular release of 17-β estradiol from cationic polyamidoamine dendrimer surface-modified poly (lactic-co-glycolic acid) microparticles improves osteogenic differentiation of human mesenchymal stromal cells. Tissue Eng Part C-Me. 2011;17(3):319-25.

107. Hong L, Wei N, Joshi V, Yu Y, Kim N, Krishnamachari Y, et al. Effects of glucocorticoid receptor small interfering RNA delivered using poly lactic-co-glycolic acid microparticles on proliferation and differentiation capabilities of human mesenchymal stromal cells. Tissue Eng Pt A. 2012;18(7-8):775-84.

108. Intra J, Salem AK. Fabrication, characterization and in vitro evaluation of poly(D,L-lactide-co-glycolide) microparticles loaded with polyamidoamine-plasmid DNA dendriplexes for applications in nonviral gene delivery. J Pharm Sci-Us. 2010;99(1):368-84.

109. Intra J, Salem AK. Rational design, fabrication, characterization and in vitro testing of biodegradable microparticles that generate targeted and sustained transgene expression in HepG2 liver cells. J Drug Target. 2011;19(6):393-408.

110. Intra J, Zhang XQ, LWilliams R, Zhu XY, Sandler AD, Salem AK. Immunostimulatory sutures that treat local disease recurrence following primary tumor resection. Biomed Mater. 2011;6(1).

111. Santillan DA, Rai KK, Santillan MK, Krishnamachari Y, Salem AK, Hunter SK. Efficacy of polymeric encapsulated C5a peptidase-based group B streptococcus vaccines in a murine model. Am J Obstet Gynecol. 2011;205(3).

112. Zhang X-Q, Dahle CE, Weiner GJ, Salem AK. A comparative study of the antigen-specific immune response induced by co-delivery of CpG ODN and antigen using fusion molecules or biodegradable microparticles. J Pharm Sci-Us. 2007;96(12):3283-92.

113. Akagi T, Baba M, Akashi M. Biodegradable nanoparticles as vaccine adjuvants and delivery systems: regulation of immune responses by nanoparticle-based vaccine. Adv Polym Sci. 2012;247:31-64.

114. Zhu Q, Talton J, Zhang GF, Cunningham T, Wang ZJ, Waters RC, et al. Large intestine-targeted, nanoparticle-releasing oral vaccine to control genitorectal viral infection. Nature Medicine. 2012;18(8):1291-6.

115. Thomas C, Rawat A, Hope-Weeks L, Ahsan F. Aerosolized PLA and PLGA nanoparticles enhance humoral, mucosal and cytokine responses to hepatitis B vaccine. Mol Pharmaceut. 2011;8(2):405-15.

116.   Goforth R, Salem AK, Zhu XY, Miles S, Zhang XQ, Lee JH, et al. Immune stimulatory antigen loaded particles combined with depletion of regulatory T-cells induce potent tumor specific immunity in a mouse model of melanoma. Cancer Immunol Immun. 2009;58(4):517-30.

117.   Lopac SK, Torres MP, Wilson-Welder JH, Wannemuehler MJ, Narasimhan B. Effect of polymer chemistry and fabrication method on protein release and stability from polyanhydride microspheres. J Biomed Mater Res B. 2009;91B(2):938-47.

118.   Göpferich A, Tessmar J. Polyanhydride degradation and erosion. Adv Drug Deliver Rev. 2002;54(7):911-31.

119.   Tamada JA, Langer R. Erosion kinetics of hydrolytically degradable polymers. Proc Natl Acad Sci U S A. 1993;90(2):552-6.

120.   Grayson ACR, Voskerician G, Lynn A, Anderson JM, Cima MJ, Langer R. Differential degradation rates in vivo and in vitro of biocompatible poly(lactic acid) and poly(glycolic acid) homo- and co-polymers for a polymeric drug-delivery microchip. J Biomat Sci-Polym E. 2004;15(10):1281-304.

121.   Huntimer L, Ramer-Tait AE, Petersen LK, Ross KA, Walz KA, Wang C, et al. Evaluation of biocompatibility and administration site reactogenicity of polyanhydride-particle-based platform for vaccine delivery. Adv Healthc Mater. 2013;2(2):369-78.

122.   Carrillo-Conde B, Schiltz E, Yu J, Minion FC, Phillips GJ, Wannemuehler MJ, et al. Encapsulation into amphiphilic polyanhydride microparticles stabilizes Yersinia pestis antigens. Acta Biomater. 2010;6(8):3110-9.

123.   Kumar N, Langer RS, Domb AJ. Polyanhydrides: an overview. Adv Drug Deliver Rev. 2002;54(7):889-910.

124.   Tamayo I, Irache JM, Mansilla C, Ochoa-Reparaz J, Lasarte JJ, Gamazo C. Poly(anhydride) nanoparticles act as active Th1 adjuvants through Toll-like receptor exploitation. Clin Vaccine Immunol. 2010;17(9):1356-62.

125.   Reboucas Jde S, Irache JM, Camacho AI, Esparza I, Del Pozo V, Sanz ML, et al. Development of poly(anhydride) nanoparticles loaded with peanut proteins: the influence of preparation method on the immunogenic properties. Eur J Pharm Biopharm. 2012;82(2):241-9.

126.   Camacho AI, Martins RD, Tamayo I, de Souza J, Lasarte JJ, Mansilla C, et al. Poly(methyl vinyl ether-co-maleic anhydride) nanoparticles as innate immune system activators. Vaccine. 2011;29(41):7130-5.

127.   Ulery BD, Kumar D, Ramer-Tait AE, Metzger DW, Wannemuehler MJ, Narasimhan B. Design of a protective single-dose intranasal nanoparticle-based vaccine platform for respiratory infectious diseases. PloS one. 2011;6(3):e17642.

128.   Zammit DJ, Cauley LS, Pham QM, Lefrancois L. Dendritic cells maximize the memory CD8 T cell response to infection. Immunity. 2005;22(5):561-70.

129.   Siegel R, DeSantis C, Virgo K, Stein K, Mariotto A, Smith T, et al. Cancer treatment and survivorship statistics, 2012. CA Cancer J Clin. 2012;62(4):220-41.

130.   Giresand O, Seliger B. Tumor-associated antigens: Identification, characterization and clinical applications. Giresand O, Seliger B, editors. Weinheim, Germany: Wiley-Blackwell; 2009.

131.   Banchereau J, Briere F, Caux C, Davoust J, Lebecque S, Liu YJ, et al. Immunobiology of dendritic cells. Annu Rev Immunol. 2000;18:767-811.

132.   Takeda K, Kaisho T, Akira S. Toll-like receptors. Annu Rev Immunol. 2003;21:335-76.

133.   Bolhassani A, Safaiyan S, Rafati S. Improvement of different vaccine delivery systems for cancer therapy. Molecular cancer. 2011;10:3.

134.   Petersen LK, Ramer-Tait AE, Broderick SR, Kong CS, Ulery BD, Rajan K, et al. Activation of innate immune responses in a pathogen-mimicking manner by amphiphilic polyanhydride nanoparticle adjuvants. Biomaterials. 2011;32(28):6815-22.

135.   Chavez-Santoscoy AV, Roychoudhury R, Pohl NLB, Wannemuehler MJ, Narasimhan B, Ramer-Tait AE. Tailoring the immune response by targeting C-type lectin receptors on alveolar macrophages using "pathogen-like" amphiphilic polyanhydride nanoparticles. Biomaterials. 2012;33(18):4762-72.

136.   Carrillo-Conde B, Song EH, Chavez-Santoscoy A, Phanse Y, Ramer-Tait AE, Pohl NLB, et al. Mannose-functionalized "pathogen-like" polyanhydride nanoparticles target C-type lectin receptors on dendritic cells. Mol Pharmaceut. 2011;8(5):1877-86.

137.   Adler AF, Petersen LK, Wilson JH, Torres MP, Thorstenson JB, Gardner SW, et al. High throughput cell-based screening of biodegradable polyanhydride libraries. Comb Chem High T Scr. 2009;12(7):634-45.

138.   Geary SM, Lemke CD, Lubaroff DM, Salem AK. Tumor immunotherapy using adenovirus vaccines in combination with intratumoral doses of CpG ODN. Cancer Immunol Immun. 2011;60(9):1309-17.

139.   Kipper MJ, Wilson JH, Wannemuehler MJ, Narasimhan B. Single dose vaccine based on biodegradable polyanhydride microspheres can modulate immune response mechanism. J Biomed Mater Res A. 2006;76(4):798-810.

140.   O'Hagan DT, Jeffery H, Davis SS. Long-term antibody responses in mice following subcutaneous immunization with ovalbumin entrapped in biodegradable microparticles. Vaccine. 1993;11(9):965-9.

141.   Petersen LK, Phanse Y, Ramer-Tait AE, Wannemuehler MJ, Narasimhan B. Amphiphilic polyanhydride nanoparticles stabilize bacillus anthracis protective antigen. Mol Pharmaceut. 2012;9(4):874-82.

142.   Petersen LK, Sackett CK, Narasimhan B. High-throughput analysis of protein stability in polyanhydride nanoparticles. Acta Biomater. 2010;6(10):3873-81.

143.   Torres MP, Wilson-Welder JH, Lopac SK, Phanse Y, Carrillo-Conde B, Ramer-Tait AE, et al. Polyanhydride microparticles enhance dendritic cell antigen presentation and activation. Acta Biomater. 2011;7(7):2857-64.

144.   Storni T, Kundig TM, Senti G, Johansen P. Immunity in response to particulate antigen-delivery systems. Adv Drug Deliver Rev. 2005;57(3):333-55.

145.   Torres MP, Vogel BM, Narasimhan B, Mallapragada SK. Synthesis and characterization of novel polyanhydrides with tailored erosion mechanisms. J Biomed Mater Res A. 2006;76(1):102-10.

146.   Schnare M, Barton GM, Holt AC, Takeda K, Akira S, Medzhitov R. Toll-like receptors control activation of adaptive immune responses. Nat Immunol. 2001;2(10):947-50.

147.   Bremers AJA, Parmiani G. Immunology and immunotherapy of human cancer: present concepts and clinical developments. Crit Rev Oncol Hemat. 2000;34(1):1-25.

148.   Brazolot Millan CL, Weeratna R, Krieg AM, Siegrist CA, Davis HL. CpG DNA can induce strong Th1 humoral and cell-mediated immune responses against hepatitis B surface antigen in young mice. Proc Natl Acad Sci U S A. 1998;95(26):15553-8.

149.   Krieg AM. CpG motifs in bacterial DNA and their immune effects. Annu Rev Immunol. 2002;20:709-60.

150.   Gould MP, Greene JA, Bhoj V, DeVecchio JL, Heinzel FP. Distinct modulatory effects of LPS and CpG on IL-18-dependent IFN-gamma synthesis. J Immunol. 2004;172(3):1754-62.

151.   Weiner GJ, Liu HM, Wooldridge JE, Dahle CE, Krieg AM. Immunostimulatory oligodeoxynucleotides containing the CpG motif are effective as immune adjuvants in tumor antigen immunization. Proc Natl Acad Sci U S A. 1997;94(20):10833-7.

152.   Wooldridge JE, Ballas Z, Krieg AM, Weiner GJ. Immunostimulatory oligodeoxynucleotides containing CpG motifs enhance the efficacy of monoclonal antibody therapy of lymphoma. Blood. 1997;89(8):2994-8.

153.   Kim JJ, Nottingham LK, Tsai A, Lee DJ, Maguire HC, Oh J, et al. Antigen-specific humoral and cellular immune responses can be modulated in rhesus macaques through the use of IFN-γ, IL-12, or IL-18 gene adjuvants. Journal of Medical Primatology. 1999;28(4-5):214-23.

154.   Gamvrellis A, Leong D, Hanley JC, Xiang SD, Mottram P, Plebanski M. Vaccines that facilitate antigen entry into dendritic cells. Immunol Cell Biol. 2004;82(5):506-16.

155.   Waeckerle-Men Y, Groettrup M. PLGA microspheres for improved antigen delivery to dendritic cells as cellular vaccines. Adv Drug Deliver Rev. 2005;57(3):475-82.

156.   Couvreur P, Vauthier C. Nanotechnology: intelligent design to treat complex disease. Pharm Res. 2006;23(7):1417-50.

157.   Ludwig C, Wagner R. Virus-like particles-universal molecular toolboxes. Curr Opin Biotechnol. 2007;18(6):537-45.

158.   Coester C, Nayyar P, Samuel J. In vitro uptake of gelatin nanoparticles by murine dendritic cells and their intracellular localisation. Eur J Pharm Biopharm. 2006;62(3):306-14.

159.   Chikh G, Schutze-Redelmeier MP. Liposomal delivery of CTL epitopes to dendritic cells. Bioscience reports. 2002;22(2):339-53.

160.   Wise DL. Encyclopedic handbook of biomaterials and bioengineering. New York: Marcel Dekker; 1995. 49 p.

161.   Audran R, Peter K, Dannull J, Men Y, Scandella E, Groettrup M, et al. Encapsulation of peptides in biodegradable microspheres prolongs their MHC class-I presentation by dendritic cells and macrophages in vitro. Vaccine. 2003;21(11-12):1250-5.

162.   Men Y, Thomasin C, Merkle HP, Gander B, Corradin G. A single administration of tetanus toxoid in biodegradable microspheres elicits T cell and antibody responses similar or superior to those obtained with aluminum hydroxide. Vaccine. 1995;13(7):683-9.

163.   Peter K, Men Y, Pantaleo G, Gander B, Corradin G. Induction of a cytotoxic T-cell response to HIV-1 proteins with short synthetic peptides and human compatible adjuvants. Vaccine. 2001;19(30):4121-9.

164.   Panda AK, Kanchan V. Interactions of antigen-loaded polylactide particles with macrophages and their correlation with the immune response. Biomaterials. 2007;28(35):5344-57.

165.   Thomas C, Gupta V, Ahsan F. Particle size influences the immune response produced by hepatitis B vaccine formulated in inhalable particles. Pharm Res. 2010;27(5):905-19.

166.   Gutierro I, Hernandez RM, Igartua M, Gascon AR, Pedraz JL. Size dependent immune response after subcutaneous, oral and intranasal administration of BSA loaded nanospheres. Vaccine. 2002;21(1-2):67-77.

167.   Lavasanifar A, Hamdy S, Molavi O, Ma ZS, Haddadi A, Alshamsan A, et al. Co-delivery of cancer-associated antigen and Toll-like receptor 4 ligand in PLGA nanoparticles induces potent CD8(+) T cell-mediated anti-tumor immunity. Vaccine. 2008;26(39):5046-57.

168.   Plebanski M, Gamvrellis A, Leong D, Hanley JC, Xiang SD, Mottram P. Vaccines that facilitate antigen entry into dendritic cells. Immunol Cell Biol. 2004;82(5):506-16.

169.   Katsikogianni G, Avgoustakis K. Poly(lactide-co-glycolide)-methoxy-poly(ethylene glycol) nanoparticles: drug loading and release properties. J Nanosci Nanotechnol. 2006;6(9-10):3080-6.

170.   Nicolas M. Spreading of a drop of neutrally buoyant suspension. J Fluid Mech. 2005;545:271-80.

171.   Deegan RD. Pattern formation in drying drops. Phys Rev E. 2000;61(1):475-85.

172.   Biswas S, Gawande S, Bromberg V, Sun Y. Effects of particle size and substrate surface properties on deposition dynamics of inkjet-printed colloidal drops for printable photovoltaics fabrication. J Sol Energ-T Asme. 2010;132(2).

173.   Lutz MB, Kukutsch N, Ogilvie ALJ, Rössner S, Koch F, Romani N, et al. An advanced culture method for generating large quantities of highly pure dendritic cells from mouse bone marrow. Journal of Immunological Methods. 1999;223(1):77-92.

174.   Lee SW, Sung YC. Immuno-stimulatory effects of bacterial-derived plasmids depend on the nature of the antigen in intramuscular DNA inoculations. Immunology. 1998;94(3):285-9.

175.   Schuler G, Schuler-Thurner B, Steinman RM. The use of dendritic cells in cancer immunotherapy. Curr Opin Immunol. 2003;15(2):138-47.

176.   Nishimura T, Iwakabe K, Sekimoto M, Ohmi Y, Yahata T, Nakui M, et al. Distinct role of antigen-specific T helper type 1 (Th1) and Th2 cells in tumor eradication in vivo. J Exp Med. 1999;190(5):617-27.

177.   Arbes SJ, Jr., Cohn RD, Yin M, Muilenberg ML, Burge HA, Friedman W, et al. House dust mite allergen in US beds: results from the First National Survey of Lead and Allergens in Housing. J Allergy Clin Immunol. 2003;111(2):408-14.

178.   Busse WW, Lemanske RF, Jr. Asthma. N Engl J Med. 2001;344(5):350-62.

179.   Lambrecht BN, Hammad H. The airway epithelium in asthma. Nature medicine. 2012;18(5):684-92.

180.   Johnson JR, Wiley RE, Fattouh R, Swirski FK, Gajewska BU, Coyle AJ, et al. Continuous exposure to house dust mite elicits chronic airway inflammation and structural remodeling. Am J Resp Crit Care. 2004;169(3):378-85.

181.   Milgrom H, Berger W, Nayak A, Gupta N, Pollard S, McAlary M, et al. Treatment of childhood asthma with anti-immunoglobulin E antibody (omalizumab). Pediatrics. 2001;108(2):E36.

182.   Barnes PJ. Severe asthma: advances in current management and future therapy. J Allergy Clin Immunol. 2012;129(1):48-59.

183.   Incorvaia C, Di Rienzo A, Celani C, Makri E, Frati F. Treating allergic rhinitis by sublingual immunotherapy: a review. Ann Ist Super Sanita. 2012;48(2):172-6.

184.   Eifan AO, Akkoc T, Yildiz A, Keles S, Ozdemir C, Bahceciler NN, et al. Clinical efficacy and immunological mechanisms of sublingual and subcutaneous immunotherapy in asthmatic/rhinitis children sensitized to house dust mite: an open randomized controlled trial. Clin Exp Allergy. 2010;40(6):922-32.

185.   Eifan AO, Calderon MA, Durham SR. Allergen immunotherapy for house dust mite: clinical efficacy and immunological mechanisms in allergic rhinitis and asthma. Expert Opin Biol Ther. 2013;13(11):1543-56.

186.   Mazzarella G, Bianco A, Catena E, De Palma R, Abbate GF. Th1/Th2 lymphocyte polarization in asthma. Allergy. 2000;55:6-9.

187.   Wills-Karp M. Immunologic basis of antigen-induced airway hyperresponsiveness. Annu Rev Immunol. 1999;17:255-81.

188.   Wohlleben G, Erb KJ. Atopic disorders: a vaccine around the corner? Trends Immunol. 2001;22(11):618-26.

189.   Burks AW, Calderon MA, Casale T, Cox L, Demoly P, Jutel M, et al. Update on allergy immunotherapy: American Academy of Allergy, Asthma & Immunology/European Academy of Allergy and Clinical Immunology/PRACTALL consensus report. J Allergy Clin Immunol. 2013;131(5):1288-96 e3.

190.   Cox L, Nelson H, Lockey R, Calabria C, Chacko T, Finegold I, et al. Allergen immunotherapy: a practice parameter third update. J Allergy Clin Immunol. 2011;127(1 Suppl):S1-55.

191.   Arlian LG, Morgan MS, Neal JS. Dust mite allergens: ecology and distribution. Current allergy and asthma reports. 2002;2(5):401-11.

192. Kidon MI, Chiang WC, Liew WK, Ong TC, Tiong YS, Wong KN, et al. Mite component-specific IgE repertoire and phenotypes of allergic disease in childhood: the tropical perspective. Pediatr Allergy Immunol. 2011;22(2):202-10.

193. Trompette A, Divanovic S, Visintin A, Blanchard C, Hegde RS, Madan R, et al. Allergenicity resulting from functional mimicry of a Toll-like receptor complex protein. Nature. 2009;457(7229):585-8.

194. Trombone APF, Tobias KRC, Ferriani VPL, Schuurman J, Aalberse RC, Smith AM, et al. Use of a chimeric ELISA to investigate immunoglobulin E antibody responses to Der p 1 and Der p 2 in mite-allergic patients with asthma, wheezing and/or rhinitis. Clin Exp Allergy. 2002;32(9):1323-8.

195. Tan LK, Huang CH, Kuo IC, Liew LM, Chua KY. Intramuscular immunization with DNA construct containing Der p 2 and signal peptide sequences primed strong IgE production. Vaccine. 2006;24(29-30):5762-71.

196. Huang TJ, MacAry PA, Eynott P, Moussavi A, Daniel KC, Askenase PW, et al. Allergen-specific Th1 cells counteract efferent Th2 cell-dependent bronchial hyperresponsiveness and eosinophilic inflammation partly via IFN-gamma. J Immunol. 2001;166(1):207-17.

197. Kline JN, Krieg AM. Toll-like receptor 9 activation with CpG oligodeoxynucleotides for asthma therapy. Drug News Perspect. 2008;21(8):434-9.

198. Fonseca DE, Kline JN. Use of CpG oligonucleotides in treatment of asthma and allergic disease. Adv Drug Deliver Rev. 2009;61(3):256-62.

199. Pulsawat P, Pitakpolrat P, Prompetchara E, Kaewamatawong T, Techakriengkrai N, Sirivichayakul S, et al. Optimization of a Der p 2-based prophylactic DNA vaccine against house dust mite allergy. Immunol Lett. 2013;151(1-2):23-30.

200. Heeg K, Zimmermann S. CpG DNA as a Th1 trigger. Int Arch Allergy Imm. 2000;121(2):87-97.

201. Mo JH, Park SW, Rhee CS, Takabayashi K, Lee SS, Quan SH, et al. Suppression of allergic response by CpG motif oligodeoxynucleotide-house-dust mite conjugate in animal model of allergic rhinitis. Am J Rhinol. 2006;20(2):212-8.

202. Simons FE, Shikishima Y, Van Nest G, Eiden JJ, HayGlass KT. Selective immune redirection in humans with ragweed allergy by injecting Amb a 1 linked to immunostimulatory DNA. J Allergy Clin Immunol. 2004;113(6):1144-51.

203. Kaburaki Y, Fujimura T, Kurata K, Masuda K, Toda M, Yasueda H, et al. Induction of Th1 immune responses to Japanese cedar pollen allergen (Cry j 1) in mice immunized with Cry j 1 conjugated with CpG oligodeoxynucleotide. Comp Immunol Microbiol Infect Dis. 2011;34(2):157-61.

204. Shirota H, Sano K, Kikuchi T, Tamura G, Shirato K. Regulation of T-helper type 2 cell and airway eosinophilia by transmucosal coadministration of antigen and oligodeoxynucleotides containing CpG motifs. Am J Resp Cell Mol. 2000;22(2):176-82.

205. Gomez JMM, Fischer S, Csaba N, Kundig TM, Merkle HP, Gander B, et al. A protective allergy vaccine based on CpG- and protamine-containing PLGA microparticles. Pharm Res. 2007;24(10):1927-35.

206. Scholl I, Kopp T, Bohle B, Jensen-Jarolim E. Biodegradable PLGA particles for improved systemic and mucosal treatment of Type I allergy. Immunol Allergy Clin North Am. 2006;26(2):349-64, ix.

207. Martinez Gomez JM, Fischer S, Csaba N, Kundig TM, Merkle HP, Gander B, et al. A protective allergy vaccine based on CpG- and protamine-containing PLGA microparticles. Pharm Res. 2007;24(10):1927-35.

208. Thorne PS, McCray PB, Howe TS, O'Neill MA. Early-onset inflammatory responses in vivo to adenoviral vectors in the presence or absence of lipopolysaccharide-induced inflammation. Am J Resp Cell Mol. 1999;20(6):1155-64.

209. George CL, White ML, Kulhankova K, Mahajan A, Thorne PS, Snyder JM, et al. Early exposure to a nonhygienic environment alters pulmonary immunity and allergic responses. Am J Physiol Lung Cell Mol Physiol. 2006;291(3):L512-22.

210. Gregory LG, Lloyd CM. Orchestrating house dust mite-associated allergy in the lung. Trends Immunol. 2011;32(9):402-11.

211. Wang X, Yang Q, Wang P, Luo L, Chen Z, Liao B, et al. Derp2-mutant gene vaccine inhibits airway inflammation and up-regulates Toll-like receptor 9 in an allergic asthmatic mouse model. Asian Pac J Allergy Immunol. 2010;28(4):287-93.

212. Daan de Boer J, Roelofs JJ, de Vos AF, de Beer R, Schouten M, Hommes TJ, et al. Lipopolysaccharide inhibits Th2 lung inflammation induced by house dust mite allergens in mice. Am J Resp Cell Mol. 2013;48(3):382-9.

213. Chung KF, Barnes PJ. Cytokines in asthma. Thorax. 1999;54(9):825-57.

214. Sumino K, Sugar EA, Irvin CG, Kaminsky DA, Shade D, Wei CY, et al. Methacholine challenge test: diagnostic characteristics in asthmatic patients receiving controller medications. J Allergy Clin Immunol. 2012;130(1):69-75 e6.

215. Akinbami LJ, Moorman JE, Bailey C, Zahran HS, King M, Johnson CA, et al. Trends in asthma prevalence, health care use, and mortality in the United States, 2001-2010. NCHS Data Brief. 2012;94:1-8.

216. Bharadwaj AS, Bewtra AK, Agrawal DK. Dendritic cells in allergic airway inflammation. Can J Physiol Pharmacol. 2007;85(7):686-99.

217.   Kündig TM, Senti G, Schnetzler G, Wolf C, Prinz Vavricka BM, Fulurija A, et al. Der p 1 peptide on virus-like particles is safe and highly immunogenic in healthy adults. J Allergy Clin Immunol. 2006;117(6):1470-6.

218.   Standley SM, Mende I, Goh SL, Kwon YJ, Beaudette TT, Engleman EG, et al. Incorporation of CpG oligonucleotide ligand into protein-loaded particle vaccines promotes antigen-specific CD8 T-cell immunity. Bioconjugate Chem. 2007;18(1):77-83.

219.   Hamdy S, Haddadi A, Hung RW, Lavasanifar A. Targeting dendritic cells with nano-particulate PLGA cancer vaccine formulations. Adv Drug Deliv Rev. 2011;63(10-11):943-55.

220.   Scholl I, Weissenbock A, Forster-Waldl E, Untersmayr E, Walter F, Willheim M, et al. Allergen-loaded biodegradable poly(D,L-lactic-co-glycolic) acid nanoparticles down-regulate an ongoing Th2 response in the BALB/c mouse model. Clin Exp Allergy. 2004;34(2):315-21.

221.   Siegel R, Ward E, Brawley O, Jemal A. Cancer statistics, 2011: the impact of eliminating socioeconomic and racial disparities on premature cancer deaths. CA Cancer J Clin. 2011;61(4):212-36.

222.   Pervaiz N, Colterjohn N, Farrokhyar F, Tozer R, Figueredo A, Ghert M. A systematic meta-analysis of randomized controlled trials of adjuvant chemotherapy for localized resectable soft-tissue sarcoma. Cancer. 2008;113(3):573-81.

223.   Gordon AN, Fleagle JT, Guthrie D, Parkin DE, Gore ME, Lacave AJ. Recurrent epithelial ovarian carcinoma: a randomized phase III study of pegylated liposomal doxorubicin versus topotecan. J Clin Oncol. 2001;19(14):3312-22.

224.   Neumann E, Engelsberg A, Decker J, Storkel S, Jaeger E, Huber C, et al. Heterogeneous expression of the tumor-associated antigens RAGE-1, PRAME, and glycoprotein 75 in human renal cell carcinoma: candidates for T-cell-based immunotherapies? Cancer Res. 1998;58(18):4090-5.

225.   Schirrmacher V, Leidig S, Griesbach A. In situ activation of syngeneic tumour-specific cytotoxic T lymphocytes: intra-pinna immunization followed by restimulation in the peritoneal cavity. Cancer Immunol Immunother. 1991;33(5):299-306.

226.   Chaudhuri D, Suriano R, Mittelman A, Tiwari RK. Targeting the immune system in cancer. Curr Pharm Biotechnol. 2009;10(2):166-84.

227.   Arlen PM, Gulley JL, Madan RA, Hodge JW, Schlom J. Preclinical and clinical studies of recombinant poxvirus vaccines for carcinoma therapy. Crit Rev Immunol. 2007;27(5):451-62.

228.   Baxevanis CN, Perez SA, Papamichail M. Combinatorial treatments including vaccines, chemotherapy and monoclonal antibodies for cancer therapy. Cancer Immunol Immunother. 2009;58(3):317-24.

229.   Sylvester RJ, Brausi MA, Kirkels WJ, Hoeltl W, Calais Da Silva F, Powell PH, et al. Long-term efficacy results of EORTC genito-urinary group randomized phase 3 study 30911 comparing intravesical instillations of epirubicin, bacillus Calmette-Guerin, and bacillus Calmette-Guerin plus isoniazid in patients with intermediate- and high-risk stage Ta T1 urothelial carcinoma of the bladder. Eur Urol. 2010;57(5):766-73.

230.   Dubensky TW, Jr., Reed SG. Adjuvants for cancer vaccines. Semin Immunol. 2010;22(3):155-61.

231.   Vollmer J, Krieg AM. Immunotherapeutic applications of CpG oligodeoxynucleotide TLR9 agonists. Adv Drug Deliver Rev. 2009;61(3):195-204.

232.   Monjazeb AM, Hsiao HH, Sckisel GD, Murphy WJ. The role of antigen-specific and non-specific immunotherapy in the treatment of cancer. J Immunotoxicol. 2012;9(3):248-58.

233.   Balsari A, Tortoreto M, Besusso D, Petrangolini G, Sfondrini L, Maggi R, et al. Combination of a CpG-oligodeoxynucleotide and a topoisomerase I inhibitor in the therapy of human tumour xenografts. Eur J Cancer. 2004;40(8):1275-81.

234.   Brody JD, Ai WZ, Czerwinski DK, Torchia JA, Levy M, Advani RH, et al. In situ vaccination with a TLR9 agonist induces systemic lymphoma regression: a phase I/II study. J Clin Oncol. 2010;28(28):4324-32.

235.   Obeid M, Tesniere A, Ghiringhelli F, Fimia GM, Apetoh L, Perfettini JL, et al. Calreticulin exposure dictates the immunogenicity of cancer cell death. Nature medicine. 2007;13(1):54-61.

236.   Casares N, Pequignot MO, Tesniere A, Ghiringhelli F, Roux S, Chaput N, et al. Caspase-dependent immunogenicity of doxorubicin-induced tumor cell death. J Exp Med. 2005;202(12):1691-701.

237.   Mizuno Y, Naoi T, Nishikawa M, Rattanakiat S, Hamaguchi N, Hashida M, et al. Simultaneous delivery of doxorubicin and immunostimulatory CpG motif to tumors using a plasmid DNA/doxorubicin complex in mice. J Control Release. 2010;141(2):252-9.

238.   Lee IH, An S, Yu MK, Kwon HK, Im SH, Jon S. Targeted chemoimmunotherapy using drug-loaded aptamer-dendrimer bioconjugates. J Control Release. 2011;155(3):435-41.

239.   Lee IH, Yu MK, Kim IH, Lee JH, Park TG, Jon S. A duplex oligodeoxynucleotide-dendrimer bioconjugate as a novel delivery vehicle for doxorubicin in in vivo cancer therapy. J Control Release. 2011;155(1):88-95.

240.   Nishikawa M, Mizuno Y, Mohri K, Matsuoka N, Rattanakiat S, Takahashi Y, et al. Biodegradable CpG DNA hydrogels for sustained delivery of doxorubicin and immunostimulatory signals in tumor-bearing mice. Biomaterials. 2011;32(2):488-94.

241.   Qiao ZY, Zhang R, Du FS, Liang DH, Li ZC. Multi-responsive nanogels containing motifs of ortho ester, oligo(ethylene glycol) and disulfide linkage as carriers of hydrophobic anti-cancer drugs. J Control Release. 2011;152(1):57-66.

242.   Janssen MJH, Crommelin DJA, Storm G, Hulshoff A. Doxorubicin decomposition on storage. Effect of pH, type of buffer and liposome encapsulation. Int J Pharm. 1985;23(1):1-11.

243.   Evangelista L, Mezzato C, Felloni G, Saladini G. Current and future perspectives in diagnostic imaging as a guide to targeted/local therapies in breast cancer recurrence. Q J Nucl Med Mol Im. 2013;57(4):367-80.

244.   Jankowitz RC, Davidson NE. Adjuvant endocrine therapy for breast cancer: how long is long enough? Oncology-Ny. 2013;27(12):1210-6.

245.   Simard S, Thewes B, Humphris G, Dixon M, Hayden C, Mireskandari S, et al. Fear of cancer recurrence in adult cancer survivors: a systematic review of quantitative studies. J Cancer Surviv. 2013;7(3):300-22.

246.   Wang ZX, Cao JX, Liu ZP, Cui YX, Li CY, Li D, et al. Combination of chemotherapy and immunotherapy for colon cancer in China: A meta-analysis. World J Gastroentero. 2014;20(4):1095-106.

247.   Buteau C, Markovic SN, Celis E. Challenges in the development of effective peptide vaccines for cancer. Mayo Clin Proc. 2002;77(4):339-49.

248.   Shetty VP, Mistry NF, Wakade AV, Ghate SD, Capadia GD, Pai VV. BCG immunotherapy as an adjunct to chemotherapy in BL-LL patients - its effect on clinical regression, reaction severity, nerve function, lepromin conversion, bacterial/antigen clearance and 'persister' M. leprae. Leprosy Rev. 2013;84(1):23-40.